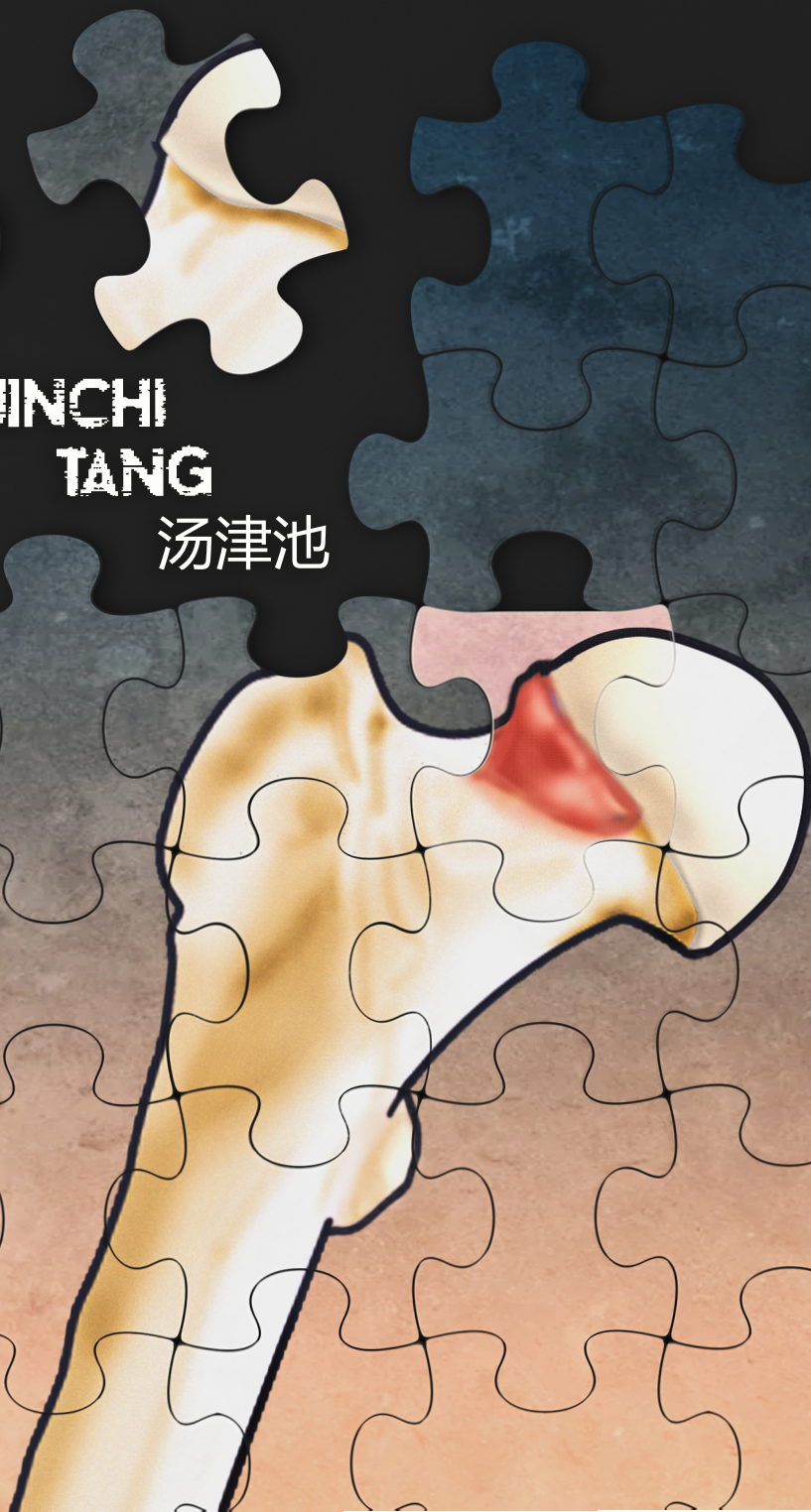


CAM MORPHOLOGY AND ITS ROLE IN HIP OSTEOARTHRITIS

JINCHI
TANG

汤津池



Cam Morphology and Its Role in Hip Osteoarthritis

Jinchi Tang

Cover design: Bernard Elsman Contreras | bernartvisuals@gmail.com

Layout: Natalia Kubalski | Natalia@ogc.nl

Printing: Optima Grafische Communicatie | www.ogc.nl

Jinchi Tang was supported by a Chinese Scholarship Council (CSC) PhD Fellowship for his PhD study in Erasmus MC, Rotterdam, the Netherlands, grant number 202006170050.

Publication of this thesis was kindly supported by the Department of Orthopaedics and Sports Medicine; Erasmus University Rotterdam; Chipsoft (<https://www.chipsoft.com>).

Cam Morphology and Its Role in Hip Osteoarthritis

Cam-morfologie en de rol ervan bij heupartrose

Thesis

to obtain the degree of Doctor from the
Erasmus University Rotterdam
by command of the
rector magnificus

Prof. dr. ir. A. J. Schuit

and in accordance with the decision of the Doctorate Board.
The public defence shall be held on

Tuesday 4 February 2025 at 10:30 hrs
by

Jinchi Tang

born in Shaanxi, China.

Erasmus University Rotterdam



DOCTORAL COMMITTEE:

Promotor: Prof. dr. S.M.A. Bierma - Zeinstra

Other members: Prof. dr. J.N. Doornberg

Dr. M. van Middelkoop

Prof. dr. J.L. Tol

Co-promotor: Dr. R. Agricola

TABLE OF CONTENTS

Chapter 1	General Introduction	7
Chapter 2	Reliability and agreement of manual and automated morphological radiographic hip measurements	21
Chapter 3	Cam morphology is strongly and consistently associated with the development of radiographic hip osteoarthritis throughout 4 follow-up visits within 10 years	53
Chapter 4	Cam morphology and the risk of developing radiographic hip osteoarthritis within 8 years: an individual participant data meta-analysis from the World COACH consortium	71
Chapter 5	The association between cam morphology and hip pain in males and females within 10 years: a national prospective cohort study (CHECK)	91
Chapter 6	The different subtypes of cam morphology as defined by statistical shape modelling and their relationship with the development of hip osteoarthritis: a nationwide prospective cohort study (CHECK) with 10 years follow-up	113
Chapter 7	Triangular index ratio as an alternative method to the alpha angle for defining the presence of cam morphology: data from the CHECK cohort	135
Chapter 8	General Discussion	149
Chapter 9	Summary/Samenvatting	167
Appendices	PhD portfolio	179
	Acknowledgments	180
	About the author	182
	List of publications	183



General Introduction

HIP OSTEOARTHRITIS

Osteoarthritis (OA) is a chronic and degenerative disease, characterized by pain, swelling, stiffness, and loss of mobility in joints^{1, 2}. It mainly affects the hyaline articular cartilage, but also the other surrounding structures, including subchondral bone, capsule, synovium, tendons, ligaments, and muscles^{3, 4}. According to the WHO's World Report on Global Ageing and Health, OA was highlighted as a leading cause of disability in the elderly aged 60 years and older, affecting 7.6% (595 million) of the global population in 2020⁵.

With the global population aging, the prevalence of OA is increasing gradually with an annual rate of 1.4% (95% CI 1.3–1.6%)⁶, accompanied by an increase in health and economic burden⁷. Globally, the age-standardized rate of years lived with disability (YLDs) accounted for up to 255 YLDs per 100,000 in 2020, establishing OA as the seventh leading cause of YLDs among the elderly⁵. The direct healthcare cost and indirect socioeconomic cost associated with OA impose a significant economic burden on both individuals and nations, collectively amounting to 1-2.5% of the gross domestic product (GDP) of high-income countries⁸.

Following knee OA, the prevalence of hip OA has been identified as the second highest among all relevant types of OA^{9, 10}, around 10%¹¹. Due to a lack of comprehensive understanding of the pathological mechanism of OA and its irreversible process of progression, no cure has been developed for the condition to date¹¹. Current management relies on non-pharmacological methods at the early stages and surgical treatments at the advanced stages^{1, 2, 12}. Therefore, the research on the prevention of hip OA, despite being in its early stages, warrants increased attention. A thorough understanding of the risk factors of hip OA may offer valuable insights into its prevention.

CAM MORPHOLOGY

To date, various risk factors for hip OA have been identified previously, which include but are not limited to demographic characteristics (older age, female sex, and obesity), genetic factors, structural morphology, previous injury, and physical activity with high loading¹³⁻¹⁹. Among structural factors of hip morphology, cam morphology has been identified as contributing to a higher risk of developing radiographic hip OA (RHOA) with growing evidence. It is characterized by the presence of additional bone formation of varying sizes around the femoral head-neck junction²⁰ (**Figure 1**). This irregularity results in a non-spherical femoral head, leading to the impingement against the acetabular rim during flexion and internal rotation of the hip²¹. Cam morphology was initially described in 1855 by Henle J²² and was systematically defined as anatomical variations of the proximal femur characterized by a significant reduction in femoral anteversion and head-neck offset on the anterior aspect of the neck in 2001²³. Over time, it has been referred to by different terms such as 'pistol grip', 'tilt deformity', or 'cam deformity'²⁴. The academic community has recently reached a consensus on its definition, agreeing that cam morphology refers to a cartilage or bony prominence of varying size usually at the anterosuperior aspect of the femoral head-neck junction of the hip²⁰.

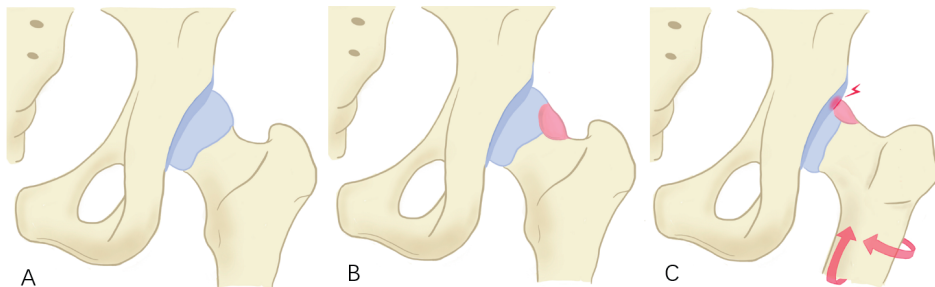


Figure 1. Comparison of normal hip (figure A) and hip with cam morphology (figure B/C)

Cam morphology can be classified as primary or secondary, depending on whether there is a pre-existing pathologic process²⁵. Comparing to primary cam morphology, secondary cam morphology arises from pre-existing pathologic processes with clear mechanisms, such as slipped capital femoral epiphysis, Legg-Calve-Perthes disease, fracture malunion, and infection²⁵. The etiology of primary cam morphology, however, remains incompletely understood.

Cam morphology mostly starts to develop before the closure of the growth plate and continues to increase in size alongside skeletal growth²⁶. Its growth halts after the closure of the proximal femoral growth plate²⁷. Engaging in high-impact sports during growth has been reported to play a significant role in this process²⁸⁻³⁰. Hence, the formation of cam morphology can be viewed as a consequence of bony structural adaptation to excessive femoral loading^{26, 31}.

The description of shape of cam morphology varied a lot, from a “pistol-grip” to a “oval shape”, suggesting the shape of cam morphology is irregular. At present, the methods used to quantify cam morphology can mainly distinguish the size of cam morphology but not its shape variations. To the best of our knowledge, there is no previous research on whether different subtypes of cam morphology as captured by the alpha angle exist and how these relate to the development of RHOA.

THE RADIOGRAPHICAL INDICES FOR CAM MORPHOLOGY

Cam morphology results in an aspherical femoral head, therefore radiographic indices used to quantify cam morphology primarily aim to measure the extent of deviation from spherical to aspherical shape of the femoral head. These indices include, but are not limited to: the alpha angle, femoral head-neck offset measure (mm) or ratio, femoroacetabular excursion angle (the beta angle), triangular index, and the relationship between the width of the femoral neck and diameter of the femoral head. Most of these indices can be measured on radiographs, dual-energy X-ray absorptiometry (DXA), CT scans, and MRI scans³² and reported as continuous and/or dichotomous variables.

The most commonly and widely used method is the alpha angle³³. It was first proposed by Notzli et al. in 2002 using MRI scans³⁴. However, it was later applied to radiographs with various views, including anteroposterior (AP) view, Dunn 45 view, Frog-leg lateral view, cross-table lateral view, false profile view, Sugioka views, von Rosen view, and Lauenstein View³². The alpha angle was measured as the angle between the longitudinal axis of the femoral neck and an auxiliary line extending from the center of the femoral head to a point where the head-neck junction begins to leave the best-fitting circle of the femoral head³⁴ (**Figure 2**). In clinical practice or research, the value of alpha angle is used as continuous in degree or dichotomous variables by a cut-off value. To date, the cut-off value used to identify the presence of cam morphology showed huge variation in prior studies, ranging from 50° to 83°³². Among them, the

threshold value of 60° recently gained a certain consensus to use for classifying cam morphology²⁰.

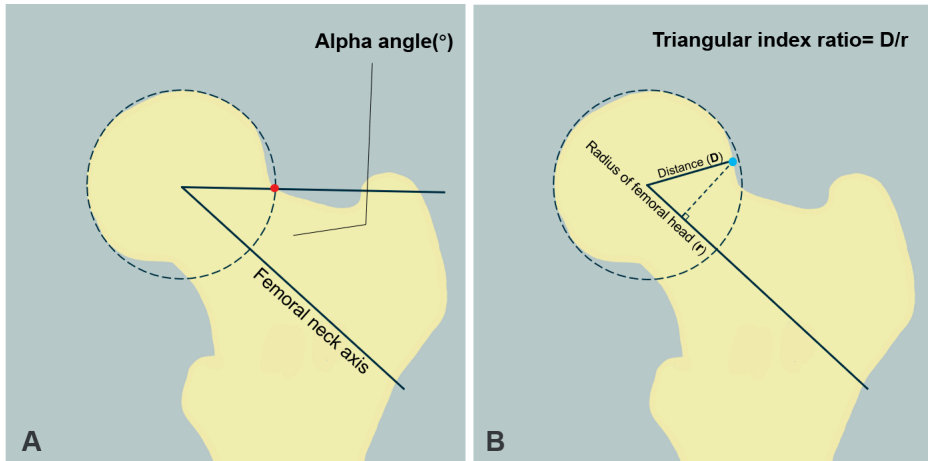


Figure 2. The measurement of alpha angle (figure A) and triangular index ratio (figure B). The alpha angle is the angle between the femoral neck axis and a line connecting the femoral head center and alpha point (red point), where the contour of the femoral head-neck junction begins to exceed the best-fitting circle of the femoral head; The triangular index ratio is the ratio of the distance (D) between the femoral head center and a point (blue point) on the femoral head-neck junction at $0.5r$ along the femoral head-neck axis and the radius of the best-fitting circle around the femoral head (r).

The triangular index ratio is an alternative method on AP radiograph to quantify cam morphology. The triangular index, the original form of the triangular index ratio, was introduced by Gosvig et al. in 2005³⁵. It compares a specific distance (D) from the center of the femoral head to a point on the cortex of the head-neck junction, taken at half the radius of the femoral head along the line passing through the femoral neck axis and the radius of the femoral head (r). Initially, the sphericity of femoral head (cam morphology) was defined by Gosvig et al. if $D \geq r + 2$ mm at 1.2 magnification³⁵ (**Figure 2**). However, this measurement relies on radiographs achieving millimeter-level accuracy, with varying magnifications depending on the radiographic protocol used. By evaluating the relationship between the 2 mm threshold and the radius of the femoral head, this linear measurement can be transformed into a ratio form to address this issue. The triangular index ratio concentrates on the distance from the most lateral part of the femoral head-neck junction to the femoral neck, which differs from the alpha angle measurement. Consequently, the triangular index ratio holds the potential to enhance the accuracy in defining the presence of cam morphology.

However, this method was seldom used in previous studies, therefore the predictive performance of cam morphology defined by this method is still unknown.

CAM MORPHOLOGY AND HIP OSTEOARTHRITIS

Cam morphology may lead to impingement against the acetabulum rim during hip motion, especially the flexion and internal rotation of the hip³⁶. This repetitive abnormal contact can induce shear forces on the acetabular labrum and articular cartilage, ultimately resulting in cartilage defects and labral tears²¹. Eventually, this wear and tear structural damage around the hip joint might evolve to hip OA.

The association between cam morphology and the development of radiographic hip OA (RHOA) has been extensively investigated in prior prospective cohort studies, consistently revealing a clear consensus that cam morphology represents a robust risk factor for the development of RHOA³⁶⁻⁴⁰. However, the strength of this association reported varies widely between different cohorts, with odds ratios varying between 2.11 (95% CI 1.55–2.87)³⁸ and 20.6 (95% CI 3.4–34.8)⁴¹. The explanation for this variance could be the difference in demographic characteristics of the studied population, definition for cam morphology and RHOA, and follow-up times used (ranging from 3 to over 25 years). Due to these variations, the findings from each previous cohort study stand independently and are not directly transferable to one another, thus rendering them underpowered for generalization to the broader population. The etiology of cam morphology leading to RHOA remains inadequately understood and warrants further attention, particularly in light of the issues mentioned above.

CAM MORPHOLOGY AND FEMOROACETABULAR IMPINGEMENT SYNDROME

Femoroacetabular impingement (FAI) syndrome has been recognized as a potential precursor to the development of idiopathic hip osteoarthritis⁴². It is characterized by abnormal contact between the proximal femur and acetabular rim, leading to its classification into two types based on morphological features: cam morphology and pincer morphology (an over coverage of the acetabulum)⁴³. The primary symptom of FAI syndrome is motion- or position-related anterior or anterolateral hip or groin pain^{36, 43-45}. However, a substantial proportion of individuals with cam morphology are asymptomatic. The association between cam morphology and hip pain remains unclear with previous conflicting findings⁴⁶⁻⁵⁴. Since all those studies only collected data

of hip pain at single time point, the fluctuating nature of pain might be an explanation for this considerable variability. To date, there is no study exploring the relationship between cam morphology and hip pain at multiple time points.

AIMS AND OUTLINE

The aims of this thesis are to:

1. Addressing current knowledge gaps by investigating the association between cam morphology and the development of RHOA at various follow-up intervals, utilizing a unified definition of cam morphology and RHOA within a comprehensive, harmonized database.
2. Examining the association between cam morphology and hip pain symptom at multiple time points.
3. Exploring shape variation of cam morphology and identifying the subtypes of cam morphology that are currently lacking.
4. Investigating the association between cam morphology defined by triangular index ratio and the development of RHOA and comparing the predictive performance for RHOA between this novel method and the currently mostly used method: alpha angle.

This thesis consists of four parts. **Part I** consists of **Chapter 2**, which is the methodology of this thesis. In this chapter, we introduced the automated algorithm for the alpha angle and triangular index ratio measured on pelvic radiographs, which forms the basis of the following chapters. In **Part II**, we focused on the association between cam morphology and the incident RHOA. In **Chapter 3**, we studied the association between cam morphology and RHOA development in the CHECK cohort at four different follow-up points. In **Chapter 4**, by an individual participant data (IPD) meta-analysis from the World COACH consortium, we tried to better understand the contribution of cam morphology to the risk of developing RHOA in a more generalized population. **Part III** consists of **Chapter 5**, in which we investigated the association of cam morphology with the presence of hip pain annually over a 10-year period. In **Part IV**, we explored the cam morphology beyond the alpha angle. In **Chapter 6**, we employed statistical shape modeling to quantify the shape of the femoral head-neck junction and aimed to identify subtypes of cam morphology. Concurrently, we investigated the association between each subtype of cam morphology and the development of RHOA at follow-up. In **Chapter 7**, acknowledging the limitations of the alpha angle, we endeavored to identify an alternative method for defining the presence of cam morphology. We assessed the predictive performance of the triangular index ratio-defined cam morphology for the development of RHOA.

REFERENCES

1. Glyn-Jones S, Palmer AJ, Agricola R, Price AJ, Vincent TL, Weinans H, et al. Osteoarthritis. *Lancet* 2015; 386: 376-387.
2. Hunter DJ, Bierma-Zeinstra S. Osteoarthritis. *Lancet* 2019; 393: 1745-1759.
3. Martel-Pelletier J, Barr AJ, Cicuttini FM, Conaghan PG, Cooper C, Goldring MB, et al. Osteoarthritis. *Nat Rev Dis Primers* 2016; 2: 16072.
4. Man GS, Mologhianu G. Osteoarthritis pathogenesis - a complex process that involves the entire joint. *J Med Life* 2014; 7: 37-41.
5. Collaborators GBDO. Global, regional, and national burden of osteoarthritis, 1990-2020 and projections to 2050: a systematic analysis for the Global Burden of Disease Study 2021. *Lancet Rheumatol* 2023; 5: e508-e522.
6. Swain S, Sarmanova A, Mallen C, Kuo CF, Coupland C, Doherty M, et al. Trends in incidence and prevalence of osteoarthritis in the United Kingdom: findings from the Clinical Practice Research Datalink (CPRD). *Osteoarthritis Cartilage* 2020; 28: 792-801.
7. Leifer VP, Katz JN, Losina E. The burden of OA-health services and economics. *Osteoarthritis Cartilage* 2022; 30: 10-16.
8. Hunter DJ, Schofield D, Callander E. The individual and socioeconomic impact of osteoarthritis. *Nat Rev Rheumatol* 2014; 10: 437-441.
9. Long H, Liu Q, Yin H, Wang K, Diao N, Zhang Y, et al. Prevalence Trends of Site-Specific Osteoarthritis From 1990 to 2019: Findings From the Global Burden of Disease Study 2019. *Arthritis Rheumatol* 2022; 74: 1172-1183.
10. Hall M, van der Esch M, Hinman RS, Peat G, de Zwart A, Quicke JG, et al. How does hip osteoarthritis differ from knee osteoarthritis? *Osteoarthritis Cartilage* 2022; 30: 32-41.
11. Katz JN, Arant KR, Loeser RF. Diagnosis and Treatment of Hip and Knee Osteoarthritis: A Review. *JAMA* 2021; 325: 568-578.
12. Kolasinski SL, Neogi T, Hochberg MC, Oatis C, Guyatt G, Block J, et al. 2019 American College of Rheumatology/Arthritis Foundation Guideline for the Management of Osteoarthritis of the Hand, Hip, and Knee. *Arthritis Care Res (Hoboken)* 2020; 72: 149-162.
13. Prieto-Alhambra D, Judge A, Javaid MK, Cooper C, Diez-Perez A, Arden NK. Incidence and risk factors for clinically diagnosed knee, hip and hand osteoarthritis: influences of age, gender and osteoarthritis affecting other joints. *Ann Rheum Dis* 2014; 73: 1659-1664.
14. Lane NE, Gore LR, Cummings SR, Hochberg MC, Scott JC, Williams EN, et al. Serum vitamin D levels and incident changes of radiographic hip osteoarthritis: a longitudinal study. *Study of Osteoporotic Fractures Research Group. Arthritis Rheum* 1999; 42: 854-860.
15. Eleni A, Panagiotis P. A systematic review and meta-analysis of vitamin D and calcium in preventing osteoporotic fractures. *Clin Rheumatol* 2020; 39: 3571-3579.
16. Kim M, Rubab A, Chan WCW, Chan D. Osteoarthritis year in review 2022: Genetics, genomics and epigenetics. *Osteoarthritis Cartilage* 2023; 31: 865-875.
17. Jiang L, Rong J, Wang Y, Hu F, Bao C, Li X, et al. The relationship between body mass index and hip osteoarthritis: a systematic review and meta-analysis. *Joint Bone Spine* 2011; 78: 150-155.
18. Casartelli NC, Maffiuletti NA, Valenzuela PL, Grassi A, Ferrari E, van Buuren MMA, et al. Is hip morphology a risk factor for developing hip osteoarthritis? A systematic review with meta-analysis. *Osteoarthritis Cartilage* 2021; 29: 1252-1264.

19. Kolber MJ, Hanney WJ, Cheatham SW, Salanh PA. Risk Factors for Hip Osteoarthritis: Insight for the Strength and Conditioning Professional. *Strength & Conditioning Journal* 2017; 39: 35-41.
20. Dijkstra HP, Mc Auliffe S, Ardern CL, Kemp JL, Mosler AB, Price A, et al. Oxford consensus on primary cam morphology and femoroacetabular impingement syndrome: part 1-definitions, terminology, taxonomy and imaging outcomes. *Br J Sports Med* 2022; 57: 325-341.
21. Heerey J, Kemp J, Agricola R, Srinivasan R, Smith A, Pizzari T, et al. Cam morphology is associated with MRI-defined cartilage defects and labral tears: a case-control study of 237 young adult football players with and without hip and groin pain. *BMJ Open Sport Exerc Med* 2021; 7: e001199.
22. Henle J. *Handbuch der systematischen Anatomie des Menschen* von J. Henle: *Handbuch der Gefäßlehre des Menschen*, Friedrich Vieweg und Sohn 1868.
23. Ito K, Minka MA, 2nd, Leunig M, Werlen S, Ganz R. Femoroacetabular impingement and the cam-effect. A MRI-based quantitative anatomical study of the femoral head-neck offset. *J Bone Joint Surg Br* 2001; 83: 171-176.
24. Matsumoto K, Ganz R, Khanduja V. The history of femoroacetabular impingement. *Bone Joint Res* 2020; 9: 572-577.
25. Morris WZ, Li RT, Liu RW, Salata MJ, Voos JE. Origin of Cam Morphology in Femoroacetabular Impingement. *Am J Sports Med* 2018; 46: 478-486.
26. van Klij P, Heijboer MP, Ginai AZ, Verhaar JAN, Waarsing JH, Agricola R. Cam morphology in young male football players mostly develops before proximal femoral growth plate closure: a prospective study with 5-year follow-up. *Br J Sports Med* 2019; 53: 532-538.
27. Agricola R, Heijboer MP, Ginai AZ, Roels P, Zadpoor AA, Verhaar JA, et al. A cam deformity is gradually acquired during skeletal maturation in adolescent and young male soccer players: a prospective study with minimum 2-year follow-up. *Am J Sports Med* 2014; 42: 798-806.
28. Agricola R, Bessems JH, Ginai AZ, Heijboer MP, van der Heijden RA, Verhaar JA, et al. The development of Cam-type deformity in adolescent and young male soccer players. *Am J Sports Med* 2012; 40: 1099-1106.
29. Siebenrock KA, Ferner F, Noble PC, Santore RF, Werlen S, Mamisch TC. The cam-type deformity of the proximal femur arises in childhood in response to vigorous sporting activity. *Clin Orthop Relat Res* 2011; 469: 3229-3240.
30. Nepple JJ, Vigdorich JM, Clohisy JC. What Is the Association Between Sports Participation and the Development of Proximal Femoral Cam Deformity? A Systematic Review and Meta-analysis. *Am J Sports Med* 2015; 43: 2833-2840.
31. Roels P, Agricola R, Oei EH, Weinans H, Campoli G, Zadpoor AA. Mechanical factors explain development of cam-type deformity. *Osteoarthritis Cartilage* 2014; 22: 2074-2082.
32. Dijkstra HP, Ardern CL, Serner A, Mosler AB, Weir A, Roberts NW, et al. Primary cam morphology; bump, burden or bog-standard? A concept analysis. *Br J Sports Med* 2021; 55: 1212-1221.
33. Nouh MR, Schweitzer ME, Rybak L, Cohen J. Femoroacetabular impingement: can the alpha angle be estimated? *AJR Am J Roentgenol* 2008; 190: 1260-1262.
34. Notzli HP, Wyss TF, Stoecklin CH, Schmid MR, Treiber K, Hodler J. The contour of the femoral head-neck junction as a predictor for the risk of anterior impingement. *J Bone Joint Surg Br* 2002; 84: 556-560.

35. Gosvig KK, Jacobsen S, Palm H, Sonne-Holm S, Magnusson E. A new radiological index for assessing asphericity of the femoral head in cam impingement. *J Bone Joint Surg Br* 2007; 89: 1309-1316.
36. Agricola R, Heijboer MP, Bierma-Zeinstra SM, Verhaar JA, Weinans H, Waarsing JH. Cam impingement causes osteoarthritis of the hip: a nationwide prospective cohort study (CHECK). *Ann Rheum Dis* 2013; 72: 918-923.
37. Ahedi H, Winzenberg T, Bierma-Zeinstra S, Blizzard L, van Middelkoop M, Agricola R, et al. A prospective cohort study on cam morphology and its role in progression of osteoarthritis. *Int J Rheum Dis* 2022; 25: 601-612.
38. Saberi Hosnijeh F, Zuiderwijk ME, Versteeg M, Smeele HT, Hofman A, Uitterlinden AG, et al. Cam Deformity and Acetabular Dysplasia as Risk Factors for Hip Osteoarthritis. *Arthritis Rheumatol* 2017; 69: 86-93.
39. Hoch A, Schenk P, Jentzsch T, Rahm S, Zingg PO. FAI morphology increases the risk for osteoarthritis in young people with a minimum follow-up of 25 years. *Arch Orthop Trauma Surg* 2021; 141: 1175-1181.
40. Nicholls AS, Kiran A, Pollard TC, Hart DJ, Arden CP, Spector T, et al. The association between hip morphology parameters and nineteen-year risk of end-stage osteoarthritis of the hip: a nested case-control study. *Arthritis Rheum* 2011; 63: 3392-3400.
41. Bardakos NV, Villar RN. Predictors of progression of osteoarthritis in femoroacetabular impingement: a radiological study with a minimum of ten years follow-up. *J Bone Joint Surg Br* 2009; 91: 162-169.
42. Kowalczyk M, Yeung M, Simunovic N, Ayeni OR. Does Femoroacetabular Impingement Contribute to the Development of Hip Osteoarthritis? A Systematic Review. *Sports Med Arthrosc Rev* 2015; 23: 174-179.
43. Griffin DR, Dickenson EJ, O'Donnell J, Agricola R, Awan T, Beck M, et al. The Warwick Agreement on femoroacetabular impingement syndrome (FAI syndrome): an international consensus statement. *Br J Sports Med* 2016; 50: 1169-1176.
44. Pun S, Kumar D, Lane NE. Femoroacetabular impingement. *Arthritis Rheumatol* 2015; 67: 17-27.
45. Clohisy JC, Dobson MA, Robison JF, Warth LC, Zheng J, Liu SS, et al. Radiographic structural abnormalities associated with premature, natural hip-joint failure. *J Bone Joint Surg Am* 2011; 93 Suppl 2: 3-9.
46. Allen D, Beaulé PE, Ramadan O, Doucette S. Prevalence of associated deformities and hip pain in patients with cam-type femoroacetabular impingement. *J Bone Joint Surg Br* 2009; 91: 589-594.
47. Khanna V, Caragianis A, Diprimio G, Rakhra K, Beaulé PE. Incidence of hip pain in a prospective cohort of asymptomatic volunteers: is the cam deformity a risk factor for hip pain? *Am J Sports Med* 2014; 42: 793-797.
48. Guler O, Isyar M, Karatas D, Ormeci T, Cerci H, Mahirogullari M. A retrospective analysis on the correlation between hip pain, physical examination findings, and alpha angle on MR images. *J Orthop Surg Res* 2016; 11: 140.
49. Abrahamson J, Jonasson P, Sansone M, Aminoff AS, Todd C, Karlsson J, et al. Hip pain and its correlation with cam morphology in young skiers-a minimum of 5 years follow-up. *J Orthop Surg Res* 2020; 15: 444.

50. van Klip P, Ginai AZ, Heijboer MP, Verhaar JAN, Waarsing JH, Agricola R. The relationship between cam morphology and hip and groin symptoms and signs in young male football players. *Scand J Med Sci Sports* 2020; 30: 1221-1231.
51. Gosvig KK, Jacobsen S, Sonne-Holm S, Gebuhr P. The prevalence of cam-type deformity of the hip joint: a survey of 4151 subjects of the Copenhagen Osteoarthritis Study. *Acta Radiol* 2008; 49: 436-441.
52. Nardo L, Parimi N, Liu F, Lee S, Jungmann PM, Nevitt MC, et al. Femoroacetabular Impingement: Prevalent and Often Asymptomatic in Older Men: The Osteoporotic Fractures in Men Study. *Clin Orthop Relat Res* 2015; 473: 2578-2586.
53. Faber BG, Ebsim R, Saunders FR, Frysz M, Gregory JS, Aspden RM, et al. Cam morphology but neither acetabular dysplasia nor pincer morphology is associated with osteophytosis throughout the hip: findings from a cross-sectional study in UK Biobank. *Osteoarthritis Cartilage* 2021; 29: 1521-1529.
54. Larson CM, Sikka RS, Sardelli MC, Byrd JW, Kelly BT, Jain RK, et al. Increasing alpha angle is predictive of athletic-related "hip" and "groin" pain in collegiate National Football League prospects. *Arthroscopy* 2013; 29: 405-410.

2

Reliability and Agreement of Manual and Automated Morphological Radiographic Hip Measurements

Fleur Boel, Noortje S. Riedstra, **Jinchi Tang**, David F. Hanff, Harbeer Ahedi, Vahid Arbabi, Nigel K. Arden, Sita Bierma-Zeinstra, Michiel M.A. van Buuren, Flavia M. Cicuttini, Tim F. Cootes, Kay M. Crossley, Denise Eygendaal, David T. Felson, Willem P. Gielis, Joshua Heerey, Graeme Jones, Stefan Kluzek, Nancy E. Lane, Claudia Lindner, John A. Lynch, Joyce van Meurs, Amanda E. Nelson, Andrea Mosler, Michael C. Nevitt, Edwin H.G. Oei, Jos Runhaar, Harrie Weinans, Rintje Agricola.

ABSTRACT

Objective: To determine the reliability and agreement of manual and automated morphological measurements, and agreement in morphological diagnoses.

Methods: Thirty pelvic radiographs were randomly selected from the World COACH consortium. Manual and automated measurements of acetabular depth-width ratio (ADR), modified acetabular index (mAI), alpha angle (AA), Wiberg center edge angle (WCEA), lateral center edge angle (LCEA), extrusion index (EI), neck-shaft angle (NSA), and triangular index ratio (TIR) were performed. Bland-Altman plots and intraclass correlation coefficients (ICCs) were used to test reliability. Agreement in diagnosing acetabular dysplasia, pincer and cam morphology by manual and automated measurements was assessed using percentage agreement. Visualizations of all measurements were scored by a radiologist.

Results: The Bland-Altman plots showed no to small mean differences between automated and manual measurements for all measurements except for ADR. Intraobserver ICCs of manual measurements ranged from 0.26 (95%CI 0-0.57) for TIR to 0.95 (95%CI 0.87-0.98) for LCEA. Interobserver ICCs of manual measurements ranged from 0.43 (95%CI 0.10-0.68) for AA to 0.95 (95%CI 0.86-0.98) for LCEA. Intermethod ICCs ranged from 0.46 (95%CI 0.12-0.70) for AA to 0.89 (95%CI 0.78-0.94) for LCEA. Radiographic diagnostic agreement ranged from 47%-100% for the manual observers and 63%-96% for the automated method as assessed by the radiologist.

Conclusion: The automated algorithm performed equally well compared to manual measurement by trained observers, attesting to its reliability and efficiency in rapidly computing morphological measurements. This validated method can aid clinical practice and accelerate hip osteoarthritis research.

INTRODUCTION

There is evidence that hip morphology is a leading contributing factor to the development of hip osteoarthritis (OA)¹. Furthermore, studies have shown that specific hip morphologies, such as acetabular dysplasia (undercoverage of the femoral head by the acetabulum), pincer morphology (excessive coverage of the femoral head by the acetabulum) and cam morphology (aspherical femoral head) are associated with radiographic hip OA¹⁻⁶.

In order to quantify hip morphology, morphological measurements can be performed on pelvic anteroposterior (AP) radiographs, which are inexpensive and routinely obtained in clinical practice. Manual morphological measurements, however, are time-consuming and can be unreliable when performed by different observers⁷. Additionally, a lack of consistency exists in the current definitions for some morphological measurements⁸.

Automated morphological measurements could enhance reproducibility while facilitating rapid assessment of multiple measurements per radiograph. Automation, therefore, has the potential to aid clinical practice and allows for the quantification of hip morphology in large cohort studies. There are currently few open-access, publicly available algorithms, and those that are available are sometimes poorly described⁹⁻¹¹.

We aim to study the reliability and agreement of manual and our in-house developed, open access, automated morphological hip measurements through quantitative and qualitative assessment of both methods. This ensures that results from future studies where this automated method is applied are clinically relevant. The secondary aim was to assess the agreement in making radiographic morphological diagnoses based on manual and automated measurements.

METHODS

Participants

The Worldwide Collaboration of OsteoArthritis prediCtion of the Hip (World COACH) consortium is a global collaboration of all prospective cohort studies with available sequential pelvic or hip imaging. The included cohorts are Cohort Hip and Cohort Knee (CHECK), the Multi-center OSteoarthritis sTudy (MOST), the OsteoArthritis Initiative (OAI), the Rotterdam Study-I (RS-I), the Rotterdam Study-II (RS-II), the Rotterdam Study-III (RS-III), the Chingford Study, the Johnston County Project (JoCo), the Study

of Osteoporotic Fractures (SOF), and the Tasmanian Older Adults Cohort (TASOAC). The World COACH consortium currently counts 37,732 participants aged 42-100 (mean 65.72 years) at baseline, and 71.33 % are female individuals. The consortium profile and protocol have previously been published in detail¹². From the consortium, 30 baseline radiographs were selected proportionate to the cohort size in the consortium for qualitative and quantitative assessment of the manual and automated morphological measurements. A power analysis was performed assuming type I errors of 0.05, type II errors of 0.20, two replications, a minimally acceptable level of reliability of 0.75 and an expected level of reliability between 0.8 and 0.9, a minimum of 27 inclusions was needed. Therefore, we selected a total of 30 random radiographs for inclusion¹³. A flowchart of the radiograph selection is shown in **Figure 1**.

The baseline characteristics were: 18 females (60%), the mean age was 62.5 ± 8.6 years (range 47-78), and the mean BMI was 26.5 ± 3.9 kg/m². All included hips had no definite RHOA as defined by Kellgren and Lawrence classification, modified Croft classification or modified OA score of 0 or 1.

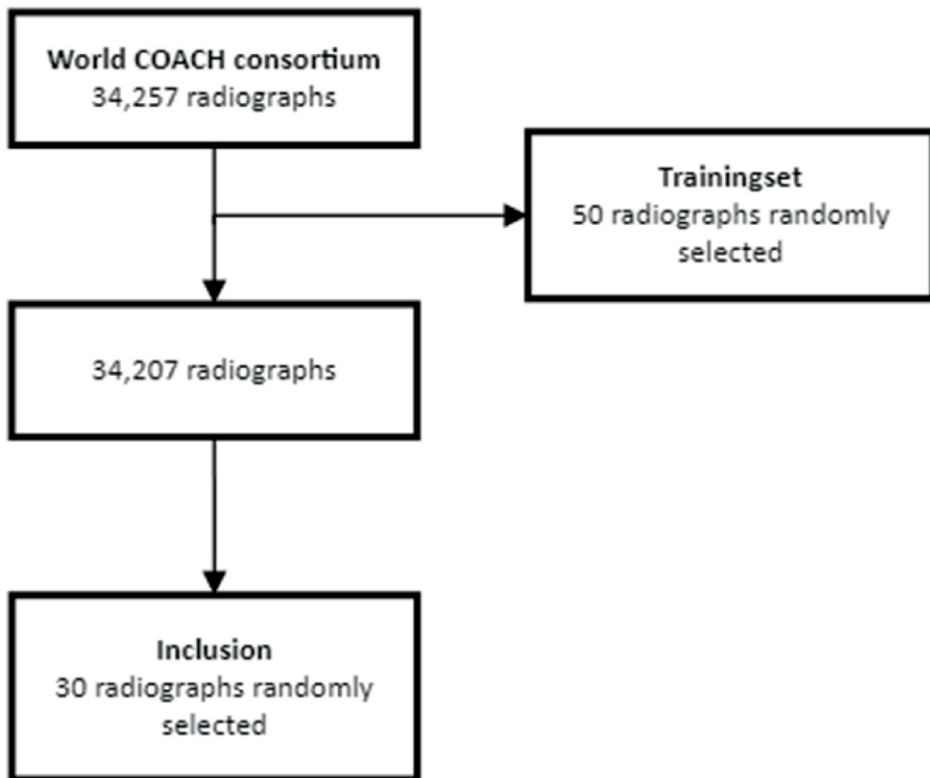


Figure 1. Flowchart of the radiograph selection.

Radiographs

The AP pelvic radiographs were obtained according to a protocol previously decided on by each cohort, and details on cohort-specific radiographic protocols can be found in the World COACH description paper¹². Seven cohorts (CHECK, MOST, OAI, RS-I, RS-II, RS-III, TASSOAC) contained weight-bearing AP pelvic radiographs. In contrast, three cohorts (the Chingford Study, JoCo, and SOF) contained supine AP pelvic radiographs.

Hip morphology and morphological measurements

Morphological measures used in this manuscript to determine acetabular dysplasia include the acetabular depth-width ratio (ADR), the modified acetabular index (mAI), the Wiberg center edge angle (WCEA), and the extrusion index (EI)¹⁴⁻¹⁶. The lateral center edge (LCEA) angle determined pincer morphology¹⁷⁻¹⁹. Cam morphology was defined by the alpha angle (AA) and the triangular index ratio (TIR)^{4, 20, 21}. The neck-shaft angle (NSA) is used to determine coxa valga and vara²². All measurements are shown in **Figure 2** and are explained in detail elsewhere²³; a brief overview, including radiological thresholds for radiographic diagnosis, is provided below.

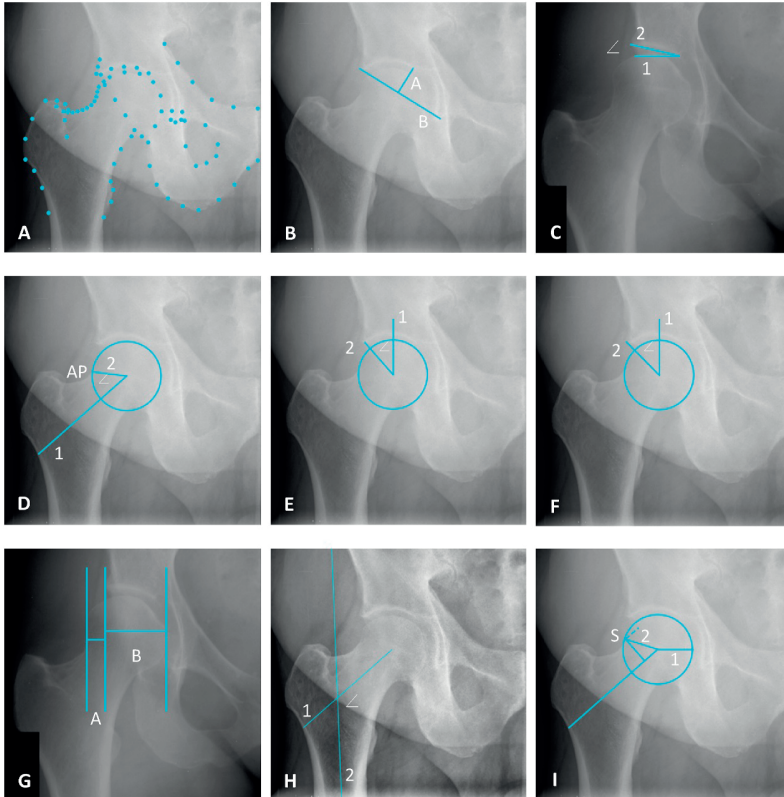


Figure 2. Definition of morphological measurements. **A:** Overview of the landmarks. **B: Acetabular depth-width ratio (ADR)** – the ratio between the acetabular depth (line A) measured from the most medial point of the acetabular sourcil to line B, and the acetabular width (line B) measured from the most lateral bony edge of the acetabulum to the most caudal point of the teardrop, $ADR = A/B \times 1000$. **C: The modified acetabular index (mAI)** – The angle between the horizontal reference line of the pelvis (HRLP) (line 1) and the line between the most lateral bony edge of the acetabulum and the most medial point of the acetabular sourcil (line 2). **D: The alpha angle (AA)** – the angle between the femoral head neck axis (line 1) and line 2 connecting the femoral head center and alpha point (AP), where the contour of the femoral head-neck junction leaves the best-fitting circle around the femoral head. **E: The Wiberg center edge angle (WCEA)** – The angle between line 1, a vertical line through the femoral head center perpendicular to the HRLP, and line 2 connecting the most lateral point of the acetabular sourcil and the femoral head center. **F: The lateral center edge angle (LCEA)** – The angle between line 1, a vertical line through the femoral head center perpendicular to the HRLP, and line 2 connecting the most lateral bony edge of the acetabulum and the femoral head center. **G: the extrusion index (EI)** – $EI = A/(A+B) \times 100\%$, where A is the distance between the most lateral point of the femoral head and the most lateral bony edge of the acetabulum, and B is the distance between the most lateral bony point of the acetabulum and the most medial point of the femoral head. **H: The neck-shaft angle** – the angle between the femoral head-neck axis (line 1) and the longitudinal axis of the femoral shaft (line 2). **I: The triangular index ratio (TIR)** – The ratio between the radius of the best-fitting circle around the femoral head (line 1) and the distance between the femoral head center and point S on the femoral head-neck junction at $0.5r$ along the femoral head-neck axis (line 2).

Acetabular depth-width ratio

The acetabular depth-width ratio (ADR) quantifies the depth of the acetabulum. The acetabular width was defined by a line from the lateral bony edge of the acetabulum to the pelvic teardrop to measure the acetabular opening. Next, the acetabular depth was defined by a line perpendicular to the acetabular width, extending from the most medial point of the sourcil (Figure 2B). The ADR is the depth ratio to the width multiplied by 1000. Acetabular dysplasia is diagnosed by an $ADR \leq 250^{24}$.

Modified acetabular index

The modified acetabular index (mAI) measures the acetabular roof's inclination. The original acetabular index is applied to hips with an open triradiate cartilage; a modified version was created to obtain this measurement in adults. The mAI measures the angle between the line from the medial sourcil to the lateral bony edge of the acetabulum and the horizontal reference line of the pelvis (Figure 2C). Acetabular dysplasia is defined by $mAI \geq 13^\circ$, acetabular overcoverage is defined by $mAI \leq 3^{o24, 25}$.

Wiberg center edge angle

The degrees of weight-bearing coverage of the femoral head by the acetabulum is measured by the Wiberg center edge angle (WCEA)²⁴. The WCEA is formed by a vertical line through the center of the femoral head, perpendicular to the horizontal reference line of the pelvis, and a second line from the center of the femoral head to the most lateral weight bearing part of the sourcil (Figure 2E). Although the threshold has been debated, acetabular dysplasia is generally defined by a $WCEA \leq 25^\circ$ in prospective studies^{1, 11, 26, 27}.

Lateral center edge angle

The degrees of bony coverage of the femoral head by the acetabulum is measured by the lateral center edge angle (LCEA)^{1, 4, 28}. The LCEA is formed by a vertical line through the center of the femoral head, perpendicular to the horizontal reference line of the pelvis, and a second line from the center of the femoral head to the most lateral bony part of the acetabulum (Figure 2F). Pincer morphology is generally defined by an $LCEA \geq 40^\circ$ in prospective studies^{1, 17}.

Extrusion index

The extrusion index (EI) quantifies bony femoral head coverage by the acetabulum. The EI is obtained by dividing the horizontal distance of the lateral uncovered femoral head by the total width of the femoral head and multiplying that by 100 to express it as a percentage (Figure 2G). Acetabular dysplasia is defined by an $EI \geq 25\%^{25}$.

Alpha angle

The alpha angle (AA) is the most commonly used measurement to define cam morphology and quantify the sphericity of the femoral head-neck junction. The AA is constructed by two lines, one from the femoral head center through the middle of the femoral neck, the femoral head-neck axis, and a second line from the center of the femoral head through the point where the contour of the femoral head-neck junction extends from the best fitting circle around the femoral head (Figure 2D)²⁹. An AA $\geq 60^\circ$ threshold is commonly used in literature to define cam morphology²¹.

Triangular index ratio

The triangular index ratio (TIR) measures femoral asphericity and defines cam morphology. Compared to the alpha angle, the TIR is measured at a specific point on the femoral head neck junction. It is the ratio between the radius of the best-fitting circle around the femoral head and the distance between the femoral head center and the femoral head-neck junction at 0.5r along the head-neck axis (Figure 2I). When, for instance, the resultant distance at 0.5r along the axis of the femoral neck at the head-neck junction exceeds the radius of the femoral head, this indicates that, the femoral head is aspherical, possibly indicating the presence of cam morphology²⁰.

Neck-shaft angle

The neck-shaft angle (NSA) is the angle between the longitudinal axis of the femoral shaft and the femoral head-neck axis (Figure 2H). It has been hypothesized that hips with a more varus neck orientation experience increased subchondral bone stress and, therefore, increased risk of degeneration in individuals with cam morphology³⁰. Conversely, a relative increase in femoral neck shaft angle combined with acetabular undercoverage also leads to RHOA³⁰. Coxa valga is generally defined by NSA $> 140^\circ$, and coxa vara by NSA $< 120^\circ$ ³¹.

Automated morphological measurements

The bony outline of the proximal femur and acetabulum were annotated automatically on all AP pelvic radiographs with landmarks (Figure 2A) (BoneFinder® software (www.bonefinder.com;The University of Manchester, UK)³². The protocol for the 80 landmarks used in this automated hip shape annotation can be found in supplementary material 1. The landmarks were used to automatically derive the hip morphology measurements using in house-built Python-based software²³. This software is a pipeline to automatically determine radiographic measurements based on radiographic landmarks. The radiographic measurements are performed in accordance to the definitions provided in this manuscript²³. To assess the impact of automated landmark placement on the morphological measurements, a second set of landmarks was cre-

ated on the same set of radiographs where all landmarks were manually assessed and adjusted, if necessary, after which the morphological measurements were derived again.

Manual morphological measurements

Two researchers (JT and NSR) were trained in performing manual assessment of all previously described morphological measurements. A random set of 50 radiographs from the World COACH consortium was used to train the researchers. Radiographs were selected at random from the consortium such that the number of radiographs chosen from each cohort was proportional to the total number of radiographs available in that cohort. After all measurements were performed on all 50 radiographs by both researchers, measurements were compared under supervision of an experienced orthopedic surgeon (RA), and inconsistencies were discussed. This was repeated 3 times with the same radiographs until both researchers were proficient in performing measurements. Next, the two trained researchers (JT and NSR) performed on the 30 randomly selected radiographs from the World COACH consortium, with the same proportionality as previously mentioned. Information on whether the hips had morphological variations, hip OA, or clinical symptoms was blinded to all researchers. The measurements were repeated on the same radiographs approximately four weeks later. The radiographs were presented to the readers in a different random order each time. Measurements were performed using the DICOM viewer (Synedra View, Version 21.0.0, Synedra Information Technologies). All radiographs were presented in a blinded fashion and random order to the observers. The mean of the individual observers' first and second round of measurements was used for interobserver analyses. The mean of all four manual measurements was used as the reference standard to which the automated method was compared.

Agreement

The agreement within the two rounds of manual measurements for each observer and between observers, and between methods with regard to radiographic diagnoses solely based on morphological measurements of acetabular dysplasia, pincer and cam morphology, and coxa vara and valga was tested.

Qualitative assessment of morphological measurements

A musculoskeletal radiologist (DFH) visually inspected the second round of manual morphological measurements and the automated measurements based on the unadjusted landmarks and qualitatively rated the measurements as acceptable or unacceptable. "Acceptable" is if the radiologist would measure the same morphological measurements based on the landmark points. "Unacceptable" is if the radiologist

would perform the measurements differently. This was done in order to ensure the automated measurements were correct from a clinical perspective of an MSK radiologist. In order to blind the radiologist to which method was used, Printscreens of the manual and automated measurements were visually presented in a way which made it impossible to distinguish between methods and in a random order. Printscreens were used because automated measurements were obtained in Python and manual measurements in Synedra Viewer, which would distinguish between methods. Additionally, this ensured that our reference standard of manual measurements were also approved by the MSK radiologist. An example of the ADR is shown in supplementary material 2. No additional information was disclosed about whether the measurements were performed manually or obtained by the automated method.

Statistical analysis

The agreement between the manual observers and the agreement between the automated and manual methods was visualized using Bland-Altman plots for each morphological measurement. In this study, in order to distinguish between random and systematic error, a mean difference larger than 2.5° was defined as a systematic error for mAI, AA, WCEA, LCEA and NSA. A mean difference larger than 1% of the measurement was defined as a systematic error for ADR, EI and TIR. These thresholds are based on expert agreement. Outliers identified by the Bland-Altman plots were visually inspected to analyze whether consistencies in measurement error occurred.

Intraclass correlation coefficients (ICCs) were used to test reliability and were reported with 95% confidence intervals (CI). Intraobserver reliability was tested with a 2-way mixed effects model, single rater, absolute agreement ICC. Interobserver reliability between manual observers and between the automated determination of the measurements on the manually adjusted and unadjusted landmarks was tested with a 2-way random-effects model, single rater, absolute agreement ICC. Lastly, inter-method reliability between the mean of all manual and automated measurements on manually adjusted and unadjusted landmarks was tested with a 2-way mixed-effects model, single rater, absolute agreement ICC. ICCs were rated as poor (<0.50), moderate ($0.50-0.75$), good ($0.76-0.90$), or excellent (>0.90)³³.

The agreement within and between observers, and between methods with regard to radiographic diagnoses was tested using percentage agreement. Based on the qualitative rating of the measurements by the musculoskeletal radiologist, the percentage of acceptable measurements was determined for each morphological measurement by the two manual observers and the automated method, respectively. The percent-

age of acceptable measurements was rated as poor (<50%), moderate (50-70%), good (71-90%), or excellent (>90%).

Statistical analyses were performed using R statistical software (v4.1.0; R Core Team 2021). The ggplot2-package in R was used to create Bland-Altman plots. The irr-package in R was used to calculate the ICCs and the percentage agreement³⁴.

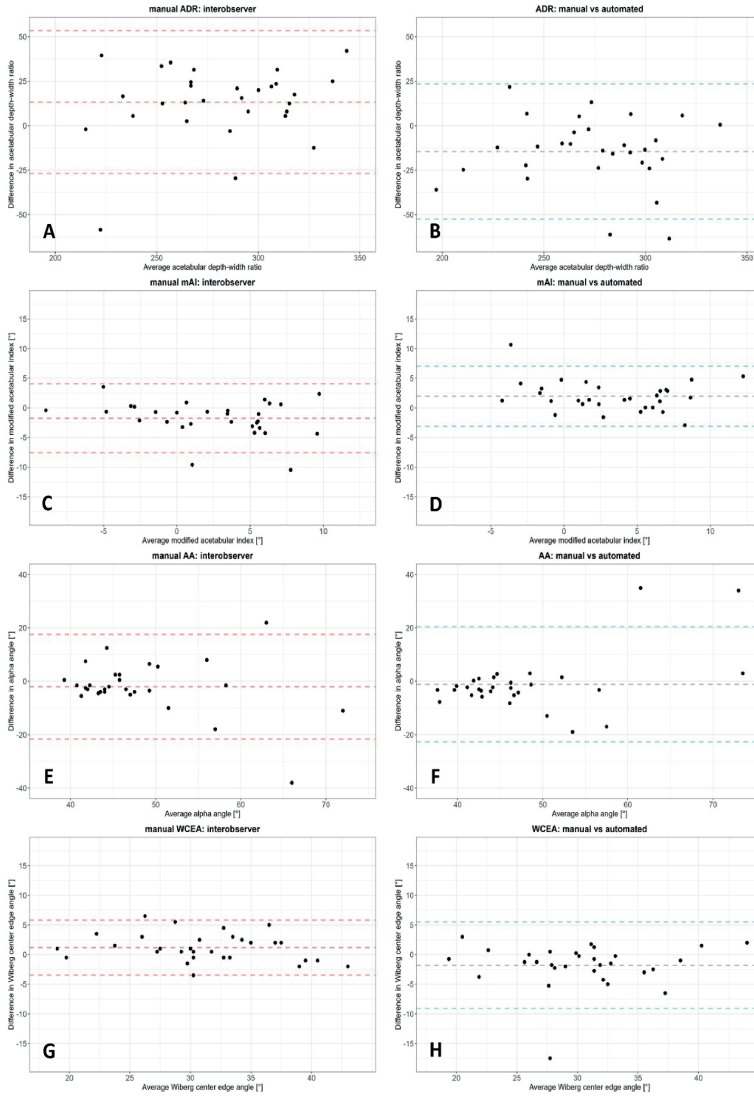
RESULTS

All morphological measurements could automatically be performed in all 30 hips, except for NSA, which could not be performed on two images as too little of the femoral shaft was depicted on the radiograph.

Agreement

The Bland-Altman plots for agreement between the two observers and the agreement between the manual and automated measurements based on unadjusted landmarks are presented in **Figure 3**, and the corresponding mean difference and limits of agreement are summarized in **Table 1**. The AA, WCEA, LCEA, mAI, and EI showed no to small mean differences between automated and manual measurements. However, both the interobserver and inter-method agreement of ADR and the interobserver NSA and TIR showed a bias. Observer 1 consistently measured ADR and TIR higher than observer 2, while the opposite was observed for NSA. When comparing the manual and automated ADR, the mean of the manual measurements was consistently higher than the automated measurement. The intermethod limits of agreement were mainly smaller or similar to the interobserver limits of agreement for all morphological measurements except for WCEA and LCEA.

The intermethod limits of agreement were mainly smaller or similar to the interobserver limits of agreement for all morphological measurements except for WCEA and LCEA.



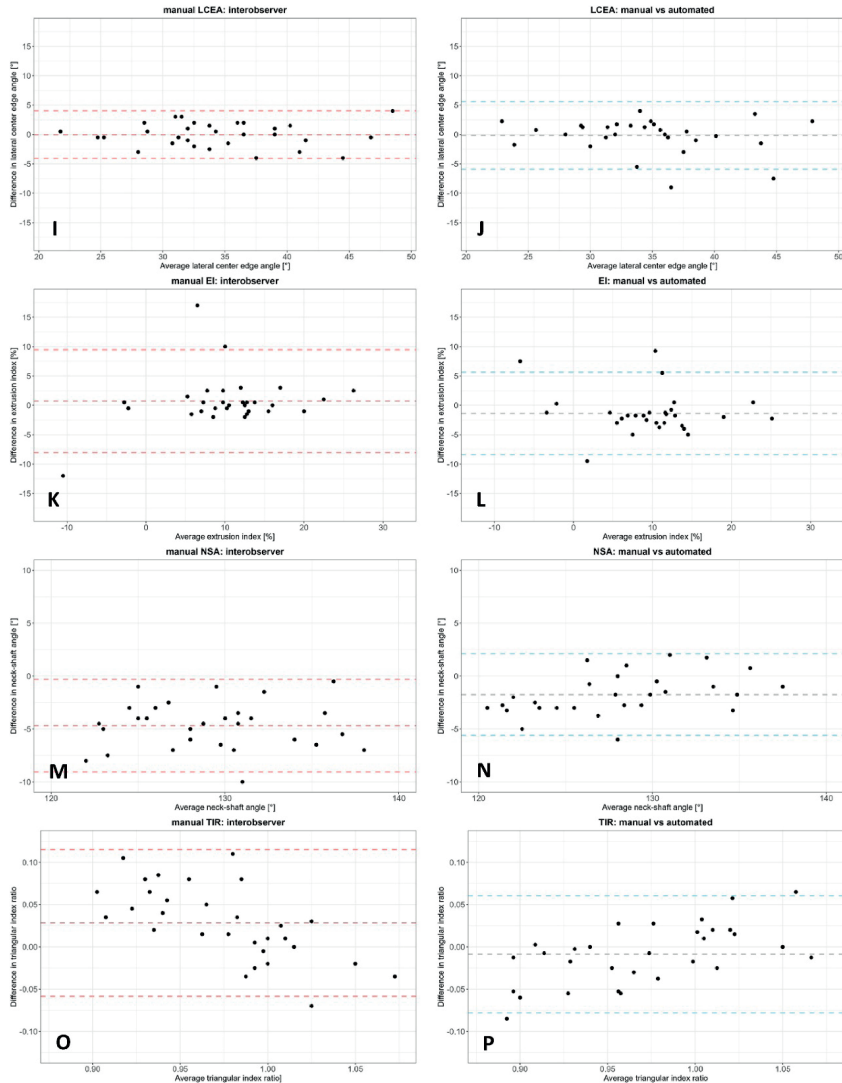


Figure 3. Bland-Altman plots of the morphological measurements. **A:** The acetabular depth-width ratio (ADR) – observer 1 vs observer 2. **B:** ADR – manual vs automated measurements based on unadjusted landmarks. **C:** The modified acetabular index (mAI) – observer 1 vs observer 2. **D:** mAI – manual vs automated measurements based on unadjusted landmarks. **E:** The alpha angle (AA) – observer 1 vs observer 2. **F:** AA – manual vs automated measurements based on unadjusted landmarks. **G:** The Wiberg center edge angle (WCEA) – observer 1 vs observer 2. **H:** WCEA – manual vs automated measurements based on unadjusted landmarks. **I:** The lateral center edge angle (LCEA) – observer 1 vs observer 2. **J:** LCEA – manual vs automated measurements based on unadjusted landmarks. **K:** The extrusion index (EI) – observer 1 vs observer 2. **L:** EI – manual vs automated measurements based on unadjusted landmarks. **M:** The neck-shaft angle (NSA) – observer 1 vs observer 2. **N:** NSA – manual vs automated measurements based on unadjusted landmarks. **O:** The triangular index ratio (TIR) – observer 1 vs observer 2. **P:** TIR – manual vs automated measurements based on unadjusted landmarks.

Table 1. Summary of mean interobserver and intermethod bias and limits of agreement of manual morphological measurements and manual vs automated morphological measurements based on the unadjusted landmarks.

Measurement	Manual		Manual vs Automated	
	Interobserver bias (mean)	Interobserver limits of agreement	Intermethod bias (mean)	Intermethod limits of agreement
Acetabular depth-width ratio	13	-27 to 53	-15	-52 to 13
Modified acetabular index [°]	-1.8	-7.6 to 4.1	2.0	-3.1 to 7.0
Alpha angle [°]	-2	-22 to 18	-1	-23 to 20
Wiberg center edge angle [°]	1	-3 to 6	-2	-9 to 5
Lateral center edge angle [°]	0	-4 to 4	0	-6 to 6
Extrusion index [%]	1	-8 to 9	-1	-8 to 5
Neck-shaft angle [°]	-5	-9 to 0	-2*	-6 to 2*
Triangular index ratio	0.028	-0.058 to 0.115	-0.009	-0.078 to 0.061

*Bland-Altman interobserver and intermethod bias (mean difference) and limits of agreement, n=30. *Based on 28 hips.*

Reliability

The intra- and interobserver and intermethod reliability defined by ICCs for all measurements are shown in **Table 2**. The intermethod reliability between the manual and automated measurements based on both the manually adjusted and unadjusted landmarks was comparable to or better than the interobserver reliability, except for WCEA in which case the manual measurements were more reliable. Additionally, we found that manually adjusted landmarks impacted the ADR and mAI most. This led to lower reliability between manually adjusted compared to unadjusted automated ADR and mAI measurements. These measurements are calculated based on only on few specific landmarks. Conversely, measurements that do not rely on few specific landmarks from the point set like AA, NSA and TIR, showed excellent reliability between the automated measurements performed using the adjusted vs unadjusted landmarks.

Table 2. Intra- and interobserver reliability between manual measurements by observer 1 and observer 2, interobserver reliability between adjusted and unadjusted landmarks and intermethod reliability between manual and automated morphological measurements

Empty Cell	Manual		Automated		Manual vs automated	
	Observer 1	Observer 2	Observer 1 vs observer 2	Adjusted vs unadjusted landmarks	Unadjusted landmarks	Adjusted landmarks
Measurement	Intraobserver ICC (95% CI)	Intraobserver ICC (95% CI)	Interobserver ICC (95% CI)	Interobserver ICC (95% CI)	Intermethod ICC (95% CI)	Intermethod ICC (95% CI)
Acetabular depth-width ratio	0.67 (0.41 – 0.82)	0.89 (0.77 – 0.94)	0.79 (0.49 – 0.91)	0.70 (0.47 – 0.85)	0.78 (0.39 – 0.91)	0.80 (0.60 – 0.90)
Modified Acetabular Index	0.65 (0.36 – 0.82)	0.82 (0.61 – 0.91)	0.77 (0.48 – 0.89)	0.83 (0.67 – 0.91)	0.75 (0.34 – 0.90)	0.82 (0.30 – 0.94)
Alpha Angle	0.36 (0.01 – 0.63)	0.67 (0.42 – 0.83)	0.43 (0.10 – 0.68)	0.98 (0.97 – 0.99)	0.46 (0.12 – 0.70)	0.5 (0.17 – 0.73)
Wiberg center edge angle	0.87 (0.74 – 0.93)	0.94 (0.88 – 0.97)	0.91 (0.78 – 0.96)	0.94 (0.88 – 0.97)	0.77 (0.54 – 0.89)	0.88 (0.70 – 0.95)
Lateral center edge angle	0.89 (0.78 – 0.95)	0.95 (0.87 – 0.98)	0.95 (0.86 – 0.98)	0.91 (0.8 – 0.96)	0.89 (0.78 – 0.94)	0.95 (0.88 – 0.98)
Extrusion Index	0.74 (0.51 – 0.87)	0.80 (0.51 – 0.91)	0.83 (0.67 – 0.91)	0.94 (0.87 – 0.97)	0.86 (0.71 – 0.93)	0.88 (0.65 – 0.95)
Neck Shaft Angle	0.89 (0.78 – 0.94)	0.86 (0.73 – 0.93)	0.58 (0 – 0.87)	0.995 (0.989 – 0.998) *	0.86 (0.44 – 0.95) *	0.88 (0.51 – 0.96) *
Triangular Index Ratio	0.26 (0 – 0.57)	0.49 (0.12 – 0.73)	0.99 (0.98 – 0.996)		0.78 (0.59 – 0.89)	0.79 (0.61 – 0.89)

*Intraclass correlation coefficients (ICC) of intra- and interobserver, and intermethod reliability of the morphological measurements. ICCs are presented with 95% confidence interval (CI). The mean of all four manual measurements was used as the reference standard for the intermethod measurements. Intraobserver reliability was tested with a 2-way mixed-effects model, single rater, absolute agreement ICC. Interobserver reliability between both manual observers, as well as between the automated determination on adjusted and unadjusted landmarks, was tested with a 2-way random-effects model, single rater, absolute agreement ICC. Intermethod reliability was tested with a 2-ways mixed-effects model, single rater, absolute agreement ICC. All ICCs were measured using 30 hips. *ICCs measured using 28 hips. Interpretation: poor (<0.50), moderate (0.50-0.75), good (0.76-0.90), or excellent (>0.90).*

Radiographic diagnostic agreement

Percentage agreement in radiographic diagnosis based on morphological measurements is summarized in **Table 3**. The intermethod radiographic diagnostic agreement was better than or similar to the interobserver radiographic diagnostic agreement. Except for the radiographic diagnostic agreement of dysplasia based on mAI of the manual versus automated measurements based on the manually adjusted landmarks.

Table 3. Prevalence and diagnostic intraobserver and interobserver agreement between observer 1 and observer 2, interobserver agreement between adjusted and unadjusted automated measurements, and intermethod agreement.

Empty Cell	Manual		Observer 2		Observer 1 vs Observer 2		Automated		Manual vs automated		Adjusted landmarks	
	Observer 1	Observer 2	Intraobserver percent agreement	Intraobserver percent agreement	Interobserver percent agreement	Interobserver percent agreement	Adjusted vs unadjusted landmarks	Prevalence	Reference standard	Prevalence	Unadjusted landmarks	Adjusted landmarks
Measurement	Intraobserver percent agreement	Intraobserver percent agreement	Intraobserver percent agreement	Intraobserver percent agreement	Interobserver percent agreement	Interobserver percent agreement	Adjusted vs unadjusted landmarks	Prevalence	Reference standard	Prevalence	Unadjusted landmarks	Adjusted landmarks
Acetabular depth-width ratio ≤ 250	90.0	83.3	86.7	93.3	90.0	96.7	16.7%	26.7%	90.0	90.0	90.0	90.0
Modified acetabular Index $\geq 13^\circ$	96.7	96.7	96.7	90.0	90.0	96.7	0%	3.3%	96.7	96.7	86.7	86.7
Alpha Angle $\geq 60^\circ$	90.0	90.0	86.7	96.7	96.7	96.7	10.0%	10.0%	86.7	86.7	83.3	83.3
Wiberg center edge angle $\leq 25^\circ$	100.0	100.0	93.3	90.0	93.3	90.0	13.3%	23.3%	96.7	96.7	93.3	93.3
Lateral center edge angle $\geq 40^\circ$	90	93.3	93.3	96.7	96.7	96.7	20.0%	16.7%	96.7	96.7	100	100
Extrusion Index $\geq 25\%$	96.7	96.7	100	100	100	100	0%	0%	100	100	100	100
Neck Shaft Angle $<120^\circ$ & $>140^\circ$	90	96.7	90	96.7	90	96.7	$<120^\circ: 0\%$ $>140^\circ: 0\%$	$<120^\circ: 3.3\%$ $>140^\circ: 0\%$	96.7	96.7	100	100

The reference standard consists of the mean of all manual measurements. Intermethod percent agreement was determined using the reference standard. n = 30.

Qualitative assessment

The results of the qualitative assessment as performed by the MSK radiologist are presented in **Table 4**. The majority of automated measurements were deemed acceptable by the musculoskeletal radiologist. The percentage of acceptable measurements was moderate to excellent for all measurements, except for the EI measurements by observer 2.

Table 4. The qualitative assessment of the morphological measurements

Measurement	Manual		Automated
	Observer 1	Observer 2	Unadjusted landmarks
Acetabular depth-width ratio	77	80	73
Modified Acetabular Index	70	53	70
Alpha Angle	93	90	77
Wiberg center edge angle	73	80	63
Lateral center edge angle	70	90	80
Extrusion Index	53	47	63
Neck Shaft Angle	93	100	96*
Triangular Index Ratio	63	100	73

*Percentage of acceptable measurements. Qualitative assessment was performed on 30 hips. *Based on only 28 hips. Interpretation: poor (<50%), moderate (50-70%), good (71-90%), or excellent (>90%).*

DISCUSSION

This study investigated the agreement and reliability of manual and automated morphological measurements including ADR, mAI, AA, WCEA, LCEA, EI, NSA, and TIR on AP pelvic radiographs. The presented algorithm performed equally well compared to current best practice of manual measurement by trained readers, attesting to its reliability and efficiency in rapidly computing radiological measurements on an AP pelvic radiograph.

The reported intra- and interobserver reliability of morphological measurements varies in literature. The reported ICCs in the present study were compared to the reliability of various morphological measurements in literature. The ICCs reported in literature for the Wiberg and lateral CEA (ICC= 0.7 (95% CI 0.58-0.86) to 0.98 (CI 0.97–0.99)^{11, 33, 35-37}, the NSA (ICC=0.58 (0.31-0.76) to 0.98 (0.95-0.99)¹¹, the mAI (or Tönnis angle) (ICC=0.71 (95% CI 0.45-0.83) to 0.92 (95% CI 0.85-0.95)^{33, 35, 38}, the EI (ICC= 0.68 (0.57-0.79) to 0.98 (no CI reported)^{33, 35-37}, and the ADR (ICC= 0.62 to 0.84^{15, 37, 38}, are similar to the ICCs found in our study. The reported reliability in literature for the AA (ICC= 0.78 (95% CI 0.61-0.87) to 0.99 (no CI reported)³⁹⁻⁴¹, is higher than observed in the present study. No reliability has been reported for the TIR, although one study did report on the triangular index height in 10 individuals ($\kappa = 0.74-0.78$)³³.

In terms of reliability and agreement in the current study, the AA showed the worst reliability in the manual method between and within observers, as well as in terms of intermethod reliability. The AA also showed large limits of agreement in the Bland-Altman plots and erratic behavior in the higher AA values (representing cam hips). These results are likely caused by small differences in femoral head circle fit, which may cause large measurement variation due to movement of the alpha point (Fig. 3). Faber et al. showed similar outliers and erratic behavior within the Bland-Altman analysis when comparing manual and automated AA measurements⁹. Similar results, although less extreme, were found for TIR, as expected since this measurement is also largely dependent on the circle fit. However, the erratic behavior observed in the AA Bland-Altman plots in hips with cam morphology is absent in the TIR Bland-Altman plots. This may be caused by the fact that compared to the location of the alpha point, the location of point S (Fig. 2I) is less influenced by the best-fitting circle around the femoral head.

ADR and mAI are two measurements which are calculated based on only two to three landmarks and, therefore highly dependent on correct landmarks recognition and placement. This is reflected in similar reliability and limits of agreement for the intra-

and interobserver, and intermethod comparisons. The outliers in these measurements were all caused by different landmarks recognition and placement of both the most lateral bony edge of the acetabulum and the most medial point of the weight-bearing sourcil. Additionally, we found that the mean of the manual measurements by the trained researchers was consistently higher than the automated measurement, implying that we may under diagnose acetabular dysplasia based on manual ADR measurements. Alternatively, it may also be the case that the medial point of the ADR on the sourcil is difficult to identify for the automated measurement. This may also influence the automated ADR.

The correct identification of the most lateral bony edge of the acetabulum also influenced the LCEA and EI measurements. The reliability was good to excellent for all analyses, and the limits of agreement were similar between the interobserver and intermethod analyses.

The WCEA, as determined using the automated method, was slightly worse than the LCEA when comparing the automated method to manual measurements. This is likely due to more difficult assessment of the sourcil, than the more distinct lateral bony acetabular rim. This is also observed in literature with higher reliability for LCEA reported compared to WCEA^{32-35, 37}. Overall, this landmark needed more adjustment than the most lateral bony part of the acetabulum during the manual assessment of landmarks placement. This was reflected in the higher reliability of the manual versus automated measurement when the WCEA was performed based on the manually adjusted landmarks.

The majority of manual measurements were deemed acceptable by the musculoskeletal radiologist. This implies that the reported manual measurement ICCs represent clinically acceptable reliability. In terms of automated measurements, we can conclude that the automated ADR, mAI, AA, LCEA, NSA and TIR measurements are valid in a clinical setting and can be applied to establish radiographic morphological hip diagnoses. According to our study, performance of manual as well as automated EI measurements does not reach the threshold for good agreement. We hypothesize that in case of less sphericity of the femoral head, the identification of the most lateral point of the femoral head becomes difficult leading to unreliability in the measurement. As there are other measurements that quantify acetabular coverage, these may be more appropriate in a clinical setting to study hip morphology.

Using automated morphological measurements may advance research and have important clinical implications. First, automated measurements may improve accuracy

and consistency in morphological measurements reported in literature. Measurement variability and bias could be reduced dramatically if all measurements are performed uniformly, allowing for comparison of results across studies. This holds especially true in terms of the femoral head circle fit, which is essential in many morphological measurements. The present automated method is published open-access, which promotes collaboration in future hip (OA) studies. While the method is still reliant on correct landmark identification, this was also automated to achieve more consistency and speed. This method can be applied in future studies to study whether these measurements are associated with clinical outcomes such as symptomatic hip OA. The automated method was tested on supine and standing pelvic radiographs from various cohorts in the World COACH consortium, potentially making the results more generalizable to a larger population. Furthermore, the automated method can improve efficiency by accommodating the collection of large amounts of morphological data. This will allow researchers to carry out studies with increased statistical power, advancing our understanding of hip morphology as a risk factor for hip OA.

No gold standard is available for these morphological measurements, so we extensively trained researchers to obtain measurements which could be used as a reference standard. We found order to ensure that these measurements resemble clinical practice, an MSK radiologist visually inspected all manual and automated measurements. Secondly, it should be kept in mind that this study includes a rather small set of 30 hips. A larger dataset would likely show increased variation in hip morphology and therefore provide a more robust assessment of the described methods. Furthermore, as the participants from the World COACH consortium are either from the general population or from a population selected based on having symptoms or risk factors for hip OA, the hips are a representation of the normal population. Therefore, gross bony deformations as seen in hospital populations are underrepresented in the World COACH consortium and results from the automated measures should be validated in this population first. All thresholds used to define radiographic morphological diagnoses are based on literature, but what the “right” threshold is remains unknown⁴².

With regards to the qualitative assessment, the radiologist evaluated printscreens of measurements, which made it impossible to adjust contrast setting on the images as preferred by the radiologist. As a result of this, the measurements that were impossible to visually inspect were labeled as unacceptable, although in reality they may have been correct. This issue may be avoided in the future by using DICOM images on PACS viewer rather than printscreens of radiographs. Another limitation of this study is that all morphological measurements were performed on AP pelvic radiographs although it is known that some morphological diagnoses require additional radiographic views

to assess hip morphology^{18, 25, 33, 37}. Furthermore, acetabular morphology is influenced by pelvic orientation, which can vary significantly in terms of tilt⁴². This provides a future opportunity to also develop automated measurements in various radiographic views.

In conclusion, automated morphological measurements are a reliable and reproducible method to quantify the ADR, WCEA, LCEA mAI, TIR, EI and NSA. This method makes morphological hip measurements viable in large population studies, as it enables reliable analysis of large amounts of data. Additionally, it may be a useful tool in clinical practice, as it reduces reader bias and the landmarks allow for insightful measurements. Access to fast, externally validated, reliable methods to quantify hip morphology may aid in the quest for modifiable risk factors for hip OA in future studies.

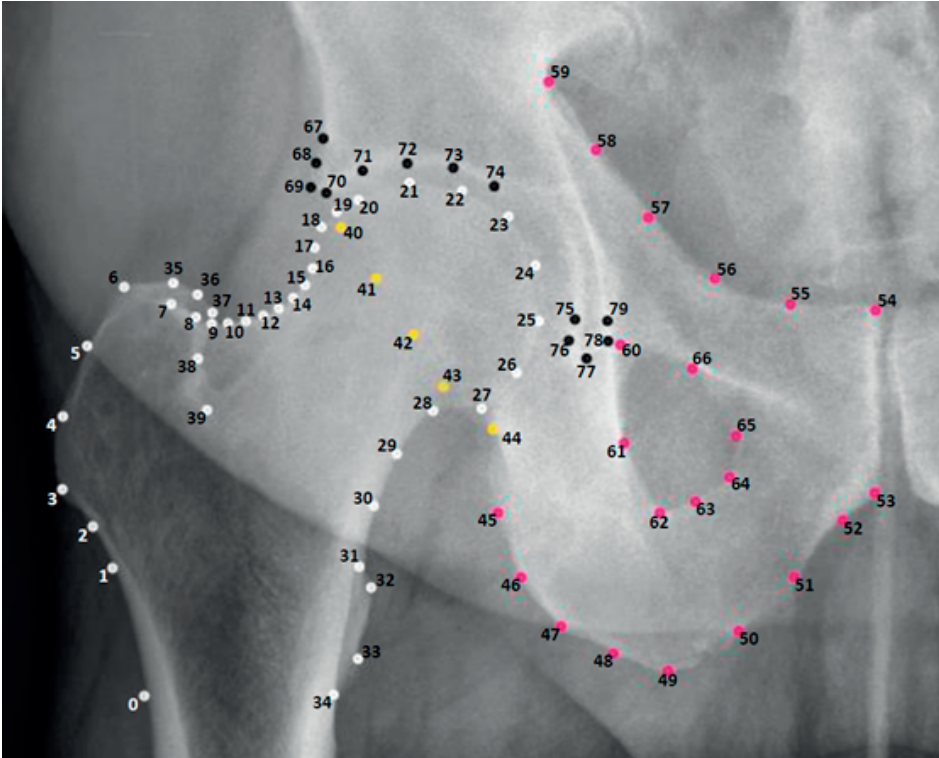
REFERENCES

1. Casartelli NC, Maffiuletti NA, Valenzuela PL, Grassi A, Ferrari E, van Buuren MMA, et al. Is hip morphology a risk factor for developing hip osteoarthritis? A systematic review with meta-analysis. *Osteoarthritis Cartilage* 2021; 29: 1252-1264.
2. Harris-Hayes M, Royer NK. Relationship of acetabular dysplasia and femoroacetabular impingement to hip osteoarthritis: a focused review. *PM R* 2011; 3: 1055-1067 e1051.
3. Thomas G, Kiran A, Batra R, Hart D, Spector T, Taylor A, et al. The association between hip morphology and end-stage osteoarthritis at 12-year follow up. *Osteoarthritis and Cartilage* 2012; 20: S204.
4. van Klij P, Heerey J, Waarsing JH, Agricola R. The Prevalence of Cam and Pincer Morphology and Its Association With Development of Hip Osteoarthritis. *J Orthop Sports Phys Ther* 2018; 48: 230-238.
5. Hoch A, Schenk P, Jentsch T, Rahm S, Zingg PO. FAI morphology increases the risk for osteoarthritis in young people with a minimum follow-up of 25 years. *Arch Orthop Trauma Surg* 2021; 141: 1175-1181.
6. Beck M, Kalhor M, Leunig M, Ganz R. Hip morphology influences the pattern of damage to the acetabular cartilage: femoroacetabular impingement as a cause of early osteoarthritis of the hip. *J Bone Joint Surg Br* 2005; 87: 1012-1018.
7. Hanson JA, Kapron AL, Swenson KM, Maak TG, Peters CL, Aoki SK. Discrepancies in measuring acetabular coverage: revisiting the anterior and lateral center edge angles. *J Hip Preserv Surg* 2015; 2: 280-286.
8. Griffin DR, Dickenson EJ, O'Donnell J, Agricola R, Awan T, Beck M, et al. The Warwick Agreement on femoroacetabular impingement syndrome (FAI syndrome): an international consensus statement. *Br J Sports Med* 2016; 50: 1169-1176.
9. Faber BG, Ebsim R, Saunders FR, Frysz M, Davey Smith G, Cootes T, et al. Deriving alpha angle from anterior-posterior dual-energy x-ray absorptiometry scans: an automated and validated approach. *Wellcome Open Res* 2021; 6: 60.
10. Archer H, Reine S, Alshaihsalama A, Wells J, Kohli A, Vazquez L, et al. Artificial intelligence-generated hip radiological measurements are fast and adequate for reliable assessment of hip dysplasia : an external validation study. *Bone Jt Open* 2022; 3: 877-884.
11. Schwarz GM, Simon S, Mitterer JA, Huber S, Frank BJ, Aichmair A, et al. Can an artificial intelligence powered software reliably assess pelvic radiographs? *Int Orthop* 2023; 47: 945-953.
12. van Buuren MMA, Riedstra NS, van den Berg MA, Boel F, Ahedi H, Arbabi V, et al. Cohort profile: Worldwide Collaboration on OsteoArthritis prediCtion for the Hip (World COACH) - an international consortium of prospective cohort studies with individual participant data on hip osteoarthritis. *BMJ Open* 2024; 14: e077907.
13. Walter SD, Eliasziw M, Donner A. Sample size and optimal designs for reliability studies. *Stat Med* 1998; 17: 101-110.
14. Umer M, Thambyah A, Tan WT, Das De S. Acetabular morphometry for determining hip dysplasia in the Singaporean population. *J Orthop Surg (Hong Kong)* 2006; 14: 27-31.
15. Engesaeter IO, Laborie LB, Lehmann TG, Sera F, Fevang J, Pedersen D, et al. Radiological findings for hip dysplasia at skeletal maturity. Validation of digital and manual measurement techniques. *Skeletal Radiol* 2012; 41: 775-785.

16. Engesaeter IO, Laborie LB, Lehmann TG, Fevang JM, Lie SA, Engesaeter LB, et al. Prevalence of radiographic findings associated with hip dysplasia in a population-based cohort of 2081 19-year-old Norwegians. *Bone Joint J* 2013; 95-B: 279-285.
17. Agricola R, Heijboer MP, Roze RH, Reijman M, Bierma-Zeinstra SM, Verhaar JA, et al. Pincer deformity does not lead to osteoarthritis of the hip whereas acetabular dysplasia does: acetabular coverage and development of osteoarthritis in a nationwide prospective cohort study (CHECK). *Osteoarthritis Cartilage* 2013; 21: 1514-1521.
18. Saberi Hosnijeh F, Zuiderwijk ME, Versteeg M, Smeele HT, Hofman A, Uitterlinden AG, et al. Cam Deformity and Acetabular Dysplasia as Risk Factors for Hip Osteoarthritis. *Arthritis Rheumatol* 2017; 69: 86-93.
19. Faber BG, Ebsim R, Saunders FR, Frysz M, Gregory JS, Aspden RM, et al. Cam morphology but neither acetabular dysplasia nor pincer morphology is associated with osteophytosis throughout the hip: findings from a cross-sectional study in UK Biobank. *Osteoarthritis Cartilage* 2021; 29: 1521-1529.
20. Gosvig KK, Jacobsen S, Palm H, Sonne-Holm S, Magnusson E. A new radiological index for assessing asphericity of the femoral head in cam impingement. *J Bone Joint Surg Br* 2007; 89: 1309-1316.
21. van Klij P, Reiman MP, Waarsing JH, Reijman M, Bramer WM, Verhaar JAN, et al. Classifying Cam Morphology by the Alpha Angle: A Systematic Review on Threshold Values. *Orthop J Sports Med* 2020; 8: 2325967120938312.
22. Ramkumar PN, Karnuta JM, Haeberle HS, Sullivan SW, Nawabi DH, Ranawat AS, et al. Radiographic Indices Are Not Predictive of Clinical Outcomes Among 1735 Patients Indicated for Hip Arthroscopic Surgery: A Machine Learning Analysis. *Am J Sports Med* 2020; 48: 2910-2918.
23. Boel F, de Vos-Jakobs S, Riedstra NS, Lindner C, Runhaar J, Bierma-Zeinstra SMA, et al. Automated radiographic hip morphology measurements: An open-access method. *Osteoarthr Imaging* 2024; 4: 100181.
24. Wilkin GP, Ibrahim MM, Smit KM, Beaulé PE. A Contemporary Definition of Hip Dysplasia and Structural Instability: Toward a Comprehensive Classification for Acetabular Dysplasia. *J Arthroplasty* 2017; 32: S20-S27.
25. Tannast M, Hanke MS, Zheng G, Steppacher SD, Siebenrock KA. What are the radiographic reference values for acetabular under- and overcoverage? *Clin Orthop Relat Res* 2015; 473: 1234-1246.
26. Reijman M, Hazes JM, Pols HA, Koes BW, Bierma-Zeinstra SM. Acetabular dysplasia predicts incident osteoarthritis of the hip: the Rotterdam study. *Arthritis Rheum* 2005; 52: 787-793.
27. Thomas GE, Palmer AJ, Batra RN, Kiran A, Hart D, Spector T, et al. Subclinical deformities of the hip are significant predictors of radiographic osteoarthritis and joint replacement in women. A 20 year longitudinal cohort study. *Osteoarthritis Cartilage* 2014; 22: 1504-1510.
28. Harris JD, Gerrie BJ, Varner KE, Lintner DM, McCulloch PC. Radiographic Prevalence of Dysplasia, Cam, and Pincer Deformities in Elite Ballet. *Am J Sports Med* 2016; 44: 20-27.
29. Notzli HP, Wyss TF, Stoecklin CH, Schmid MR, Treiber K, Hodler J. The contour of the femoral head-neck junction as a predictor for the risk of anterior impingement. *J Bone Joint Surg Br* 2002; 84: 556-560.

30. van Buuren MMA, Arden NK, Bierma-Zeinstra SMA, Bramer WM, Casartelli NC, Felson DT, et al. Statistical shape modeling of the hip and the association with hip osteoarthritis: a systematic review. *Osteoarthritis Cartilage* 2021; 29: 607-618.
31. Arévalo N, Santamaría NA, Diez EM, Molinero JG, Barez MG. Imaging findings of developmental dysplasia of the hip in adults. 2016.
32. Lindner C, Thiagarajah S, Wilkinson JM, arc OC, Wallis GA, Cootes TF. Fully automatic segmentation of the proximal femur using random forest regression voting. *IEEE Trans Med Imaging* 2013; 32: 1462-1472.
33. Nicholls AS, Kiran A, Pollard TC, Hart DJ, Arden CP, Spector T, et al. The association between hip morphology parameters and nineteen-year risk of end-stage osteoarthritis of the hip: a nested case-control study. *Arthritis Rheum* 2011; 63: 3392-3400.
34. M. Gamer JL, M.M. Gamer, A. Robinson, W. Kendall's. Package'irr'. R Package, vol. 12012.
35. Nelson AE, Stiller JL, Shi XA, Leyland KM, Renner JB, Schwartz TA, et al. Measures of hip morphology are related to development of worsening radiographic hip osteoarthritis over 6 to 13 year follow-up: the Johnston County Osteoarthritis Project. *Osteoarthritis Cartilage* 2016; 24: 443-450.
36. Yang W, Ye Q, Ming S, Hu X, Jiang Z, Shen Q, et al. Feasibility of automatic measurements of hip joints based on pelvic radiography and a deep learning algorithm. *Eur J Radiol* 2020; 132: 109303.
37. Tontanahal S, Madhuri V. Reproducibility of Radiographic Measurements Made in the Active Stages of Legg-Calvé-Perthes Disease: Evaluation of a Prognostic Indicator and an Interim Outcome Measure. *Journal of Pediatric Orthopaedics* 2021; 41: e938-e939.
38. Powell J, Gibly RF, Faulk LW, Carry P, Mayer SW, Selberg CM. Can EOS Imaging Substitute for Conventional Radiography in Measurement of Acetabular Morphology in the Young Dysplastic Hip? *J Pediatr Orthop* 2020; 40: 294-299.
39. Mast NH, Impellizzeri F, Keller S, Leunig M. Reliability and agreement of measures used in radiographic evaluation of the adult hip. *Clin Orthop Relat Res* 2011; 469: 188-199.
40. Lerch S, Kasperczyk A, Berndt T, Ruhmann O. Ultrasound is as reliable as plain radiographs in the diagnosis of cam-type femoroacetabular impingement. *Arch Orthop Trauma Surg* 2016; 136: 1437-1443.
41. Air ME, Harrison JR, Nguyen JT, Kelly BT, Bogner EA, Moley PJ. Correlation of Measurements of the Prearthritic Hip Between Plain Radiography and Computed Tomography. *PM R* 2019; 11: 158-166.
42. Tannast M, Siebenrock KA, Anderson SE. Femoroacetabular impingement: radiographic diagnosis--what the radiologist should know. *AJR Am J Roentgenol* 2007; 188: 1540-1552.

Supplement 1: Protocol for landmark annotation



Proximal femur (white points)

Lesser trochanter

Point (34): Where the lesser trochanter starts bending off the shaft distally. If the lesser trochanter is seen behind the shaft, place this point on the cortex of the shaft at this level. If the lesser trochanter is not visible at all: missing points.

Point (31): Where the lesser trochanter joins the shaft proximally. If the lesser trochanter is seen behind the shaft, place this point on the cortex of the shaft at this level. If the lesser trochanter isn't visible at all: missing points.

Point (32)+(33): Respectively on the lower and upper corners of the lesser trochanter. If there are no clear corners: space them equally between (31) and (34) along the bony contour of the lesser trochanter.

Rest of proximal femur

Point (0) + (1): Respectively across (34) and (31) on the lateral femoral shaft. If point (1) would be above point (3) based on the position of point (34), place point (1) just under point (3).

Point (3): On the lower lateral corner of the greater trochanter.

Point (2): Equally spaced between (1) and (3).

Point (6): On the upper lateral corner of the (anterior) greater trochanter.

Point (4)+(5): Equally spaced between (3) and (6).

Point (7): On the medial upper corner of the anterior greater trochanter. If not visible, place this point equally spaced between (6) and (8) on the contour of the anterior greater trochanter.

Point (8): Where the anterior greater trochanter intersects the femoral.

Point (18): On the superolateral side of the femoral head, where the "best fitting circle" around the convexity of the femoral head seems to start. In case of a cam bump, osteophyte, or other irregularity: place (18) right after this bump ends, and the circle begins.

Point (27): On the inferomedial side of the femoral head, where the convexity of the femoral head seems to end. (The neck bends off after this point).

Point (20-26): Place these points equally spaced between (18) and (27) following the femoral head contour, unless there is a clear fovea dip, in which case the adjacent points, usually (24) and (25), are placed just outside of the fovea. Point (23) will be approximately placed halfway across the 'semi'-circle between (18) and (27).

Point (9-17): Place these points equally spaced between (8) and (18) following the lateral femoral neck contour. In case of irregularities like a cam bump or osteophyte, follow the outlining contour as closely as possible.

Point (19): Place this point equally spaced between (18) and (20) on the femoral head contour.

Point (28): At the deepest point of the inferomedial concavity of the femoral neck, so that (27-31) will follow the medial cortex of the femoral neck as closely as possible.

Point (29)+(30): Place these points equally spaced between (28) and (31), following the medial cortex of the femoral neck.

Greater trochanter, posterior part

** If the posterior greater trochanter is not visible: (35-39) missing points.

Point (36): On the upper medial corner of the posterior greater trochanter.

Point (35): Between (6) and (36), following the contour. If there is a clear corner, put it there.

Point (37): On the medial corner of the posterior greater trochanter, where it starts to drop downwards (caudal). This is independent of the femoral neck, so it can be before or after it dips behind the femoral neck, depending on the rotation of the proximal femur.

Point (38): Where the posterior greater trochanter is dropping straight down, right before it bends medially.

Point (39): On the end of the sclerotic line right after the medial bend, following the contour of the posterior greater trochanter.

Posterior wall of acetabulum (yellow points)

Point (40): On the uppermost visible part of the posterior wall of the acetabulum (usually right below the lateral edge of the weight-bearing surface or lateral osteophyte/pincer).

Point (44): Where the posterior wall joins the ischium (where the ischium usually proceeds vertically down).

Point (41-43): Place these points equally spaced between (40) and (44), following the contour of the posterior wall of the acetabulum.

Ischium & Pubis (pink points)

Point (49): On the most caudal point of the ischium (ischial tuberosity). If the ischial tuberosity appears as a straight line, put it in the middle of the ischial tuberosity.

Point (45-48): Place these points equally spaced between (44) and (49) along the contour of the ischial tuberosity.

Point (52): In the concavity before the symphysis.

Point (50)+(51): Place these points equally spaced between (49) and (52), following the caudal contour of the inferior pubic ramus.

Point (53): On the most caudal point of the pubic symphysis.

Point (54): On the most cranial point of the pubic symphysis.

Point (59): On the iliopectineal line of the pelvis, at the height where the ilioischial line splits off.

Point (55-58): Place these points equally spaced between (54) and (59). Follow the iliopectineal line, ignoring the ischial spine.

Point (60): In the superolateral corner of the obturator foramen.

Point (62): In the inferolateral corner of the obturator foramen.

Point (61): Equally spaced between (60) and (62), following the contour of the lateral rim of the obturator foramen.

Point (64): In the inferomedial corner of the obturator foramen.

Point (63): Place this point equally spaced between (62) and (64), following the contour/angle of the inferior rim of the obturator foramen.

Point (65): In the superomedial corner of the obturator foramen.

Point (66): Place this point equally spaced between (65) and (60), following the contour/angle of the superior rim of the obturator foramen.

Acetabulum (black points)

Acetabular roof

** Points (70-74) along the weight-bearing zone (sourcil) are placed on the inferior rim of the sclerotic line.

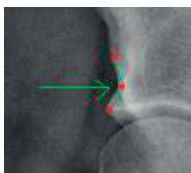
Point (69): On the most lateral point of the acetabulum, this can also be a lip/osteophyte.

Point (70): On the most lateral point of the weight-bearing zone (sourcil) of the acetabulum (most lateral point of sclerotic line).

Point (74): On the most medial point of the weight-bearing zone (sourcil) of the acetabulum, this is also the most superolateral point of the acetabular fossa. Usually there is a clear angle in the (sclerotic) line at the transition of weight-bearing zone to fossa. If the acetabular fossa is not visible at all, just place it on the most medial point of the sclerotic line.

Point (71-73): Along the underside of the sourcil, place these points equally spaced between (70) and (74), following the contour of the weight-bearing zone.

Point (68): On the 'dimple' above (70), where the acetabular lip contour has a bend. When the acetabular lip forms a straight line, equally space point (68) and (67) above point (69), with the same distance as points (71-72).



Point (67): Above (68), following the most lateral sclerotic line, with a similar distance between points (67-68) as points (71-72).

Pelvic teardrop

Point (75): On the superolateral corner of the visible teardrop (on the wall of the acetabular fossa)

Point (77): On the most caudal point of the teardrop.

Point (79): Across (75) on the other side of the teardrop.

Point (76)+(78): Across each other between (75-77-79), at the corners of the teardrop, where the more vertical (diverging) lines change direction to more oblique (converging) lines. This can be a very acute angle or more gradual.

Curve model:

Proximal femur curve:

0-1-2-3-4-5-6-7-8-9-10-11-12-13-14-15-16-17-18-19-20-21-22-23-24-25-26-27-28-29-30-31-32-33-34

Greater trochanter curve:

6-35-36-37-38-39

Posterior wall curve:

40-41-42-43-44

Ischium & pubis curve:

44-45-46-47-48-49-50-51-52-53-54-55-56-57-58-59

Foramen curve:

60-61-62-63-64-65-66

Acetabular roof curve:

67-68-69-70-71-72-73-74

Pelvic teardrop curve:

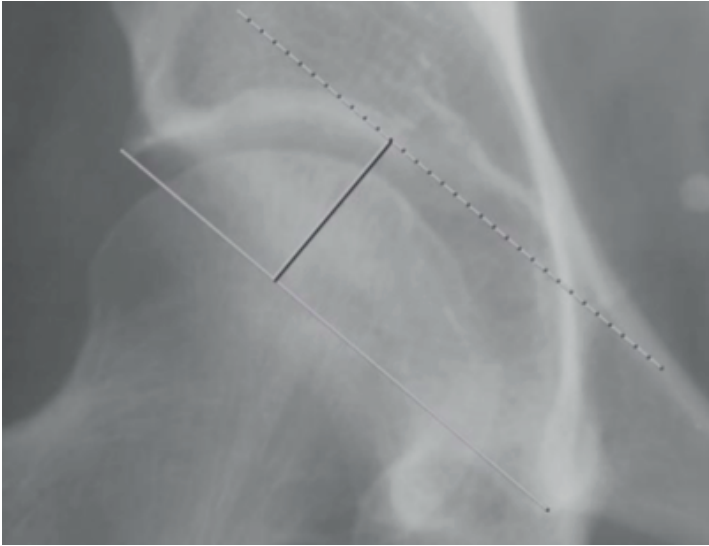
75-76-77-78-79

General rules:

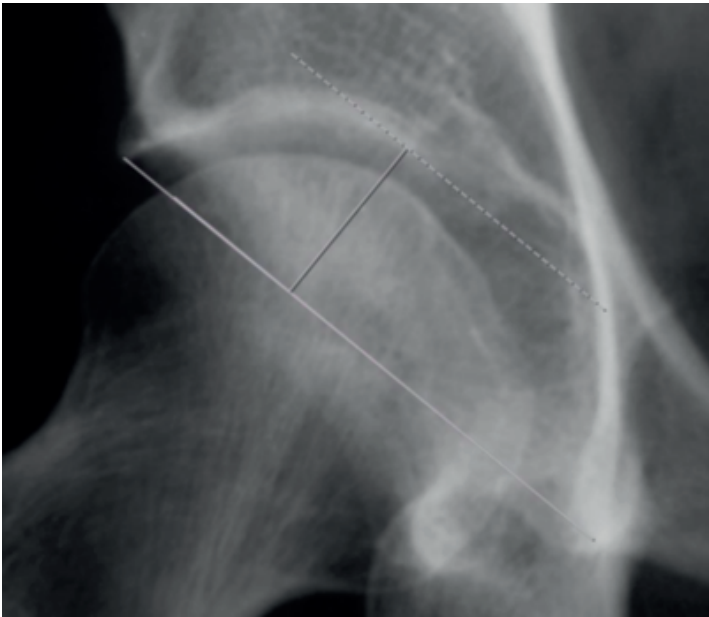
- Osteophytes of the femoral head are included in the model. Follow the outermost contour. We can later correct for these with the radiological assessment data.
- Non-identifiable landmarks: missing points (write in separate log file)
- Only follow clear bony structures, not projecting shadows.
- Every hip is different, so not all anatomical landmarks might be clearly visible in each radiograph. In case of systematic doubt or error: discuss!

Supplement 2: Example of the images for qualitative assessment

Below are depicted the visualizations of the acetabular depth-width ratio measurements as performed by observer 1, observer 2 and the automated method which were presented to the musculoskeletal radiologist for qualitative assessment of the measurement.



Visualization of the acetabular depth-width ratio measurement as performed by observer 1.



Visualization of the acetabular depth-width ratio measurement as performed by observer 2.



Visualization of the automated acetabular depth-width measurement on unadjusted landmark points.

3

Cam Morphology Is Strongly and Consistently Associated with the Development of Radiographic Hip Osteoarthritis Throughout 4 Follow-up Visits within 10 Years

Jinchi Tang, Michiel M A van Buuren, Noortje S Riedstra, Fleur Boel, Jos Runhaar, Sita Bierma-Zeinstra, Rintje Agricola.

ABSTRACT

Objective: To determine the association between cam morphology and the development of radiographic hip osteoarthritis (RHOA) at four time points within 10-year follow-up.

Design: The nationwide prospective Cohort Hip and Cohort Knee (CHECK) study includes 1,002 participants aged 45-65 years with 2-, 5-, 8-, and 10-year follow-ups. The associations of cam morphology (alpha angle $>60^\circ$) and large cam morphology (alpha angle $>78^\circ$) in hips free of OA at baseline (Kellgren & Lawrence (KL) grade <2) with the development of both incident RHOA (KL grade ≥ 2) and end-stage RHOA (KL grade ≥ 3) were estimated using logistic regression with generalized estimating equation at each follow-up and using Cox regression over 10 years, adjusted for age, sex, and body mass index.

Results: Both cam morphology and large cam morphology were associated with the development of incident RHOA at all follow-ups with adjusted Odd Ratios (aORs) ranging from 2.7 (95% CI 1.8-4.1) to 2.9 (95% CI 2.0-4.4) for cam morphology and ranging from 2.5 (95% CI 1.5-4.3) to 4.2 (95% CI 2.2-8.3) for large cam morphology. For end-stage RHOA, cam morphology resulted in aORs ranging from 4.9 (95% CI 1.8-13.2) to 8.5 (95% CI 1.1-64.4) and aORs for large cam morphology ranged from 6.7 (95% CI 3.1-14.7) to 12.7 (95% CI 1.9-84.4).

Conclusion: Cam morphology poses the hip at a 2 to 13 times increased odds for developing RHOA within 10-year follow-up. The association was particularly strong for large cam morphology and end-stage RHOA, while the strength of association was consistent over time.

Keywords: radiographic hip osteoarthritis; cam morphology; cohort study

INTRODUCTION

Hip osteoarthritis (OA) is one of the most prevalent musculoskeletal conditions affecting the elderly, causing hip pain and functional disability¹. The social and economic impact of hip OA is steadily rising as the population ages².

In recent years, hip morphology, including hip dysplasia and cam morphology, has been identified as an important risk factor for the development of radiographic hip osteoarthritis (RHOA)³⁻⁷. Cam morphology represents extra cartilage or bone formation at any location around the femoral head-neck junction, which results in a non-spherical femoral head⁸. During hip motion, the cam morphology might impinge against and be forced into the acetabular rim, causing repetitive stress on the acetabular labrum and articular cartilage^{9,10}.

The association between cam morphology and RHOA has been shown in some prospective cohort studies^{5,7,11-16}. However, there is considerable heterogeneity between those cohorts. Therefore, the strength of association reported varies widely between different cohorts, with odds ratios varying between 2.11 (95% CI 1.55–2.87)⁷ and 20.6 (95% CI 3.4–34.8)¹². One of the explanations for the variance in the strength of association between cam morphology and RHOA is the different follow-up times used, ranging from 3¹⁴ to over 25 years¹⁵. It has been hypothesized that cam morphology leads to rapid development of hip OA¹¹ meaning hip OA develops within a few years of follow-up rather than a gradual development over a decade or more. Other reasons could be the different definitions used for RHOA and different definitions to quantify cam morphology^{5,13,16}. To the best of our knowledge, there are no studies showing the strength of association over time within the same cohort. Studying different definitions for both cam morphology and RHOA, as well as their association at multiple follow-up times, can provide a more detailed understanding of the relation between cam morphology and RHOA, which is currently lacking.

The aim of this study was therefore to determine the strength of association of cam morphology and large cam morphology with the development of both incident RHOA and incident end-stage incident RHOA at 2-, 5-, 8-, and 10-year follow-up (T2, T5, T8 and T10).

METHODS

Study population

The Cohort Hip and Cohort Knee (CHECK) is a nationwide multicenter prospective cohort study of 1,002 individuals. From October 2002 until September 2005, all participants were recruited in the Netherlands through i) invitation by general practitioners (GP), ii) advertisements and articles in local newspapers and iii) the Dutch Arthritis Foundation website.

Individuals were eligible to participate if they had first onset pain and/or stiffness of the knee or hip, were aged between 45 and 65 years, and had not yet consulted their GPs for these symptoms, or the first consultation was within 6 months before entry. Individuals were excluded from the study if they had any other pathological condition that could explain the symptoms (for hip: previous trauma, fracture, subluxation, rheumatoid arthritis, previous hip surgery, bursitis, tendinitis, previously diagnosed congenital dysplasia, osteochondritis dissecans, septic arthritis or Perthes' disease), any comorbidity precluding physical evaluation and/or follow-up of at least 10 years, malignancy in the past 5 years or inability to understand the Dutch language^{17, 18}. Radiological data were collected from 11 general and academic hospitals in the Netherlands.

The study was approved by the medical ethics committees of all participating centers, and written informed consent was obtained from all participants.

Radiography

Standardized weight-bearing anteroposterior (AP) radiographs of the pelvis or hip were obtained at baseline and T2, T5, T8 and T10. During acquisition of the AP pelvic radiograph, participants were positioned with the lower extremities parallel and with 15° internal rotation, resulting in the touch of the medial side of the distal part of the first phalanx. The X-ray beam was centered on the proximal edge of the pubic symphysis. The tube to film distance was 100 cm. Only the first 124 participants who entered the CHECK study had an AP hip radiograph of each hip obtained according to the same protocol, but with the X-ray beam centered on the groin.

Radiographic measurements

The alpha angle was used to quantify cam morphology. The alpha angle is constructed by one line from the femoral head center through the middle of the femoral neck and a second line from the femoral head center through a point where the contour of the femoral head-neck junction exceeds the radius of the best fitting circle of the femoral

head¹⁹ (Figure 1). In this study, the alpha angle was calculated automatically in AP radiographs using Matlab (V.7.1.0) by a set of landmark points.

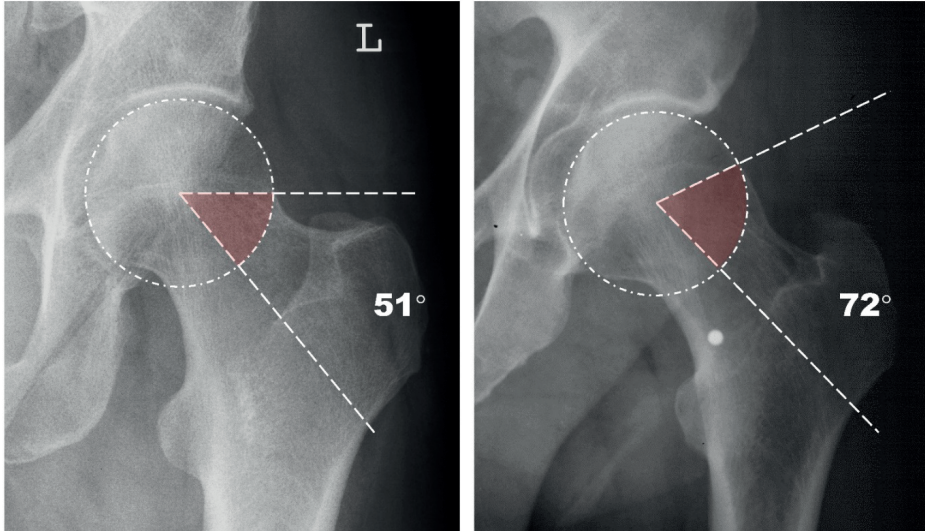


Figure 1. The measurement of alpha angle on an anteroposterior pelvic radiograph. The radiograph on the left shows a normal hip with an alpha angle of 51° whereas the right radiograph shows a hip with cam morphology resulting in an alpha angle of 72°.

We used a previously validated threshold value of $> 60^\circ$ to define the presence of cam morphology²⁰. As previous studies²¹ showed a higher risk of developing OA with increasing alpha angle, we also used a threshold of $> 78^\circ$ to define a large cam morphology. This threshold previously showed the best discriminative ability between hips that developed and did not develop hip OA²¹.

Outcome measures

At baseline and T2, T5, T8 and T10, the AP pelvic and hip radiographs were scored for osteoarthritis according to the Kellgren and Lawrence (KL) classification. All available radiographs of each participant were scored simultaneously, so that the information of all images was used for the KL scoring at each time point. This approach has been shown to be more reliable compared to scoring every radiograph independently²². From the hips without definite RHOA at baseline (KL grade < 2), the development of incident RHOA was defined by a KL grade equal or greater than two or a total hip replacement (THR) at follow-up and the development of incident end-stage RHOA was defined by a KL grade equal or greater than three, or a THR at follow-up. THR was included because all hips underwent THR due to hip OA and it was assumed that

there will be RHOA present in a more advanced stage before this procedure is being performed. This was confirmed by the RHOA grades at the visit prior to the THR procedure, which almost all showed a KL grade >1.

Statistics

Differences in characteristics between included and excluded hips and between hips with and without cam morphology at baseline were evaluated. We used the Mann-Whitney U test for continuous variables (age and body mass index (BMI) and alpha angle) and the chi-square test for dichotomous variable (sex and baseline KL grade). To study the association between cam morphology and the development of RHOA on a hip level at each follow-up, we used logistic regression with generalized estimating equation (GEE), as GEE accounted for statistical dependency between two hips within one subject. For each follow-up time point, the inclusion criterion for analysis was the availability of a radiograph both at baseline and at the given follow-up time point. The comparator group for both alpha angle threshold values for cam morphology was hips without cam morphology (alpha angle <60°). The comparator group for both RHOA outcomes was hips free of definite RHOA (KL grade <2). Therefore, hips with an alpha angle between 60° to 78° as well as with KL grade equal to two were excluded from the analysis when respectively large cam morphology as predictor or end-stage RHOA as an outcome were used. In addition to quantifying cam morphology as a dichotomous variable, we also present the results of the alpha angle as a continuous variable as supplemental data. Cox proportional hazard regression using the same predictors and outcomes as the logistic regression model was also used to provide better insight in the association between cam morphology and RHOA over time and to allow for incomplete follow-up of participants. The strength of association was expressed in odds ratios (OR) or hazard ratios (HR) with 95% confidence intervals and corrected for age, sex, and BMI. The effect was considered significant at $P < 0.05$. All statistical analyses were performed in IBM SPSS V.26.0 (Windows).

RESULTS

Population

Of the 2004 hips from 1,002 individuals in the CHECK cohort, 1,514 baseline hips were included (**Table 1**). Of the 490 excluded hips, there were 22 hips that did not have baseline radiographs available, 6 hips did not have baseline BMI values, 244 hips had unavailable alpha angle values due to insufficient quality of radiographs, and 218 hips had a K&L score equal or greater than two at baseline. The complete flow of participants (included hips) is provided in the flowchart (**Figure 2**).

Table 1. The difference in baseline characteristics between included and excluded hips.

Baseline characteristics	CHECK study n=2004		P value
	Included hips n=1514	Excluded hips n=490	
Age in years: mean (SD)	55.6 (5.2)	56.7 (5.2)	<0.001
Women, No (%)	1233 (81.4)	347 (70.8)	<0.001
BMI, kg/m ² : mean (SD)	26.2 (4.1)	26.0 (3.6)	0.183
KL grade 0, No (%)	1121 (74.0)	162 (33.1)	<0.001
KL grade 1, No (%)	393 (26.0)	88 (18.0)	<0.001
Alpha angle: mean (SD)	46.3(12.1)	55.6(18.3)	<0.001

BMI: body mass index; KL: Kellgren & Lawrence.

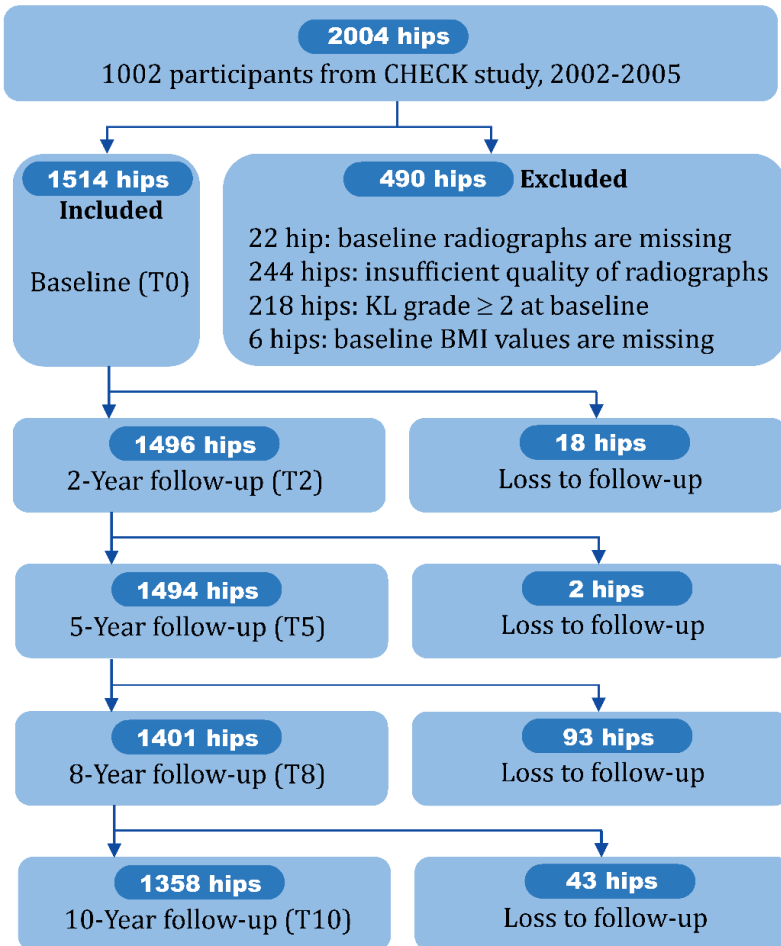


Figure 2. The flow of subjects (hips) from the beginning of the study to baseline and different follow-up time points.

Radiographic hip osteoarthritis

At T2, the prevalence of incident RHOA and incident end-stage RHOA was 5.9% (88 hips) and 0.5% (7 hips), respectively. Over the next eight years, the prevalence increased steadily with respective values of 14.6% (218 hips) and 1.6% (24 hips) at T5, 24.7% (346 hips) and 3.2% (45 hips) at T8, and 43.4% (589 hips) and 5.2% (70 hips) at T10.

Association between cam morphology and RHOA

The baseline prevalence of cam morphology (alpha angle $>60^\circ$) was 8.9% (134 hips) and the prevalence of large cam morphology (alpha angle $>78^\circ$) was 4.7% (71 hips). Cam morphology was more prevalent in men than in women, see Supplementary Table S1 for all differences in baseline characteristics between hips with and without cam morphology. The absolute risk to develop RHOA in hip with cam morphology ranged from 14.4% at T2 to 69.2% at T10 (**Table 2**), while the corresponding values in hip without cam morphology were relatively lower (5.1% at T2, 12.8% at T5, 21.6% at T8 and 40.9% at T10). Cam morphology at baseline was significantly associated with the development of both incident and end-stage RHOA at all follow-up time points (Table 2). The strength of association between cam morphology and incident RHOA ranged between 2.7 (95% CI 1.8 -4.1) at T10 and 2.9 (95% CI 2.0-4.3) at T5. For end-stage RHOA, the association ranged between 5.3 (95% CI 2.6-10.6) at T8 and 8.5 (95% CI 1.1-64.4) at T2.

Table 2. Logistic regression model: association between predictors and the development of incident or end-stage RHOA at four follow-ups over 10 years.

Predictors	Follow-up	Hips with predictor (%)	Outcome: development of incident RHOA				Outcome: development of end-stage RHOA							
			Absolute risk (%)		Crude OR (95% CI)	P value	Absolute risk (%)		Crude OR (95% CI)	P value				
			In hips with predictor	In hips without predictor			In hips with predictor	In hips without predictor						
Cam morphology (alpha angle>60°)	T2	132(8.8)	19/132(14.4)	69/1364(5.1)	3.0(1.7-5.1)	<0.001	2.8 (1.6-4.9)	0.001	4/132(3.0)	3/1364(0.2)	15.3(3.4-68.9)	<0.001	8.5(1.1-64.4)	0.037
	T5	132(8.8)	44/132(33.3)	174/1362(12.8)	3.3(2.2-4.8)	<0.001	2.9(2.0-4.4)	<0.001	7/132(5.3)	17/1362(1.2)	5.5(2.3-13.4)	<0.001	4.9(1.8-13.2)	0.002
	T8	121(8.6)	57/121(47.1)	277/1280(21.6)	2.9(2.0-4.1)	<0.001	2.7(1.9-4.0)	<0.001	12/121(9.9)	33/1280(2.6)	5.5(2.9-10.5)	<0.001	5.3(2.6-10.6)	<0.001
	T10	120(8.8)	83/120(69.2)	506/1238(40.9)	2.9(2.0-4.3)	<0.001	2.7(1.8-4.1)	<0.001	18/120(15.0)	52/1238(4.2)	5.7(3.2-10.3)	<0.001	5.4(2.9-10.2)	<0.001
	T2	70(4.7)	14/70(20.0)	69/1364(5.1)	4.5(2.3-8.6)	<0.001	4.2(2.2-8.3)	<0.001	3/70(4.3)	3/1364(0.2)	23.1(4.6-116.1)	<0.001	12.7(1.9-84.4)	0.008
Large cam morphology (alpha angle>78°)	T5	70(4.7)	28/70(40.0)	174/1362(12.8)	4.5(2.7-7.4)	<0.001	4.1(2.4-6.9)	<0.001	6/70(8.6)	17/1362(1.2)	10.0(3.8-26.2)	<0.001	8.1(2.8-23.5)	<0.001
	T8	64(4.6)	33/64(51.6)	277/1280(21.6)	3.2(2.0-5.1)	<0.001	3.1(1.9-5.1)	<0.001	8/64(12.5)	33/1280(2.6)	7.8(3.5-17.1)	<0.001	6.9(3.0-15.7)	<0.001
	T10	64(4.7)	44/64(68.8)	506/1238(40.9)	2.7(1.6-4.5)	<0.001	2.5(1.5-4.3)	<0.001	13/64(20.3)	52/1238(4.2)	7.8(5.4-22.8)	<0.001	6.7(3.1-14.7)	<0.001
	T2	64(4.7)	14/64(21.9)	69/1364(5.1)	4.5(2.3-8.6)	<0.001	4.2(2.2-8.3)	<0.001	3/64(4.7)	3/1364(0.2)	23.1(4.6-116.1)	<0.001	12.7(1.9-84.4)	0.008

RHOA: radiographic hip osteoarthritis; aOR: adjusted Odds Ratio; T2-T10: 2- to 10-year. Results are adjusted for age, sex and body mass index.

Large cam morphology was also associated with both incident and end-stage RHOA at all follow-up time points (Table 2) and this association seemed to be stronger compared to cam morphology defined by an alpha angle > 60°. The association with development of incident RHOA ranged between 2.5 (95% CI 1.5 -4.3, T10) and 4.2 (95% CI 2.0 -8.3, T2). For end-stage RHOA the association ranged from 6.7 (95% CI 3.1-14.7) at T10 to 12.7 (95% CI 1.5-84.4) at T2.

At each follow-up visit, the alpha angle as a continuous variable was associated with development of both incident and end-stage RHOA with aORs ranging from 1.02 (95% CI 1.01-1.03) to 1.06 (95% CI 1.02-1.09) for every degree increase in alpha angle (Supplementary Table S2).

Similar results were also found from the Cox regression model as all of predictors (cam morphology, large cam morphology and continuous alpha angle) showed significant association with both incident and end-stage RHOA over 10 years follow-up period (Table 3 and Supplementary Table S3).

Table 3. Cox regression model: association between predictors and the development of incident or end-stage radiographic hip osteoarthritis over 10 years.

Predictors	Outcome: development of incident RHOA				Outcome: development of end-stage RHOA			
	Crude HR (95% CI)	P value	aHR (95% CI)	P value	Crude HR (95% CI)	P value	aHR (95% CI)	P value
Cam morphology (alpha angle>60°)	2.2 (1.7-2.7)	<0.001	2.1(1.7-2.6)	<0.001	4.4 (2.7-7.1)	<0.001	4.1 (2.5-6.8)	<0.001
Large cam morphology (alpha angle>78°)	2.3 (1.7-3.1)	<0.001	2.1(1.5-2.8)	<0.001	6.2 (3.6-10.7)	<0.001	5.8 (3.4-9.9)	<0.001

RHOA: radiographic hip osteoarthritis; aHR: adjusted Hazard Ratio. Results are adjusted for age, sex and body mass index.

DISCUSSION

This prospective cohort study showed a consistent association between cam morphology and the development of RHOA within 10 years follow-up. For large cam morphology (alpha angle > 78°), the association with the development of RHOA seemed to be stronger than cam morphology (alpha angle > 60°). Also, for both cam morphology and large cam morphology, the association was stronger when using end-stage RHOA (KL grade≥3) as an outcome as compared to incident RHOA (KL grade≥2). Considering the wide confidence interval around the odds ratios, further validation on the magnitude of association is required for these findings in future larger studies.

In previously published longitudinal studies on the association between cam morphology and the development of incident RHOA, there seemed to be a trend of weaker associations with a longer follow-up time^{7, 11, 15}. This trend contrasts with our findings which showed a consistent strength of association for at least 10 years follow-up. Previously published prospective cohort studies^{5, 7, 11, 13-16}, however, only used one follow-up time point and the trend of association over time in those cohorts is therefore unknown. The differences in strength of association between

previously published cohorts might therefore also be explained by differences in cohort characteristics and definitions of RHOA and cam morphology which we showed to influence the strength of association. A possibility to overcome this would be to harmonize data from previously published cohort studies which might be a topic of future research.

The alpha angle threshold value for defining cam morphology is still under debate, with a review²³ reporting threshold values previously used ranging from 50.5° up to 83°. However, a recent systematic review²⁰, aiming to identify a threshold value, suggested a 60° cutoff to distinguish between hips with and without cam morphology, but also mentioned that a higher threshold value might increase the risk of developing hip OA. Our findings also supported this, showing a stronger association with RHOA for large cam morphology. We reported the alpha angle with threshold values for its interpretability and because the alpha angle previously showed a clear bimodal distribution in this cohort, thereby having a naturally distinction between hips with and without cam morphology²¹. However, this approach might have some statistical drawbacks (loss of power and incomplete correction for confounding factors²⁴⁻²⁶) which is why we also presented the alpha angle as a continuous measure.

The baseline BMI was included as a covariate in present study. It is indeed unclear whether BMI is truly associated with hip OA. Although the relationship between hip OA and obesity is not as pronounced as that of knee OA, the causal role of BMI in both knee and hip OA has recently been demonstrated in a previous study using first-release data from the UK Biobank²⁷. Moreover, a recent cohort study with over 18000 subjects also found positive association between BMI and hip OA²⁸. Given the fact that there is still uncertainty around a potential effect of BMI, we decided to include it as a confounder in our analysis.

The differences in strength of association between cam morphology and large cam morphology might be explained mechanically. A larger cam morphology might create an earlier premature contact between the cam and acetabulum during hip motion. This earlier premature contact potentially also results in more rapid or extensive cartilage damage¹⁰. Moreover, during large ranging hip motion, a larger cam morphology could cause higher peak contact pressures on the acetabular cartilage⁶, compared with a smaller size cam morphology.

Our data suggested that the presence of both cam morphology and large cam morphology seemed to have stronger associations with the development of incident end-stage RHOA than incident RHOA at all follow-up time points over 10 years. The pathogenesis of hip OA is heterogeneous and includes mechanical, inflammatory, metabolic, biological and genetic factors amongst others²⁹. Cam morphology is a typical mechanical risk factor, known to develop during adolescence. Hip OA is therefore probably the result of a cumulating effect in which the cam is repetitively forced into the acetabulum. It is known that this abnormal contact between cam morphology and the acetabulum can lead to a complete delamination of the cartilage from the subchondral bone, particularly in the anterosuperior region³⁰. The mechanism of cam impingement has therefore been suggested that end-stage OA changes in imaging can be detected within a 2-to 5-year time frame, which we confirmed with the results of our study. Therefore, more research is urgently needed on how we can reverse this association through primary or secondary prevention.

Our findings may have important clinical implications. In these participants who consulted the GP for the first time with first onset of either hip or knee pain, but without definite signs of RHOA, a simple measurement (alpha angle) on the same AP radiograph can be obtained to assess the risk for developing future RHOA. The risk was 6 to 13-times increased for a large cam morphology, depending on the follow-up time. The absolute risk of hips with cam morphology developing incident RHOA increased from 14.4% at T2 to 69.2% at T10, with an a priori chance of 5.9% and 43.4% respectively.

Identifying such a high-risk subgroup is important to test interventions that might prevent or delay the development of hip OA in these individuals.

The main limitation of this study is the use of AP radiographs, as this view only captures the outline of the femoral head-neck junction in the coronal plane. As cam morphology is a three-dimensional structure mostly located at the anterolateral aspect of the femoral head-neck junction, we may have underestimated the prevalence of cam morphology in this study. Still, quantifying cam morphology only on AP view was highly predictive for the development of hip RHOA. Also, the reader should be aware that participants of CHECK cohort study had first onset symptoms of either hip or knee or both and were aged 45-65 years at baseline. Our findings can therefore not be generalized to individuals without symptoms or younger and athletic individuals. Also, although we excluded hips with definite RHOA at baseline, we cannot rule out that these symptoms were already the first sign of OA. Finally, the reader should bear in mind that the CHECK cohort excluded those with a suspected non-OA pathological condition that could explain the symptoms (such as childhood hip diseases, fracture, bursitis amongst others). However, it is difficult to estimate what the influence of this exclusion criteria on the results is, because the distribution of cam morphology in these groups is unknown.

In conclusion, cam morphology and large cam morphology were consistently associated with the development of incident and end-stage RHOA over 10 years. The association was stronger in hips with large cam morphology than cam morphology and for the development of end-stage RHOA as compared with incident RHOA. Depending on the size of cam morphology and definition of RHOA used, odds ratios ranged from 2 to 13 and the absolute risk ranged from 15% to 69%. Cam morphology can be diagnosed before hip OA is present and might therefore be an interesting target for prevention of RHOA.

REFERENCES

1. Murphy NJ, Eyles JP, Hunter DJ. Hip Osteoarthritis: Etiopathogenesis and Implications for Management. *Adv Ther* 2016; 33: 1921-1946.
2. Hunter DJ, Bierma-Zeinstra S. Osteoarthritis. *Lancet* 2019; 393: 1745-1759.
3. Faber BG, Frysz M, Tobias JH. Unpicking observational relationships between hip shape and osteoarthritis: hype or hope? *Curr Opin Rheumatol* 2020; 32: 110-118.
4. Agricola R, Waarsing JH, Arden NK, Carr AJ, Bierma-Zeinstra SM, Thomas GE, et al. Cam impingement of the hip: a risk factor for hip osteoarthritis. *Nat Rev Rheumatol* 2013; 9: 630-634.
5. Ahedi H, Winzenberg T, Bierma-Zeinstra S, Blizzard L, van Middelkoop M, Agricola R, et al. A prospective cohort study on cam morphology and its role in progression of osteoarthritis. *Int J Rheum Dis* 2022; 25: 601-612.
6. Liu Q, Wang W, Thoreson AR, Zhao C, Zhu W, Dou P. Finite element prediction of contact pressures in cam-type femoroacetabular impingement with varied alpha angles. *Comput Methods Biomech Biomed Engin* 2017; 20: 294-301.
7. Saberi Hosnijeh F, Zuiderwijk ME, Versteeg M, Smeele HT, Hofman A, Uitterlinden AG, et al. Cam Deformity and Acetabular Dysplasia as Risk Factors for Hip Osteoarthritis. *Arthritis Rheumatol* 2017; 69: 86-93.
8. Dijkstra HP, Mc Auliffe S, Arden CL, Kemp JL, Mosler AB, Price A, et al. Oxford consensus on primary cam morphology and femoroacetabular impingement syndrome: part 1-definitions, terminology, taxonomy and imaging outcomes. *Br J Sports Med* 2022; 57: 325-341.
9. Heerey J, Kemp J, Agricola R, Srinivasan R, Smith A, Pizzari T, et al. Cam morphology is associated with MRI-defined cartilage defects and labral tears: a case-control study of 237 young adult football players with and without hip and groin pain. *BMJ Open Sport Exerc Med* 2021; 7: e001199.
10. Rogers MJ, Sato EH, LaBelle MW, Ou Z, Presson AP, Maak TG. Association of Cam Deformity on Anteroposterior Pelvic Radiographs and More Severe Chondral Damage in Femoroacetabular Impingement Syndrome. *Am J Sports Med* 2022; 50: 2980-2988.
11. Agricola R, Heijboer MP, Bierma-Zeinstra SM, Verhaar JA, Weinans H, Waarsing JH. Cam impingement causes osteoarthritis of the hip: a nationwide prospective cohort study (CHECK). *Ann Rheum Dis* 2013; 72: 918-923.
12. Bardakos NV, Villar RN. Predictors of progression of osteoarthritis in femoroacetabular impingement: a radiological study with a minimum of ten years follow-up. *J Bone Joint Surg Br* 2009; 91: 162-169.
13. Doherty M, Courtney P, Doherty S, Jenkins W, Maciewicz RA, Muir K, et al. Nonspherical femoral head shape (pistol grip deformity), neck shaft angle, and risk of hip osteoarthritis: a case-control study. *Arthritis Rheum* 2008; 58: 3172-3182.
14. Gosvig KK, Jacobsen S, Sonne-Holm S, Palm H, Troelsen A. Prevalence of malformations of the hip joint and their relationship to sex, groin pain, and risk of osteoarthritis: a population-based survey. *J Bone Joint Surg Am* 2010; 92: 1162-1169.
15. Hoch A, Schenk P, Jentsch T, Rahm S, Zingg PO. FAI morphology increases the risk for osteoarthritis in young people with a minimum follow-up of 25 years. *Arch Orthop Trauma Surg* 2021; 141: 1175-1181.

16. Nicholls AS, Kiran A, Pollard TC, Hart DJ, Arden CP, Spector T, et al. The association between hip morphology parameters and nineteen-year risk of end-stage osteoarthritis of the hip: a nested case-control study. *Arthritis Rheum* 2011; 63: 3392-3400.
17. Wesseling J, Boers M, Viergever MA, Hilberdink WK, Lafeber FP, Dekker J, et al. Cohort Profile: Cohort Hip and Cohort Knee (CHECK) study. *Int J Epidemiol* 2016; 45: 36-44.
18. Wesseling J, Dekker J, van den Berg WB, Bierma-Zeinstra SM, Boers M, Cats HA, et al. CHECK (Cohort Hip and Cohort Knee): similarities and differences with the Osteoarthritis Initiative. *Ann Rheum Dis* 2009; 68: 1413-1419.
19. Notzli HP, Wyss TF, Stoecklin CH, Schmid MR, Treiber K, Hodler J. The contour of the femoral head-neck junction as a predictor for the risk of anterior impingement. *J Bone Joint Surg Br* 2002; 84: 556-560.
20. van Klij P, Reiman MP, Waarsing JH, Reijman M, Bramer WM, Verhaar JAN, et al. Classifying Cam Morphology by the Alpha Angle: A Systematic Review on Threshold Values. *Orthop J Sports Med* 2020; 8: 2325967120938312.
21. Agricola R, Waarsing JH, Thomas GE, Carr AJ, Reijman M, Bierma-Zeinstra SM, et al. Cam impingement: defining the presence of a cam deformity by the alpha angle: data from the CHECK cohort and Chingford cohort. *Osteoarthritis Cartilage* 2014; 22: 218-225.
22. Macri EM, Runhaar J, Damen J, Oei EHG, Bierma-Zeinstra SMA. Kellgren/Lawrence Grading in Cohort Studies: Methodological Update and Implications Illustrated Using Data From a Dutch Hip and Knee Cohort. *Arthritis Care Res (Hoboken)* 2022; 74: 1179-1187.
23. Sankar WN, Nevitt M, Parvizi J, Felson DT, Agricola R, Leunig M. Femoroacetabular impingement: defining the condition and its role in the pathophysiology of osteoarthritis. *J Am Acad Orthop Surg* 2013; 21 Suppl 1: S7-S15.
24. Altman DG, Royston P. The cost of dichotomising continuous variables. *BMJ* 2006; 332: 1080.
25. Naggara O, Raymond J, Guilbert F, Roy D, Weill A, Altman DG. Analysis by categorizing or dichotomizing continuous variables is inadvisable: an example from the natural history of unruptured aneurysms. *AJNR Am J Neuroradiol* 2011; 32: 437-440.
26. Royston P, Altman DG, Sauerbrei W. Dichotomizing continuous predictors in multiple regression: a bad idea. *Stat Med* 2006; 25: 127-141.
27. Zengini E, Hatzikitoulas K, Tachmazidou I, Steinberg J, Hartwig FP, Southam L, et al. Genome-wide analyses using UK Biobank data provide insights into the genetic architecture of osteoarthritis. *Nat Genet* 2018; 50: 549-558.
28. Badley EM, Zahid S, Wilfong JM, Perruccio AV. Relationship Between Body Mass Index and Osteoarthritis for Single and Multisite Osteoarthritis of the Hand, Hip, or Knee: Findings From a Canadian Longitudinal Study on Aging. *Arthritis Care Res (Hoboken)* 2022; 74: 1879-1887.
29. Morris WZ, Li RT, Liu RW, Salata MJ, Voos JE. Origin of Cam Morphology in Femoroacetabular Impingement. *Am J Sports Med* 2018; 46: 478-486.
30. Scholes MJ, Kemp JL, Mentiplay BF, Heerey JJ, Agricola R, King MG, et al. Are cam morphology size and location associated with self-reported burden in football players with FAI syndrome? *Scand J Med Sci Sports* 2022; 32: 737-753.

Supplementary Table S1. The difference in baseline characteristics between included hips with and without cam morphology.

Baseline characteristics	Hips with cam morphology n=134	Hips without cam morphology n=1380	P value
Age in years: mean (SD)	56.6(5.1)	55.6(5.2)	0.032
Women, No (%)	67(50.0)	1166(84.5)	<0.001
BMI, kg/m ² : mean (SD)	27.5(4.4)	26.1(4.1)	0.001
KL grade 0, No (%)	68(50.7)	1053(76.3)	<0.001
Hip pain symptom, No (%)	52(38.8)	540(39.1)	0.941
Knee pain symptom, No (%)	79(59.0)	908(65.8)	0.112
Dropout T2, No (%)	2(1.5)	16(1.2)	1
Dropout T5, No (%)	0(0.0)	2(0.1)	1
Dropout T8, No (%)	11(8.2)	82(5.9)	0.297
Dropout T10, No (%)	1(0.7)	42(3.0)	0.209

BMI: body mass index; KL: Kellgren & Lawrence; T2-T10: 2- to 10-year follow-up; Dropout: the number of new dropout cases at each follow-up.

Supplementary Table S2. Logistic regression model: association between continuous alpha angle and the development of incident or end-stage RHOA at four follow-ups over 10 years.

Predictors	Follow-up	Outcome: development of incident RHOA				Outcome: development of end-stage RHOA			
		Crude OR (95% CI)	P value	aOR (95% CI)	P value	Crude OR (95% CI)	P value	aOR (95% CI)	P value
Continuous alpha angle	T2	1.03 (1.021.04)	<0.001	1.03 (1.021.04)	<0.001	1.06 (1.041.09)	<0.001	1.06 (1.021.09)	0.001
	T5	1.03 (1.021.04)	<0.001	1.03 (1.021.04)	<0.001	1.04 (1.021.06)	<0.001	1.04 (1.021.06)	<0.001
	T8	1.02 (1.021.03)	<0.001	1.02 (1.011.03)	<0.001	1.04 (1.021.05)	<0.001	1.04 (1.021.05)	<0.001
	T10	1.02 (1.011.03)	<0.001	1.02 (1.011.03)	<0.001	1.04 (1.031.05)	<0.001	1.04 (1.031.05)	<0.001

RHOA: radiographic hip osteoarthritis; aOR: adjusted Odds Ratio; T2-T10: 2- to 10-year follow-up. Results are adjusted for age, sex and body mass index.

Supplementary Table S3. Cox regression model: association between continuous alpha angle and the development of incident or end-stage radiographic hip osteoarthritis over 10 years.

Predictors	Outcome: development of incident RHOA				Outcome: development of end-stage RHOA			
	Crude HR (95% CI)	P value	aHR (95% CI)	P value	Crude HR (95% CI)	P value	aHR (95% CI)	P value
Continuous alpha angle	1.02 (1.01-1.02)	<0.001	1.02 (1.01-1.02)	<0.001	1.04 (1.03-1.05)	<0.001	1.04 (1.03-1.05)	<0.001

RHOA: radiographic hip osteoarthritis; aHR: adjusted Hazard Ratio. Results are adjusted for age, sex, and body mass index.

4

Cam Morphology and the Risk of Developing Radiographic Hip Osteoarthritis within 8 Years: an Individual Participant Data Meta-analysis from the World COACH Consortium

Jinchi Tang, Fleur Boel, Michiel M.A. van Buuren, Noortje S. Riedstra, Myrthe A. van den Berg, Harbeer Ahedi, Nigel K. Arden, Sita Bierma-Zeinstra, Cindy G. Boer, Flavia M. Cicuttini, Tim F. Cootes, Kay M. Crossley, David T. Felson, Willem P. Gielis, Graeme Jones, Stefan Kluzek, Nancy E. Lane, Claudia Lindner, John A. Lynch, Joyce van Meurs, Amanda E. Nelson, Michael C. Nevitt, Edwin H.G. Oei, Jos Runhaa, Harrie Weinans, Rintje Agricola.

Manuscript submitted.

ABSTRACT

Importance: Cam morphology, an extra bone formation around the femoral head-neck junction, has been reported as a risk factor for the development of radiographic hip osteoarthritis (RHOA), but the strength of association is not well understood. By using all globally available prospective cohort data on RHOA and by applying uniform radiographic measurements, the results can be more accurate and generalizable.

Objective: To assess the relationship between cam morphology and the development of RHOA, overall and in subgroups based on age, biological sex, and body mass index (BMI).

Design, setting, and participants: In this individual participant data meta-analysis of prospective cohort studies, the association between baseline cam morphology and the development of RHOA was assessed by a three-level mixed-effects logistic regression model (hip side, individual, and cohort). A total of 23,886 hips from the World COACH consortium, with 4-8 years follow-up, were included (mean age: 62.2±8.4 years; 70.6% female; BMI: 27.4±4.5).

Exposure: 1. Baseline cam morphology defined as an alpha angle $\geq 60^\circ$. 2. The alpha angle as a continuous measure.

Main Outcome: The development of incident RHOA was defined by the transition from free RHOA at baseline to definite RHOA at 4-8 years follow-up.

Results: Cam morphology prevalence was 9.5% at baseline, and 2.1% of all hips developed RHOA. Significant associations were observed between cam morphology and the development of incident RHOA (odds ratio: 1.87, 95%CI 1.36-2.59), and greater alpha angle and RHOA (odds ratio 1.02, 95%CI 1.01-1.03 for every degree increase). The overall relative risk of developing RHOA in hips with cam morphology was 1.62 (95%CI 1.26-2.07), greatest for those aged 51-60 years (2.15, 95%CI 1.55-2.98) and in males (2.50, 95%CI 1.67-3.73).

Conclusion and Relevance: Hips with cam morphology have nearly double the odds of developing RHOA within 4-8 years, compared to hips without cam morphology. The relative risk was highest in subgroups of participants aged 51-60 years and males, making cam morphology an interesting target for primary or secondary prevention of RHOA.

Keywords: cam morphology; radiographic hip osteoarthritis; prospective cohort study.

INTRODUCTION

Osteoarthritis (OA) is a highly prevalent musculoskeletal condition worldwide, affecting 15% of individuals aged 30 and older¹. Its global prevalence (7.6% in 2020) is expected to surge in the coming decades, followed by its heavy socioeconomic costs². Currently, hip OA management remains predominantly reactive, given the absence of curative treatments. This underscores the imperative need for a deeper and more thorough understanding of its aetiology and risk factors.

A potential risk factor for radiographic hip OA (RHOA) is cam morphology³. It is characterized by the presence of additional bone formation of varying size around the femoral head-neck junction, resulting in a non-spherical femoral head⁴. This incongruity of the hip joint can result in abnormal contact between the femoral head-neck junction and the acetabulum during motion, a process referred to as femoroacetabular impingement (FAI). This may, in turn, cause pain and cartilage damage already in young adults and eventually progress to OA⁵.

The association between cam morphology and RHOA has been demonstrated previously⁶⁻¹¹. A recent systematic review could only identify three prospective studies and found odds ratios (ORs) ranging from 2.12 to 3.67 and ORs ranging from 4.57 to 10.38 in four cross-sectional studies¹². The reported inconsistency can be attributed not only to variations in the definition of cam morphology and RHOA but also to differences in demographic characteristics, and differences in measurement technique of cam morphology which limit the generalizability of findings. Combining data from existing cohort studies and uniformly measuring cam morphology to undertake individual participant data (IPD) meta-analysis could address that with a larger combined sample size, standardized automated measurements, and the ability to consider both cohort- and participant-level heterogeneity jointly¹³.

Thus, our primary aim was to assess the association between cam morphology at baseline and the subsequent development of incident RHOA over a 4-8 years follow-up period using an IPD meta-analysis based on harmonized data from nine prospective cohorts, the largest study to date. Additionally, we aimed to conduct various interaction and subgroup analyses stratified by sex, age groups, and body mass index (BMI), to comprehensively understand the role of cam morphology in the development of RHOA.

METHODS

Study population

The Worldwide Collaboration on Osteoarthritis Prediction for the Hip (World COACH) consortium is an international collaboration currently comprising eleven prospective cohort studies and has previously been described in detail¹⁴. Data from the following included studies were used in this study: the Cohort Hip and Cohort Knee (CHECK) study¹⁵, the Chingford study¹⁶, the Johnston County Osteoarthritis Project (JoCoOA)¹⁷, the Multicenter Osteoarthritis Study (MOST)¹⁸, the Osteoarthritis Initiative (OAI)¹⁹, the Rotterdam Study (RS, including three subcohorts: RS1, RS2 and RS3)²⁰, the Study of Osteoporotic Fractures (SOF)²¹.

For the current study, hips were excluded if they had missing baseline demographic data, no or insufficient quality baseline radiographs, or absence of RHOA scores at either baseline or follow-up. We only included hips that showed no signs of RHOA at baseline to focus on the development of incident RHOA, eliminating potential influence from early RHOA signs that could affect alpha angle measurements.

Radiographs

At baseline and follow-up, anteroposterior (AP) radiographs of the hip or pelvis were obtained according to the respective protocols of each cohort study¹⁵⁻²¹. The CHECK, OAI, and RS cohorts utilized standardized weight-bearing radiographs, while the Chingford, JoCoOA, and SOF cohorts employed standardized supine radiographs. Additionally, the MOST cohort used standardized weight-bearing AP full-limb radiographs of the lower extremities.

Cam morphology

The alpha angle is a recommended radiological measurement to quantify cam morphology⁴. It is measured as the angle between the femoral head-neck axis and another line drawn from the femoral head center to the first point where the bony contour of the head-neck junction leaves the best-fitting circle around the femoral head²² (**Figure 1**). In the present study, the alpha angle was automatically and uniformly measured on all baseline radiographs²³. First, the bony margin of the proximal femur was automatically annotated with landmark points using the BoneFinder® software (www.bone-finder.com; The University of Manchester, UK)²⁴. Subsequently, the alpha angle was measured by an in-house developed, open-access and validated method based on these landmarks. The automated method was validated by comparison to manual measurements, with inter-method and intraclass correlation coefficients of 0.81 (95%CI 0.46-0.92) on dual-energy x-ray absorptiometry (DXA) images²⁵ and 0.46

(95%CI 0.12-0.70) on AP pelvic radiographs²⁶, respectively. A validated alpha angle threshold value of $>60^\circ$ was used to define the presence of cam morphology^{4, 27}. As dichotomizing continuous measures may limit statistical power, we also investigated the effect of the alpha angle as a continuous variable⁴.

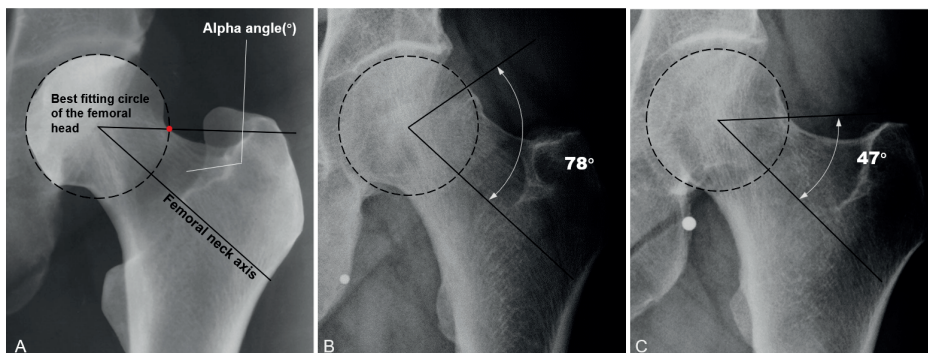


Figure 1. Measurement of the alpha angle on anteroposterior radiographs. A: the alpha angle is the angle between the femoral neck axis (which passes through the center of the femoral head and the femoral neck) and a line connecting the femoral head center and alpha point (red point), where the contour of the femoral head-neck junction begins to leave the best-fitting circle of the femoral head; B: Hip with an alpha angle of 78° ; C: Hip with an alpha angle of 47° .

Outcome measures

Among the cohorts included in the World COACH consortium, three classifications for RHOA grading were used, namely the Kellgren and Lawrence (KL)^{15-18, 20}, the Croft²¹, and the atlas of individual radiographic features in osteoarthritis (OARSI atlas)¹⁹. These RHOA scores were harmonized into three ordinal categories through a unified interpretation: 'free of RHOA' (any score of 0), 'doubtful RHOA' (any score of 1), and 'definite RHOA' (any score ≥ 2 or total hip replacement (THR)). The development of RHOA was defined by a transition from being 'free of RHOA' at baseline to having 'definite OA' at follow-up.

Statistics

Descriptive statistics were used to analyze the baseline characteristics of the included hips, stratified by cohort. Baseline characteristics were compared between hips included in the analyses versus those hips that were excluded at baseline (independent t-tests for continuous variables, and chi-square tests for categorical variables).

To assess the association between baseline cam morphology and subsequent RHOA development, a three-level mixed-effects logistic regression model (hip side, individual, and cohort) was employed. This model accounted for the clustering of two

hips from a single participant and among individuals and included cohorts. Results were expressed as odds ratios with 95% confidence intervals (CIs) and were adjusted for age, sex, and BMI. The association between the continuous alpha angle and RHOA development was assessed using the same method. All analyses were repeated for sensitivity purposes by excluding the MOST cohort, as this was the only cohort with full-limb radiographs and thus a different radiographic projection of the pelvis.

In the primary analysis, doubtful RHOA cases at follow-up were defined as the reference group together with free RHOA cases, which might influence the findings for definite RHOA. The influence of the development of 'doubtful RHOA' to 'definite RHOA' was assessed using a forward continuation ratio model, given that this transition is often considered a critical and irreversible step. This model treated RHOA as an ordinal outcome, "free of RHOA," "doubtful RHOA," and "definite RHOA", and relaxed the ordinality assumption for cam morphology. Results were presented as an effect plot of marginal probabilities, adjusted for random effects with mean baseline age and BMI and randomly selected right hip side and for female and male respectively.

We also investigated potential interaction effects between cam morphology and demographic factors (sex, age, and BMI) using unadjusted logistic regression models. Significant interactions prompted further analysis to compute odds ratios for each demographic factor, considering females as the reference group for sex, and treating age and BMI as continuous variables. Subsequent analyses stratified the data by sex, specific age groups (40-50, 51-60, 61-70, and over 70 years), and BMI categories (normal: BMI < 25, overweight: BMI ≥ 25). It was not possible to perform the aforementioned analyses in every subgroup due to restricted numbers, instead we provided descriptive statistics, including absolute risk and relative risk, for developing RHOA.

Statistical significance for the primary analyses and interaction effects was determined at a level of $P < 0.05$. Univariate analyses were performed with IBM SPSS Statistics (version: 26.0) and other analyses were conducted using R Statistical Software (version: 4.1.1, The R Foundation, used package: Lme4, GLMMadaptive, and ggplot2).

RESULTS

Baseline participant characteristics

The World COACH consortium included available data from 77,230 hips in total. After excluding those with missing or insufficient-quality data, 38,811 hips were available at baseline for this study (**Figure 2**). From this group, 14,925 hips were excluded due

to definite or doubtful signs of RHOA at baseline, leaving 23,886 hips for inclusion in the final analyses.

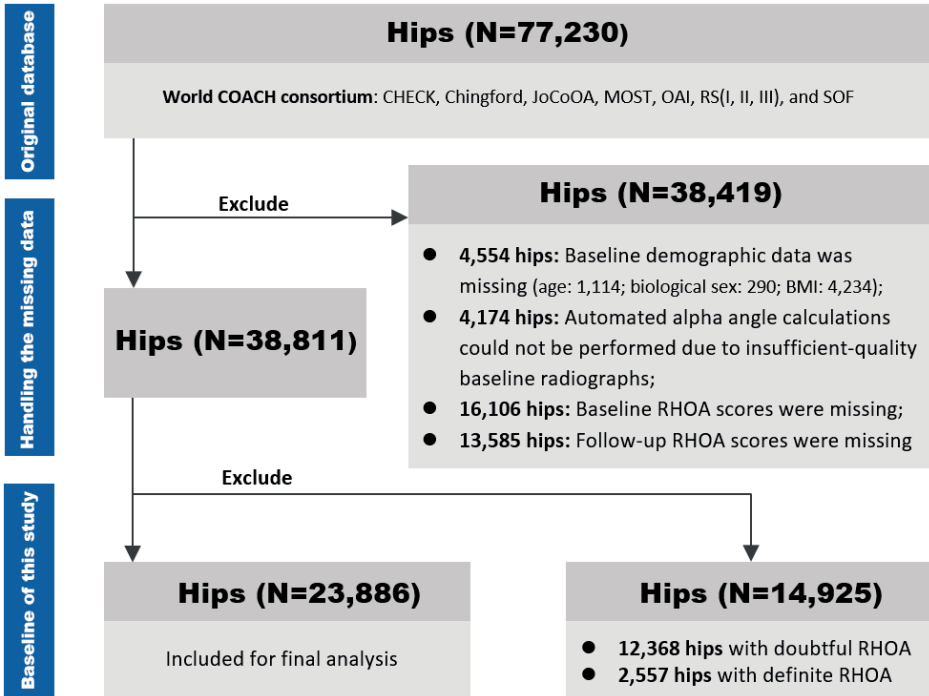


Figure 2. Complete flow of hips from the original dataset to the baseline of this study

At baseline, excluded hips were from older individuals and had a higher prevalence of cam morphology (Table 1). Results stratified by cohort are provided in supplementary Table S1.

Table 1. The difference in characteristics between included and excluded hips at baseline.

Baseline characteristic	Baseline of this study		P value
	Included hips (n=23,886)	Excluded hips (n=14,925)	
Age in years: mean (SD)	62.21(8.36)	65.40(8.43)	<0.001
Women, No (%)	16,875(70.6)	10,636(71.3)	0.195
BMI, kg/m ² : mean (SD)	27.35(4.48)	27.56(4.75)	<0.001
Alpha angle, °: mean (SD)	46.40(10.17)	48.11(11.98)	<0.001
Cam morphology: No (%)	2,271(9.51)	2,128(14.26)	<0.001
No RHOA: No (%)	23,886(100)	0(0)	-
Doubtful RHOA: No (%)	0(0)	12,368(82.90)	-
Definite RHOA: No (%)	0(0)	2,557(17.10)	-

SD: standard deviation; BMI: body mass index; RHOA: radiographic hip osteoarthritis.

Association between cam morphology and radiographic hip osteoarthritis

The prevalence of cam morphology at baseline was 9.5% (n=2,271). The incidence of RHOA was 3.2% in hips with cam morphology and 2.0% in those without. Detailed results per cohort are provided in supplementary **Table S1**. Cam morphology (alpha angle $\geq 60^\circ$) was associated with the development of incident RHOA with an odds ratio of 1.87 (95%CI 1.36-2.59). A significant association was also observed between the continuous alpha angle and RHOA development with an odds ratio of 1.02 (95%CI 1.01-1.03) for each degree increase in alpha angle (the crude ORs are provided in supplementary **Table S2**).

The effect plot of the marginal probabilities of the forward continuation ratio model is provided in **Figure 3**. All marginal probabilities were calculated in male or female aged 62 years with a BMI of 27 kg/m². Marginal probabilities indicated that cam morphology increased the likelihood of developing doubtful RHOA to 21% (95% CI:15%-27%) in females and 23% (95% CI: 16%-30%) in males, compared to 17% (95% CI:11%-23%) and 18% (95% CI: 11%-25%) in those without, respectively. For definite RHOA, probabilities were 5% (95% CI: 2%-10%) in females and 4% (95% CI: 1%-9%) in males with cam morphology, versus 2% (95% CI: 1%-6%) in females and 2% (95% CI: 1%-5%) in males without.

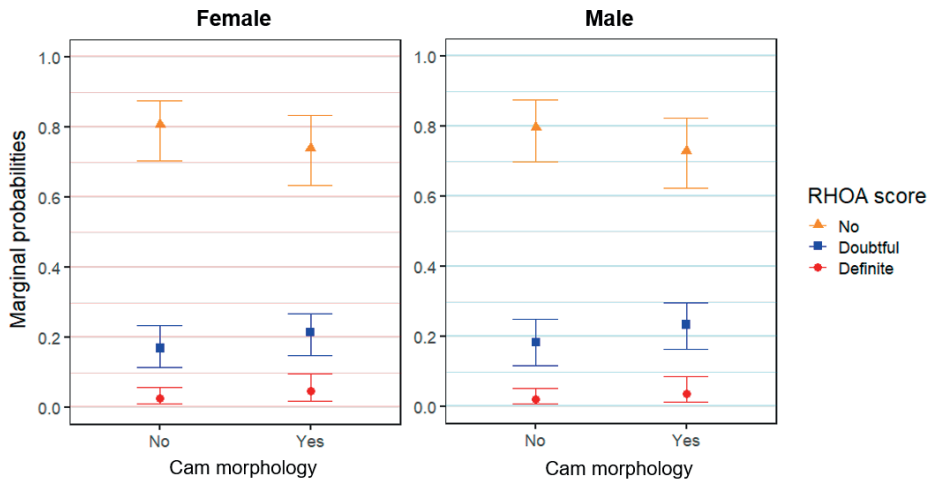


Figure 3. The effect plot of the marginal probabilities of RHOA within 4-8 years for females and males, aged 62 years, and BMI of 27 kg/m².

The sensitivity analysis excluded 2,009 hips with full-limb radiographs from the MOST cohort, leading to a total of 21,377 hips for analysis. The association between cam morphology (alpha angle $\geq 60^\circ$) and the development of incident RHOA showed similar results with an odds ratio of 1.82 (95%CI 1.31-2.52) and 1.02 (95%CI 1.01-1.03) for continuous alpha angle.

Interaction effect and subgroup analyses

The interaction analysis revealed a significant interaction between sex and cam morphology in the development of incident RHOA (P value: 0.014), but not for cam morphology with age (P value: 0.417) or BMI (P value: 0.387). Specifically, male hips with cam morphology showed an odds ratio (OR) of 3.09 (95%CI 1.38-6.90) for developing RHOA compared to those without cam morphology. In contrast, an OR of 1.36 (95%CI 0.87-2.11) was observed in female. The absolute risk and relative risk of developing RHOA for hips with cam morphology in subgroup analyses stratified by sex, age groups, and BMI categories are provided in **Table 2**. The higher relative risk was found in 51-60 years group (2.15, 95%CI 1.55-2.98) compared to other age subgroups and the male group (2.50, 95%CI 1.67-3.73) compared to the female group.

Table 2. The absolute risk and relative risk for developing RHOA stratified by age, sex, or BMI groups.

Subgroup	N (%)	Alpha angle, °: mean (±SD)	Cam morphology: No (%) in hips with cam morphology	RHOA in hips without cam morphology	Absolute Risk (%)	Relative Risk (95%CI)
Age in years	40-50	2,083 (8.7)	48.27 (11.38)	287 (13.8)	5	49 1.7 (0.261.59)
	51-60	8,155 (34.1)	46.90 (10.56)	853 (10.5)	43	171 5 (1.552.98)
	61-70	9,340 (39.1)	45.84 (9.82)	768 (8.2)	17	143 2.2 (0.812.18)
	over 70	4,308 (18.0)	45.78 (9.57)	363 (8.4)	7	61 1.9 (0.572.71)
Biological sex	Female	16,875 (70.6)	44.26 (8.65)	853 (5.1)	34	364 4 (1.242.48)
	Male	7,011 (29.4)	51.56 (11.62)	1,418 (20.2)	38	60 2.7 (1.673.73)
BMI, kg/m ²	<25	7,880 (33.0)	45.30 (9.82)	602 (7.6)	24	169 4 (1.132.61)
	≥25	16,006 (67.0)	46.95 (10.30)	1,669 (10.4)	48	255 2.9 (1.192.19)

RHOA: radiographic hip osteoarthritis

DISCUSSION

In this IPD meta-analysis, both cam morphology defined by an alpha angle $\geq 60^\circ$, as well as higher alpha angle as a continuous variable, were significantly associated with the development of incident RHOA within a 4-8 year follow-up period. By using the largest sample size to date, with a reliable automated measurement across cohorts and excluding doubtful RHOA cases at baseline, the findings of this study provide a robust estimate. Also, the large sample size allowed subgroup analysis which showed that the strength of association was highest in males and in the age group 51-60 years.

The considerable variability in previously reported findings may stem from differences in population, measurement of the alpha angle, and definition of RHOA. First, demographic characteristics varied widely in previous studies, such as a mean age below 50 years²⁸ versus over 60 years⁷, a mean BMI greater than 30²⁹ versus less than 26³⁰, and asymptomatic versus symptomatic individuals³⁰. Although recent studies consistently used an alpha angle threshold value of 60° to define the presence of cam morphology, the methods used to calculate the alpha angle differed. Lastly, some studies defined the development of RHOA as a transition from KL grade <3 at baseline

to KL grade >3 at follow-up²⁹, while others defined it as a KL grade ≥ 2 at follow-up from those with KL grade <2 at baseline. These differences limit the generalizability of each study's results, confining them to specific populations.

By taking above variabilities into account, our finding on the association between cam morphology and RHOA development showed a lower OR of 1.87 (95% CI 1.36-2.59), comparing to previous reported results. The association between the continuous alpha angle to RHOA showed similar lower strength [OR: 1.02 (95% CI 1.01-1.03)], compared to previous OR of 1.63 (95% CI 1.58-1.67) found in the UK Biobank study³¹. In our study, the harmonized database provided a more generalized population and a uniform, automated measurement of the alpha angle. Additionally, by using a three-category outcome, we defined and excluded doubtful RHOA cases at baseline from the analyses, aiming to clarify the association with incident RHOA. These points will be discussed below.

Excluding hips with doubtful RHOA at baseline impacted the observed association between cam morphology and RHOA development, likely accounting for the lower association strength compared to prior studies. Our study, with its large sample size, allowed us to analyze a substantial dataset even after removing 12,368 hips with doubtful RHOA at baseline. Previous research included these hips in their non-RHOA groups, potentially influencing the actual results, particularly the transition from being free of RHOA to developing definite RHOA. Doubtful RHOA, characterized by uncertain joint space narrowing and possible osteophyte formation³²⁻³⁴, often precedes more definitive RHOA, thereby influencing outcomes. Results from our forward continuation ratio model support this by higher marginal probabilities for both developing doubtful and definite RHOA in hips with cam morphology. For example, the CHECK study previously reported a 23.8% incidence of RHOA at the 8-year follow-up³⁰, whereas our study noted only a 13% incidence in the same cohort under the updated criteria. The inclusion of doubtful cases may overestimate RHOA prevalence and lead to baseline misclassification of cam morphology. Radiological signs of RHOA, like osteophyte formation or femoral head flattening, can alter the alpha angle, often resulting in higher measurements. This was supported by our findings, where excluded hips displayed larger alpha angles than those included, suggesting early structural changes indicative of RHOA progression.

While the AP radiograph might not be the gold standard for measuring cam morphology, its effectiveness in predicting RHOA has been demonstrated in our findings as well as in previous studies^{8, 35}. Cam morphology is a three-dimensional structure, and different planes in CT and MRI images provide more detailed information compared to

two-dimensional techniques. However, the use of CT and MRI for large-scale screening is limited due to being time-consuming, expensive, and higher requirements for facilities and radiologists. Therefore, radiographs may be the best solution as a screening tool for large samples. Cam morphology is mostly located at the anterosuperior part of the femoral head-neck junction, and the more superiorly located cam morphologies are captured well in the AP view³⁶. Our sensitivity analysis, which excluded the MOST study with full-limb radiographs, also indicates that minor differences in radiographic protocol will not obviously influence capturing and defining cam morphology. However, the readers should keep in mind that the influence of using full-limb radiographs may be underestimated due to the large overall sample size, with the MOST cohort contributing only 9% of the total sample.

Our analyses included participants' baseline age, biological sex, and BMI as confounders. Structural changes of RHOA have been found to occur with increasing age and show differences between sexes³⁷. Although the causal factor of obesity in the incidence and progression of OA is more pronounced in the knee joint compared to the hip^{38, 39}, recent studies suggest a potential causal role in hip OA as well⁴⁰⁻⁴². Generally, obesity can lead to abnormal biomechanical loading on weight-bearing joints, therefore we included BMI as a confounder in analyses, despite the current inconclusiveness of obesity's role in hip OA.

Our findings showed that cam morphology is a notable risk factor for developing RHOA in individuals without any existing radiographic signs of hip OA. Early identification through simple radiographic measurements can help identify high-risk groups before the development of complaints. This early detection enables preventive measures through lifestyle and physical activity interventions, potentially mitigating the risk of developing RHOA. These findings highlight the importance of further investigating the aetiology of cam morphology. Although cam morphology remains stable after skeletal maturity, its formation could potentially be influenced during skeletal growth making it a target for primary prevention⁴³. Interestingly, our results suggest that cam morphology may not pose as high a risk for developing RHOA as previously believed. A recent study on cam morphology showed that not all shape variants captured by alpha angle $\geq 60^\circ$ are relevant to the development of RHOA⁴⁴. Future research should focus on subtypes of cam morphology and identifying those specifically linked to RHOA. Also, cam morphology is a radiological finding, combining this with the presence of symptoms and clinical signs associated with FAI syndrome can enhance the prediction of who will develop RHOA⁴⁵.

Descriptive subgroup analyses from our study indicate that the risk of developing RHOA due to cam morphology does not consistently increase with age. Individuals aged 51-60 are at a higher risk compared to other age groups, suggesting that middle-aged individuals may especially benefit from preventative strategies. Additionally, males exhibit a higher risk of RHOA than females, likely due to the higher mean alpha angle which is associated with cartilage defects and labral tears²⁸ and absolute higher prevalence of cam morphology. However, our findings show no obvious difference in RHOA risk between individuals with a BMI below 25 and those above 25, suggesting that BMI may not significantly influence the relationship between cam morphology and RHOA. This finding aligns with the majority of previous related studies, although a few research have recently shown an association between severe cam morphology and higher BMI⁶. These insights highlight the need to consider various demographic and physical characteristics in RHOA prevention strategies.

Our study has several limitations. First, we relied solely on AP radiographs to quantify cam morphology. While we recognize the practicality of radiographs for large-scale studies, they are less detailed compared to MRI or CT scans and underestimate the prevalence of cam morphology. Second, our findings are limited by the age demographics of our sample, with a mean age of 62 years, making them less applicable to individuals under 40 years old, despite the age range spanning from 40 to over 70 years. Then, we did not consider the influence of other hip morphologies, such as hip dysplasia and pincer morphology, which may also contribute to the development of RHOA and thus impact the association between cam morphology and RHOA.

In conclusion, cam morphology defined by both alpha angle $\geq 60^\circ$ and greater continuous alpha angle is associated with the development of RHOA over 4-8 years follow-up. Important strengths of this analysis include the combination of populations from diverse cohorts, uniform calculation for alpha angle and more strict definition for the development of RHOA, supporting the robust and generalizable nature of our findings. Our results warrant further research in preventive measures for cam morphology to halt or delay the development of hip OA.

REFERENCES

1. Collaborators GBDO. Global, regional, and national burden of osteoarthritis, 1990-2020 and projections to 2050: a systematic analysis for the Global Burden of Disease Study 2021. *Lancet Rheumatol* 2023; 5: e508-e522.
2. Hunter DJ, Bierma-Zeinstra S. Osteoarthritis. *Lancet* 2019; 393: 1745-1759.
3. Agricola R, Waarsing JH, Arden NK, Carr AJ, Bierma-Zeinstra SM, Thomas GE, et al. Cam impingement of the hip: a risk factor for hip osteoarthritis. *Nat Rev Rheumatol* 2013; 9: 630-634.
4. Dijkstra HP, Mc Auliffe S, Arden CL, Kemp JL, Mosler AB, Price A, et al. Oxford consensus on primary cam morphology and femoroacetabular impingement syndrome: part 1-definitions, terminology, taxonomy and imaging outcomes. *Br J Sports Med* 2022; 57: 325-341.
5. Heerey J, Kemp J, Agricola R, Srinivasan R, Smith A, Pizzari T, et al. Cam morphology is associated with MRI-defined cartilage defects and labral tears: a case-control study of 237 young adult football players with and without hip and groin pain. *BMJ Open Sport Exerc Med* 2021; 7: e001199.
6. Ahedi H, Winzenberg T, Bierma-Zeinstra S, Blizzard L, van Middelkoop M, Agricola R, et al. A prospective cohort study on cam morphology and its role in progression of osteoarthritis. *Int J Rheum Dis* 2022; 25: 601-612.
7. Saberi Hosnijeh F, Zuiderwijk ME, Versteeg M, Smeele HT, Hofman A, Uitterlinden AG, et al. Cam Deformity and Acetabular Dysplasia as Risk Factors for Hip Osteoarthritis. *Arthritis Rheumatol* 2017; 69: 86-93.
8. Agricola R, Heijboer MP, Bierma-Zeinstra SM, Verhaar JA, Weinans H, Waarsing JH. Cam impingement causes osteoarthritis of the hip: a nationwide prospective cohort study (CHECK). *Ann Rheum Dis* 2013; 72: 918-923.
9. Bardakos NV, Villar RN. Predictors of progression of osteoarthritis in femoroacetabular impingement: a radiological study with a minimum of ten years follow-up. *J Bone Joint Surg Br* 2009; 91: 162-169.
10. Doherty M, Courtney P, Doherty S, Jenkins W, Maciewicz RA, Muir K, et al. Nonspherical femoral head shape (pistol grip deformity), neck shaft angle, and risk of hip osteoarthritis: a case-control study. *Arthritis Rheum* 2008; 58: 3172-3182.
11. Nicholls AS, Kiran A, Pollard TC, Hart DJ, Arden CP, Spector T, et al. The association between hip morphology parameters and nineteen-year risk of end-stage osteoarthritis of the hip: a nested case-control study. *Arthritis Rheum* 2011; 63: 3392-3400.
12. Casartelli NC, Maffioletti NA, Valenzuela PL, Grassi A, Ferrari E, van Buuren MMA, et al. Is hip morphology a risk factor for developing hip osteoarthritis? A systematic review with meta-analysis. *Osteoarthritis Cartilage* 2021; 29: 1252-1264.
13. Maxwell L, Shreedhar P, Carabali M, Levis B. How to plan and manage an individual participant data meta-analysis. An illustrative toolkit. *Res Synth Methods* 2024; 15: 166-174.
14. van Buuren MMA, Riedstra NS, van den Berg MA, Boel F, Ahedi H, Arbabi V, et al. Cohort profile: Worldwide Collaboration on OsteoArthritis prediCtion for the Hip (World COACH) - an international consortium of prospective cohort studies with individual participant data on hip osteoarthritis. *BMJ Open* 2024; 14: e077907.
15. Wesseling J, Boers M, Viergever MA, Hilberdink WK, Lafeber FP, Dekker J, et al. Cohort Profile: Cohort Hip and Cohort Knee (CHECK) study. *Int J Epidemiol* 2016; 45: 36-44.

16. Hart DJ, Spector TD. Cigarette smoking and risk of osteoarthritis in women in the general population: the Chingford study. *Ann Rheum Dis* 1993; 52: 93-96.
17. Nelson AE, Hu D, Arbeeve L, Alvarez C, Cleveland RJ, Schwartz TA, et al. Point prevalence of Hip Symptoms, Radiographic, And Symptomatic OA at Five Time Points: The Johnston County Osteoarthritis Project, 1991-2018. *Osteoarthr Cartil Open* 2022; 4.
18. Segal NA, Nevitt MC, Gross KD, Hietpas J, Glass NA, Lewis CE, et al. The Multicenter Osteoarthritis Study: opportunities for rehabilitation research. *PM R* 2013; 5: 647-654.
19. Nevitt M, Felson D, Lester G. The osteoarthritis initiative. Protocol for the cohort study 2006; 1.
20. Hofman A, Darwish Murad S, van Duijn CM, Franco OH, Goedegebure A, Ikram MA, et al. The Rotterdam Study: 2014 objectives and design update. *Eur J Epidemiol* 2013; 28: 889-926.
21. Cummings SR, Black DM, Nevitt MC, Browner WS, Cauley JA, Genant HK, et al. Appendicular bone density and age predict hip fracture in women. The Study of Osteoporotic Fractures Research Group. *JAMA* 1990; 263: 665-668.
22. Notzli HP, Wyss TF, Stoecklin CH, Schmid MR, Treiber K, Hodler J. The contour of the femoral head-neck junction as a predictor for the risk of anterior impingement. *J Bone Joint Surg Br* 2002; 84: 556-560.
23. Boel F, Riedstra NS, Tang J, Hanff DF, Ahedi H, Arbabi V, et al. Reliability and agreement of manual and automated morphological radiographic hip measurements. *Osteoarthr Cartil Open* 2024; 6: 100510.
24. Lindner C, Thiagarajah S, Wilkinson JM, arc OC, Wallis GA, Cootes TF. Fully automatic segmentation of the proximal femur using random forest regression voting. *IEEE Trans Med Imaging* 2013; 32: 1462-1472.
25. Boel F, de Vos-Jakobs S, Riedstra N, Lindner C, Runhaar J, Bierma-Zeinstra S, et al. Automated radiographic hip morphology measurements: An open-access method. *Osteoarthritis Imaging* 2024; 4: 100181.
26. F. Boel NSR, J. Tang, D.F. Hanff, H. Ahedi, V. Arbabi, N.K. Arden, S.M.A. Bierma-Zeinstra, M.M.A. van Buuren, F.M. Cicuttini, T.F. Cootes, K. Crossley, D. Eygendaal, D.T. Felson, W.P. Gielis, J. Heerey, G. Jones, S. Kluzek, N.E. Lane, C. Lindner, J. Lynch, J. van Meurs, A.E. Nelson, A.B. Mosler, M.C. Nevitt, E.H. Oei, J. Runhaar, H. Weinans, R. Agricola. Reliability and agreement of manual and automated morphological radiographic hip measurements. *Osteoarthritis and Cartilage Open* 2024: 100510.
27. Mascarenhas VV, Castro MO, Afonso PD, Rego P, Dienst M, Sutter R, et al. The Lisbon Agreement on femoroacetabular impingement imaging-part 2: general issues, parameters, and reporting. *Eur Radiol* 2021; 31: 4634-4651.
28. Kemp JL, Osteras N, Mathiessen A, Nordsletten L, Agricola R, Waarsing JH, et al. Relationship between cam morphology, hip symptoms, and hip osteoarthritis: the Musculoskeletal pain in Ullersaker Study (MUST) cohort. *Hip Int* 2021; 31: 789-796.
29. Nelson AE, Stiller JL, Shi XA, Leyland KM, Renner JB, Schwartz TA, et al. Measures of hip morphology are related to development of worsening radiographic hip osteoarthritis over 6 to 13 year follow-up: the Johnston County Osteoarthritis Project. *Osteoarthritis Cartilage* 2016; 24: 443-450.
30. Tang J, van Buuren MMA, Riedstra NS, Boel F, Runhaar J, Bierma-Zeinstra S, et al. Cam morphology is strongly and consistently associated with development of radiographic

- hip osteoarthritis throughout 4 follow-up visits within 10 years. *Osteoarthritis Cartilage* 2023.
31. Faber BG, Frysz M, Hartley AE, Ebsim R, Boer CG, Saunders FR, et al. A Genome-Wide Association Study Meta-Analysis of Alpha Angle Suggests Cam-Type Morphology May Be a Specific Feature of Hip Osteoarthritis in Older Adults. *Arthritis Rheumatol* 2023; 75: 900-909.
 32. Kohn MD, Sassoon AA, Fernando ND. Classifications in Brief: Kellgren-Lawrence Classification of Osteoarthritis. *Clin Orthop Relat Res* 2016; 474: 1886-1893.
 33. M. Gamer JL, M.M. Gamer, A. Robinson, W. Kendall's. Package 'irr' 2012.
 34. Altman RD, Gold GE. Atlas of individual radiographic features in osteoarthritis, revised. *Osteoarthritis Cartilage* 2007; 15 Suppl A: A1-56.
 35. Agricola R, Waarsing JH, Thomas GE, Carr AJ, Reijman M, Bierma-Zeinstra SM, et al. Cam impingement: defining the presence of a cam deformity by the alpha angle: data from the CHECK cohort and Chingford cohort. *Osteoarthritis Cartilage* 2014; 22: 218-225.
 36. Sutter R, Dietrich TJ, Zingg PO, Pfirrmann CW. How useful is the alpha angle for discriminating between symptomatic patients with cam-type femoroacetabular impingement and asymptomatic volunteers? *Radiology* 2012; 264: 514-521.
 37. Lanyon P, Muir K, Doherty S, Doherty M. Age and sex differences in hip joint space among asymptomatic subjects without structural change: implications for epidemiologic studies. *Arthritis Rheum* 2003; 48: 1041-1046.
 38. King LK, March L, Anandacoomarasamy A. Obesity & osteoarthritis. *Indian J Med Res* 2013; 138: 185-193.
 39. Wang C, Zhu Y, Liu Z, Long H, Ruan Z, Zhao S. Causal associations of obesity related anthropometric indicators and body compositions with knee and hip arthritis: A large-scale genetic correlation study. *Front Endocrinol (Lausanne)* 2022; 13: 1011896.
 40. Funck-Brentano T, Nethander M, Moverare-Skrtic S, Richette P, Ohlsson C. Causal Factors for Knee, Hip, and Hand Osteoarthritis: A Mendelian Randomization Study in the UK Biobank. *Arthritis Rheumatol* 2019; 71: 1634-1641.
 41. Badley EM, Zahid S, Wilfong JM, Perruccio AV. Relationship Between Body Mass Index and Osteoarthritis for Single and Multisite Osteoarthritis of the Hand, Hip, or Knee: Findings From a Canadian Longitudinal Study on Aging. *Arthritis Care Res (Hoboken)* 2022; 74: 1879-1887.
 42. Yuan J, Wang D, Zhang Y, Dou Q. Genetically predicted obesity and risk of hip osteoarthritis. *Eat Weight Disord* 2023; 28: 11.
 43. Agricola R, Bessems JH, Ginai AZ, Heijboer MP, van der Heijden RA, Verhaar JA, et al. The development of Cam-type deformity in adolescent and young male soccer players. *Am J Sports Med* 2012; 40: 1099-1106.
 44. van Buuren MMA, Heerey JJ, Smith A, Crossley KM, Kemp JL, Scholes MJ, et al. The association between statistical shape modeling-defined hip morphology and features of early hip osteoarthritis in young adult football players: Data from the femoroacetabular impingement and hip osteoarthritis cohort (FORCe) study. *Osteoarthr Cartil Open* 2022; 4: 100275.
 45. Agricola R, van Buuren MMA, Kemp JL, Weinans H, Runhaar J, Bierma-Zeinstra SMA. Femoroacetabular impingement syndrome in middle-aged individuals is strongly associated with the development of hip osteoarthritis within 10-year follow-up: a prospective cohort study (CHECK). *Br J Sports Med* 2024.

Table S1. The characteristic of included hips stratified by per cohort from the World COACH Consortium

Characteristic	World COACH Consortium							
	Chingford (n=1,026) (4%)	JoCoOA (n=763) (3%)	MOST (n=2,009) (9%)	SOF (n=4,807) (20%)	OAI (n=5,568) (23%)	RS-I (n=3,352) (14%)	RS-II (n=2,254) (10%)	RS-III (n=3,092) (13%)
Age in years: mean (±SD)	55.48(5.18)	53.38(5.69)	58.62(8.69)	60.92(7.39)	70.25(4.34)	60.37(8.94)	65.07(6.39)	62.95(6.36)
Women, No (%)	848(83.50)	1,026(100)	422(55.3)	1,439(71.6)	4,807(100)	3,257(58.5)	2,033(60.7)	1,282(56.9)
BMI, kg/m ² : mean (±SD)	26.21(4.03)	25.46(4.00)	29.54(6.02)	29.69(5.02)	26.42(4.35)	28.21(4.59)	26.29(3.52)	27.17(3.86)
Alpha angle, °: mean (±SD)	45.26(8.27)	51.21(12.64)	44.35(8.10)	45.77(8.31)	44.23(8.69)	47.54(10.97)	44.84(8.60)	45.10(9.14)
Cam morphology: No (%)	54(5.3)	177(17.3)	41(5.4)	114(5.7)	254(5.3)	710(12.8)	201(6.0)	156(6.9)
Harmonized RHOA score								
0: No (%)	473(46.6)	894(87.1)	384(50.3)	1,914(95.3)	3,834(79.8)	5,400(97.0)	2,955(88.2)	2,019(89.6)
Harmonized RHOA score								
1: No (%)	410(40.4)	42(4.1)	319(41.8)	85(4.2)	901(18.7)	147(2.6)	371(11.1)	227(10.1)
Harmonized RHOA score								
2: No (%)	132(13.0)	90(8.8)	60(7.9)	10(0.5)	72(1.5)	21(0.4)	26(0.8)	8(0.4)
								77(2.5)

SD: standard deviation; BMI: body mass index; Harmonized RHOA score: 0= no RHOA, 1= Doubtful RHOA, 2= Definite RHOA; CHECK: the Cohort Hip and Cohort Knee study; Chingford: the Chingford study; JoCoOA: the Johnston County Osteoarthritis Project; MOST: the Multicenter Osteoarthritis Study; SOF: the Study of Osteoporotic Fractures; OAI: the Osteoarthritis Initiative; RS: the Rotterdam Study.

Table S2. Association of cam morphology and continuous alpha angle with the development of RHOA at 4-8 years follow-up

	N	Hips develop definite RHOA at follow-up	Absolute risk (%)	Crude odds ratio (95% CI)	Adjusted odds ratio (95% CI)
Cam morphology (alpha angle $\geq 60^\circ$)	2,271	72	3.2	1.77(1.29-2.43)	1.87(1.36-2.59)
Continuous alpha angle	23,386	462	-	1.02(1.01-1.03)	1.02(1.01-1.03)

The odds ratio was adjusted for age, biological sex, and body mass index.

5

The Association between Cam Morphology and Hip Pain in Males and Females within 10 Years: a National Prospective Cohort Study (CHECK)

Jinchi Tang, Michiel M A van Buuren, Fleur Boel, Noortje S Riedstra, Myrthe A van den Berg, Jos Runhaar, Sita Bierma-Zeinstra, Rintje Agricola.

ABSTRACT

Objectives: To determine the association between baseline cam morphology and self-reported hip pain assessed at annual visits over a 10-year follow-up period stratified by biological sex. The secondary aim was to study the association between the magnitude of cam morphology and the severity of pain in symptomatic hips.

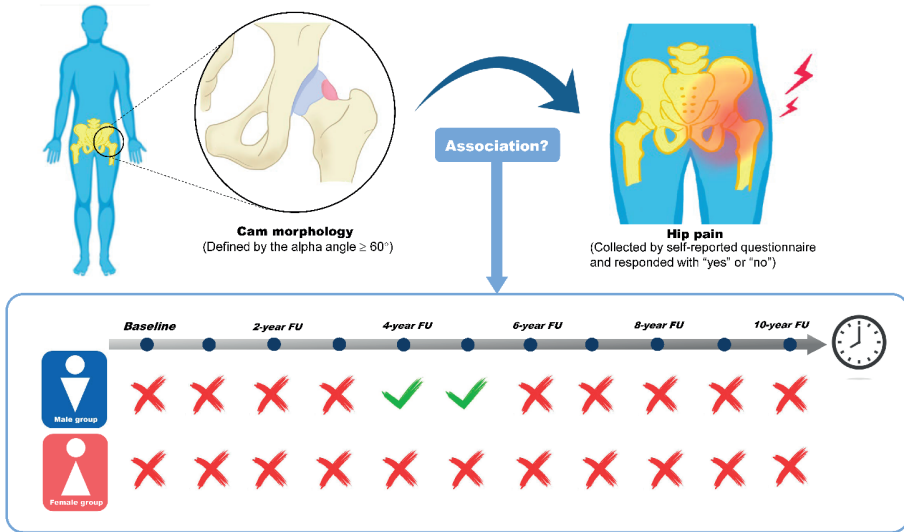
Methods: The nationwide prospective Cohort Hip and Cohort Knee (CHECK) study includes 1,002 participants aged 45-65 years. Logistic regression with generalized estimating equations were used to determine the strength of the associations between (1) baseline cam morphology (both alpha angle $\geq 60^\circ$ and as a continuous measure) and the presence of hip pain at 10 annual follow-up visits and (2) the alpha angle (continuous) and the severity of pain as classified by Numerical Rating Scale at 5-, 8-, 9-, and 10-years. The results are expressed as odds ratios (OR), adjusted for age, biological sex (only in the sex-combined group), body mass index, and follow-up Kellgren and Lawrence grade.

Results: In total, 1,658 hips were included at baseline (1,335 female hips (79.2%)). The prevalence of cam morphology was 11.1% among all hips (29.1% in males; 6.4% in females). No association was found between cam morphology at baseline and the presence of hip pain at any follow-up in the female or sex-combined group. In males, only at 5-year follow-up, significant adjusted ORs were observed for the presence of cam morphology (1.77 (95%CI: 1.01-3.09)) and the alpha angle (1.02 (95%CI:1.00-1.04)). No evidence of associations was found between the alpha angle and the severity of hip pain in any of three groups.

Conclusion: Within this study, no consistent associations were found between cam morphology and hip pain at multiple follow-ups. There might be a weak relationship between cam morphology and hip pain in males, while no such relation was found in females. We did not identify an association between the alpha angle and severity of hip pain.

Keywords: cam morphology; hip pain; femoroacetabular impingement.

GRAPHICAL ABSTRACT



INTRODUCTION

Femoroacetabular impingement syndrome (FAIs) is a motion-related clinical disorder of the hip¹ and a common cause of hip pain in young adults². It is characterized by abnormal contact (impingement) between the femoral head-neck junction and acetabular rim during hip motion, which is thought to cause damage to the acetabular labrum and articular cartilage³⁻⁵. Cam morphology has been identified as an important type of hip morphology associated with FAIs^{1,6}. It represents extra bone formation in the anterolateral head-neck junction resulting in a non-spherical femoral head⁷.

The primary symptom of FAIs is motion- or position-related anterior or anterolateral hip or groin pain^{1,2,8,9}. However, a substantial proportion of individuals with cam morphology are asymptomatic. Consequently, the precise determination of those at risk of experiencing hip pain among individuals with cam morphology remains unknown.

In previous studies, the attempts to relate cam morphology to hip pain have yielded conflicting results. Allen et al¹⁰ and Khanna et al¹¹ demonstrated that cam morphology would put individuals at 2.6- and 4.3-time higher risk of developing hip pain, respectively. Similarly, Larson et al¹² and Guler et al¹³ found in their cross-sectional studies that a greater alpha angle was associated with hip and/or groin pain in athletes. Scholes et al¹⁴ found cam morphology measured in the Dunn45° view but not in the anteroposterior (AP) view was related to worse pain. Conversely, Heery et al¹⁵ found that cam morphology was unrelated to the presence or severity of hip pain in football players. This finding was also supported by other studies¹⁶⁻²⁰.

Besides populations with different levels of hip motion activity^{16, 17, 21} and different definitions for cam morphology, there might also be other explanations for the conflicting results between cam morphology and hip pain such as the duration and frequency of follow-up and differences in biological sex. The fluctuating nature of pain may yield different outcomes within the same population using the same definition at different time points. A recent study revealed that relevant fluctuations in hip pain were found in 37% of participants over a 10-year follow-up period²². Therefore, multiple follow-ups may help to provide more concise data on hip pain. Moreover, cam morphology was recently found to be associated with hip pain in males but not in females²⁰, which raises the question of whether biological sex also plays a role in the association between cam morphology and hip pain. Cam morphology manifests differently between sexes as males usually have a higher prevalence²³ and greater magnitude of cam morphology than females^{24, 25}. This might affect the association with hip pain as well.

Exploring the relationship between cam morphology and hip pain at multiple time points and in both sexes separately could offer a more comprehensive understanding of the role of cam morphology in the presence and severity of hip pain. Therefore, the aim of this study was to determine the association between baseline cam morphology and hip pain at baseline and annual visits over 10 years of follow-up for male and females. We also aimed to determine the association between the alpha angle and the severity of hip pain in symptomatic.

METHODS

Study population

The Cohort Hip and Cohort Knee (CHECK) study constitutes a nationwide multicenter prospective cohort involving 1,002 individuals. Between October 2002 and September 2005, the study recruited all participants within the Netherlands^{26, 27}. Individuals were eligible to participate if they had first onset of pain and/or stiffness of either the knee or hip; were between 45 and 65 years old; had not yet consulted their GP for these symptoms, or the first consultation was within 6 months before entry. Individuals were excluded if they had any other pathological condition that could explain their symptoms, any comorbidity precluding physical evaluation and/or follow-up of at least 10 years, malignancy in the past 5 years or inability to understand the Dutch language. Radiological data was collected within 11 general and academic hospitals in the Netherlands.

For the present study, data was collected from the CHECK cohort at hip level. Hips without complete demographic data or a high-quality baseline radiograph were excluded from the analysis.

The study was approved by the medical ethics committees of all participating centers, and written informed consent was obtained from all participants.

Baseline radiography and cam morphology

Standardized weight-bearing anteroposterior (AP) radiographs of the pelvis or hip were obtained at baseline and 2-, 5-, 8-, and 10-year follow-ups. During acquisition of the AP pelvic radiograph, participants were positioned with the lower extremities parallel and with 15° internal rotation, resulting in the touch of the medial sides of the distal part of the big toes. The X-ray beam was centered on the proximal edge of the pubic symphysis. The tube to film distance was 100 cm. The first 124 participants

who entered the CHECK study had an AP hip radiograph of each hip obtained according to the same protocol but with the X-ray beam centered on the groin.

We used the alpha angle, a commonly applied and agreed upon method, to quantify cam morphology^{7,28}. On the baseline AP radiographs, the alpha angle was constructed by one line from the femoral head center through the middle of the femoral neck and a second line from the femoral head center through a point where the contour of the femoral head-neck junction exits the radius of the best fitting circle of the femoral head²⁹ (**Figure 1**). In this study, the alpha angle was calculated automatically on AP radiographs from the landmark points set of the SSM software by a MATLAB script (V.7.1.0). The previously published intraclass correlation coefficients were: 0.73 for interobserver reliability, and intra-observer reliability ranged from 0.85 to 0.99^{8, 30}. To determine the presence of cam morphology, a cut-off alpha angle value of $\geq 60^\circ$ was used. This specific value was validated in a recent systematic review³¹, as it best distinguished between hips having cam morphology and those without. Furthermore, we adopted this dichotomous threshold value because the CHECK cohort previously showed a bimodal distribution of the alpha angle around 60° ³².

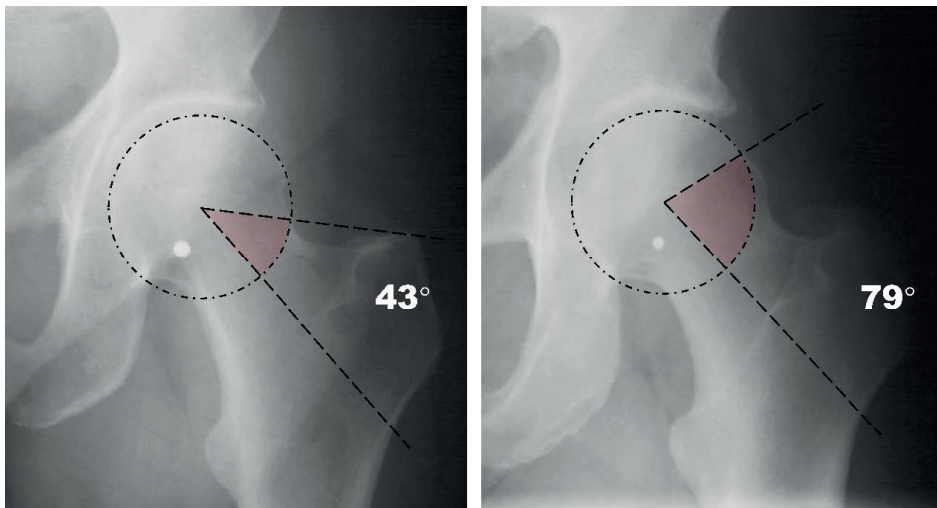


Figure 1. The alpha angle as measured on an anteroposterior pelvic radiograph (1a: alpha angle: 43° ; 1b: alpha angle: 79°).

Hip pain

At baseline and subsequent annual follow-up visits over 10 years (1-year to 10-year follow-up), data regarding hip pain were collected by self-reported questionnaires. Participants were asked to answer whether they experienced pain in their left and/or right hip (responding with “yes” or “no”) for the past week. Their answers were used to define the presence of hip pain. In addition, at 5-, 8-, 9-, and 10-year follow-ups, participants were specifically asked to report the intensity of pain they had experienced in relation to their left or right hips during the preceding week. Hip pain intensity was assessed by the Numerical Rating Scale (NRS) with score ranging from 0 to 10 (higher scores indicating more pain). Given the limited number of high NRS scores observed, scores from symptomatic hips (NRS score >0) were categorized into three groups to define the severity of hip pain: mild pain (NRS score: 1-3), moderate pain (NRS score:4-6) and severe pain (NRS score:7-10).

Statistical analysis

Descriptive statistics were used to analyze the baseline characteristics with mean and standard deviation for continuous variables and frequencies and percentage for categorical variables. The independent t-test was used for comparisons of continuous variables and chi-square test for categorical variables between the following groups: included hips vs excluded hips; hips with cam morphology vs hips without; male hips vs female hips. Hips excluded from analysis at each visit encompassed those with missing or insufficient quality of radiographs at baseline, as well as hips that underwent a total hip replacement at follow-up or those lost to follow-up. For our primary aim, binary logistic regression was used to determine the association between cam morphology and hip pain on hip-level at baseline and each follow-up visit over 10 years. Cam morphology was presented in two ways: as a dichotomous variable indicating the presence of cam morphology^{31,32} and as a continuous variable representing the alpha angle value. To determine the association between the alpha angle and hip pain severity, asymptomatic hips at each visit were excluded and ordinal logistic regression was used. All tests were independent of each other and were performed with generalized estimating equations (GEE), as GEE accounts for statistical dependency between two hips within one subject. All analyses were adjusted for age, biological sex (only in sexes combined group), body mass index (BMI) at baseline, Kellgren & Lawrence (KL) grade at follow-up and expressed in odds ratios with 95% confidence intervals. It should be noted that we only acquired follow-up KL grades at 2-,5-,8-, and 10-year follow-ups. For tests at other time points without KL grades, the nearest previously available follow-up KL grade was adjusted, taking into account the irreversible nature of pathophysiological changes in hip osteoarthritis. Subsequently, we grouped all the included hips into male and female categories based on the biological sex of

the participants and repeated the aforementioned primary analyses in the two groups separately. The effect was considered significant at $P < 0.05$. All statistical analyses were performed in IBM SPSS V.26.0 (Armonk, NY: IBM Corp).

RESULTS

Of the baseline 2,004 hips from 1,002 individuals in the CHECK cohort, 1,685 hips were included. Of 319 excluded hips, 22 hips did not have baseline radiographs available, 295 hips had unavailable alpha angle values due to insufficient quality of radiographs and 2 hips missed data of BMI. The complete flow of participants (included hips) is provided in **Figure 2**. Of 1,685 included hips, there were 674 symptomatic hips (40.0%); there were 350 hips (20.8%) from males and 1,335 hips (79.2%) from females. The participants had a mean age of 55.9 ± 5.2 years and a mean BMI of $26.2 \pm 4.1 \text{ kg/m}^2$. (**Table 1**).

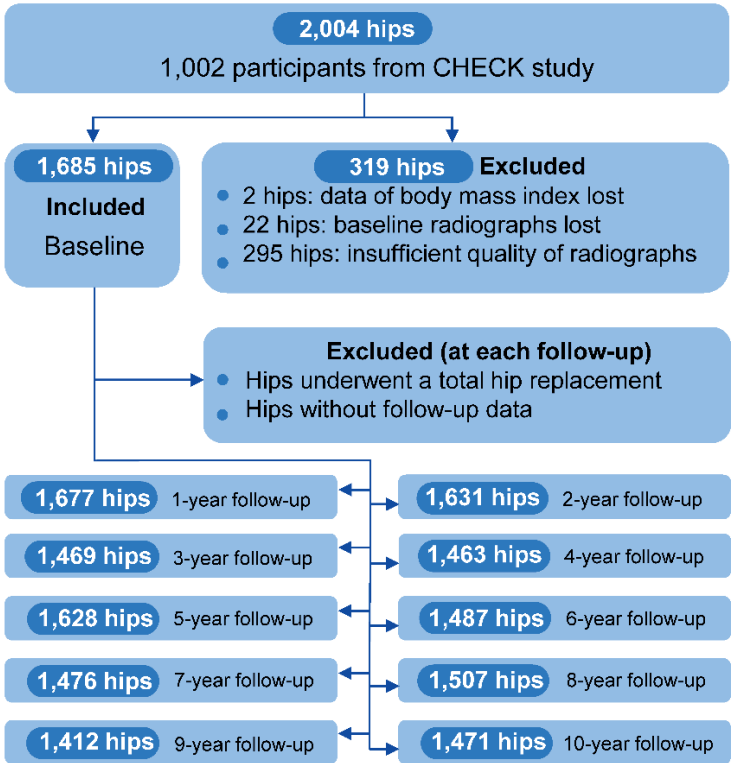


Figure 2. The flow of participants (hips) from the beginning of the study and through different follow-ups over 10 years.

Table 1. Differences in baseline characteristics among three groups: included and excluded hips, hips with and without cam morphology, and hips from males and females.

Baseline characteristics	CHECK study (n=2,004)		Included hips (n=1,685)		Included hips (n=1,685)		P value	P value
	Included hips (n=1,685)	Excluded hips (n=319)	Included hips with cam morphology (n=187)	hips without cam morphology (n=1,498)	Male group (n=350)	Female group (n=1,355)		
Age in years: mean (±SD)	55.9(5.2)	56.2(5.4)	57.1(4.9)	55.7(5.2)	56.2(5.4)	55.7(5.1)	<0.001	0.151
Women, No (%)	1,335(79.2)	245(76.8)	85(45.5)	1,250(83.3)	0(0)	1,355(100)	<0.001	-
BMI, kg/m ² : mean (±SD)	26.2(4.1)	25.9(3.6)	27.0(4.2)	26.1(4.0)	26.2(3.4)	26.2(4.2)	0.006	0.827
Alpha angle, °: mean (±SD)	47.3(13.2)	45.1(2.8)	80.9(12.9)	43.1(4.0)	54.6(16.5)	45.4(11.4)	<0.001	<0.001
Hip pain symptom, No (%)	674(40.0)	122(38.2)	79(42.2)	595(39.7)	126(36.0)	548(41.1)	0.506	0.086

BMI: body mass index.

The prevalence of hip pain fluctuated during the 10-year follow-up period, with the highest value of 40.0% at baseline and the lowest value of 27.5% at 9-year follow-up. More detailed information on the prevalence of hip pain in different subgroups is provided in **Figure 3** and the distribution of NRS scores at four follow-ups is provided in **Figure 4**.

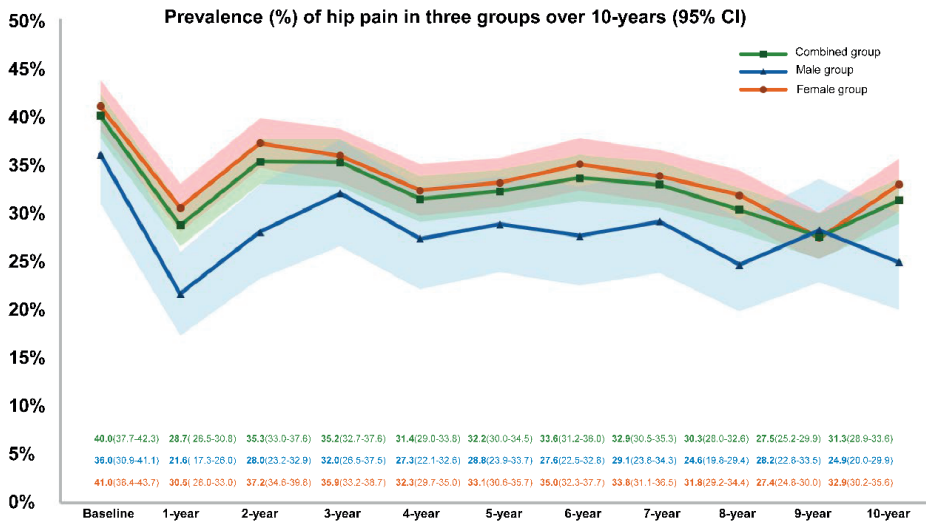


Figure 3. The prevalence of hip pain at baseline and during annual follow-ups over 10 years in three groups: combined group (green line), male group (blue line), and female group (red line). The area around the line with the same color represents the 95% confidence interval.

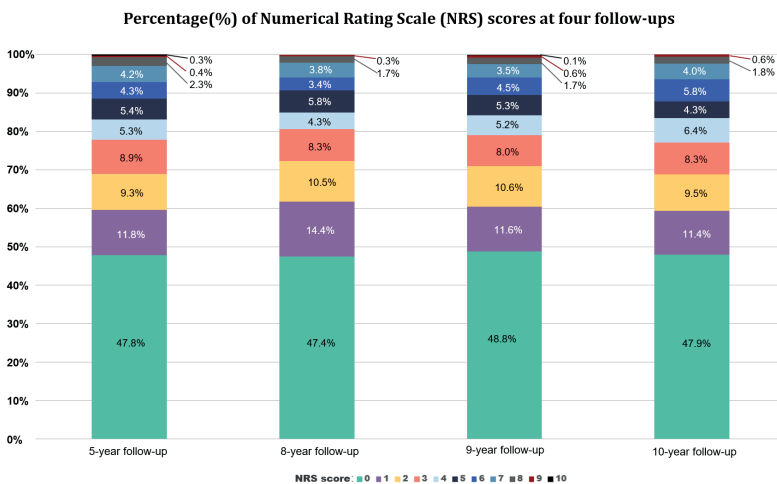


Figure 4. The distribution of Numerical Rating Scale (NRS) scores at 5-, 8-, 9-, and 10-year follow-ups.

At baseline, the prevalence of cam morphology (alpha angle $\geq 60^\circ$) was 11.1% among all hips, with a distribution of 29.1% (102/350) in male hips and 6.4% (85/1,335) in female hips. No evidence of an association between cam morphology (alpha angle $\geq 60^\circ$) and the presence of hip pain was observed at any follow-up time point in the female and combined groups. In males, cam morphology was associated with experiencing hip pain at 4-year and 5-year follow-up, but after adjustment for confounders only at 5-year follow-up (**Table 2**).

Table 2. Association between cam morphology (alpha angle $\geq 60^\circ$) and the presence of hip pain at baseline and annual follow-ups over 10 years in male, female, and sex-combined groups.

Group	Follow-up	Predictor: cam morphology (alpha angle $\geq 60^\circ$)		
		Absolute risk (%)	Crude OR (95% CI)	Adjusted OR (95% CI)
Combined	Baseline	79/187(42.2)	1.12(0.82-1.53)	0.98(0.69-1.41)
	1-year	59/182(32.4)	1.14(0.81-1.61)	1.24(0.84-1.81)
	2-year	68/173(39.3)	1.14(0.81-1.60)	1.10(0.75-1.61)
	3-year	55/153(35.9)	1.00(0.70-1.42)	0.86(0.59-1.26)
	4-year	57/154(37.0)	1.2(0.83-1.75)	1.13(0.76-1.67)
	5-year	63/168(37.5)	1.13(0.80-1.61)	1.04(0.71-1.52)
	6-year	56/149(37.6)	1.23(0.86-1.75)	1.19(0.82-1.74)
	7-year	52/151(34.4)	1.04(0.72-1.49)	0.91(0.61-1.36)
	8-year	53/149(35.6)	1.31(0.92-1.88)	1.27(0.86-1.89)
	9-year	46/138(33.3)	1.20(0.80-1.81)	1.05(0.68-1.62)
Male	Baseline	44/102(43.1)	1.60(0.99-2.60)	1.27(0.73-2.19)
	1-year	29/99(29.3)	1.68(0.95-2.94)	1.50(0.82-2.74)
	2-year	35/92(38.0)	1.55(0.90-2.67)	1.19(0.65-2.15)
	3-year	30/78(38.5)	1.32(0.74-2.34)	1.03(0.55-1.93)
	4-year	30/79(38.0)	1.86(1.04-3.31)	1.62(0.89-2.94)
	5-year	38/92(41.3)	1.94(1.14-3.28)	1.77(1.01-3.09)
	6-year	31/82(37.8)	1.74(1.00-3.03)	1.40(0.78-2.51)
	7-year	27/81(33.3)	1.26(0.76-2.07)	1.11(0.64-1.95)
	8-year	26/82(31.7)	1.38(0.85-2.25)	1.23(0.73-2.06)
	9-year	29/74(39.2)	1.48(0.85-2.58)	1.28(0.75-2.19)
10-year	27/82(32.9)	1.55(0.86-2.78)	1.40(0.76-2.58)	

Table 2. Association between cam morphology (alpha angle $\geq 60^\circ$) and the presence of hip pain at baseline and annual follow-ups over 10 years in male, female, and sex-combined groups. (continued)

Group	Follow-up	Predictor: cam morphology (alpha angle $\geq 60^\circ$)		
		Absolute risk (%)	Crude OR (95% CI)	Adjusted OR (95% CI)
Female	Baseline	35/85(41.2)	0.98(0.62-1.55)	0.80(0.49-1.31)
	1-year	30/83(36.1)	1.14(0.70-1.88)	1.08(0.65-1.81)
	2-year	33/81(40.7)	1.14(0.71-1.85)	1.01(0.61-1.68)
	3-year	25/75(33.3)	0.90(0.55-1.46)	0.74(0.45-1.23)
	4-year	27/75(36.0)	1.03(0.60-1.77)	0.89(0.51-1.55)
	5-year	25/76(32.9)	0.80(0.46-1.38)	0.68(0.39-1.20)
	6-year	25/67(37.3)	1.16(0.70-1.90)	1.03(0.62-1.72)
	7-year	25/70(35.7)	1.00(0.58-1.72)	0.80(0.45-1.44)
	8-year	27/67(40.3)	1.54(0.89-2.66)	1.33(0.75-2.37)
	9-year	17/64(26.6)	0.93(0.49-1.77)	0.81(0.41-1.58)
	10-year	17/63(27.0)	0.73(0.40-1.33)	0.67(0.37-1.24)

OR: Odds Ratio, adjusted for age, sex (only in sex-combined group), body mass index and follow-up Kellgren & Lawrence grade.

Similar results were observed when using the continuous alpha angle as a risk factor. No evidence of an association between the alpha angle and the presence of hip pain was found at any follow-up time point in the female and combined groups. In males, greater cam morphology was associated with hip pain at baseline, 5-year, and 6-year follow-ups. However, after adjusting for confounders, this association was significant only at the 5-year follow-up (**Table 3**).

Table 3. Association between continuous alpha angle and the presence of hip pain at baseline and annual follow-ups over 10 years in male, female, and sex-combined groups.

Group	Follow-up	Predictor: continuous alpha angle	
		Crude OR (95% CI)	adjusted OR (95% CI)
Combined	Baseline	1.01(1.00-1.01) *	1.00(0.99-1.01)
	1-year	1.00(1.00-1.01) *	1.01(1.00-1.01) *
	2-year	1.01(1.00-1.01) *	1.00(0.99-1.01)
	3-year	1.00(0.99-1.01)	1.00(0.99-1.01)
	4-year	1.00(0.99-1.01)	1.00(0.99-1.01)
	5-year	1.00(0.99-1.01)	1.00(0.99-1.01)
	6-year	1.01(1.00-1.01) *	1.00(1.00-1.01) *
	7-year	1.00(0.99-1.01)	0.99(0.98-1.00)†
	8-year	1.01(1.00-1.02) *	1.00(0.99-1.02)
	9-year	1.00(0.99-1.01)	1.00(0.99-1.01)
	10-year	1.00(0.99-1.01)	1.00(0.99-1.01)
Male	Baseline	1.02(1.00-1.03) **	1.01(0.99-1.03)
	1-year	1.01(1.00-1.03) *	1.01(0.99-1.03)
	2-year	1.02(1.00-1.03)	1.01(0.99-1.02)
	3-year	1.01(0.99-1.03)	1.00(0.99-1.02)
	4-year	1.02(1.00-1.03) *	1.01(0.99-1.03)
	5-year	1.02(1.01-1.04)	1.02(1.00-1.04) **
	6-year	1.02(1.00-1.04) **	1.01(1.00-1.03) *
	7-year	1.01(0.99-1.02)	1.00(0.98-1.02)
	8-year	1.01(0.99-1.03)	1.01(0.99-1.02)
	9-year	1.01(0.99-1.03)	1.01(0.99-1.02)
	10-year	1.01(0.99-1.03)	1.01(0.99-1.02)
Female	Baseline	1.00(1.00-1.01) *	1.00(0.99-1.01)
	1-year	1.01(0.99-1.02)	1.00(0.99-1.01)
	2-year	1.01(1.00-1.02) *	1.00(0.99-1.01)
	3-year	1.00(0.99-1.01)	0.99(0.98-1.01)
	4-year	1.00(0.99-1.01)	1.00(0.98-1.01)
	5-year	1.00(0.98-1.01)	0.99(0.98-1.00)†
	6-year	1.00(0.99-1.01)	1.00(0.99-1.01)
	7-year	1.00(0.99-1.01)	0.99(0.98-1.00)
	8-year	1.01(1.00-1.02) *	1.00(0.99-1.02)
	9-year	1.00(0.98-1.01)	0.99(0.98-1.01)
	10-year	0.99(0.98-1.01)	0.99(0.98-1.00)†

The lower bound of 95% CI is approximately equal but less (*) or more (**) than 1; The upper bound of 95% CI is approximately equal but more than 1 (†); OR: Odds Ratio, represented every 1-degree increase in the alpha angle and adjusted for age, sex (only in the combined group), body mass index and follow-up Kellgren & Lawrence grade.

The distribution of the severity of hip pain at four follow-ups is shown in **Table 4**. No evidence of an association was observed between the alpha angle and severity of hip pain in all three groups (**Table 5**).

Table 4. The distribution of the severity of hip pain in symptomatic hips at 5-, 8-, 9-, and 10-year follow-ups.

Group	Follow-up	Included hips	The severity of hip pain		
			Mild pain (%)	Moderate pain (%)	Severe pain (%)
Combined	5-year	834	480(57.6)	239(28.7)	115(13.8)
	8-year	784	495(63.1)	201(25.6)	88(11.2)
	9-year	710	419(59.0)	208(29.3)	83(11.7)
	10-year	749	420(56.1)	238(31.8)	91(12.1)
Male	5-year	140	86(61.4)	44(31.4)	10(7.1)
	8-year	149	108(72.5)	29(19.5)	12(8.1)
	9-year	138	92(66.7)	39(28.3)	7(5.1)
	10-year	150	99(66.0)	40(26.7)	11(7.3)
Female	5-year	694	394(56.8)	195(28.1)	105(15.1)
	8-year	635	387(60.9)	172(27.1)	76(12.0)
	9-year	572	327(57.2)	169(29.5)	76(13.3)
	10-year	599	321(53.6)	198(33.1)	80(13.4)

Table 5. Association between the alpha angle and the severity of hip pain at 5-, 8-, 9-, and 10-year follow-ups in male, female, and sex-combined groups.

Group	Follow-up	Predictor: the alpha angle (continuous value)			
		Crude OR (95% CI)	P value	adjusted OR (95% CI)	P value
Combined	5-year	1.00 (0.99-1.01)	0.396	1.00(0.99-1.01)	0.524
	8-year	1.00(0.99-1.01)	0.82	1.00(0.99-1.01)	0.911
	9-year	1.00(0.99-1.02)	0.598	1.00(0.99-1.01)	0.811
	10-year	1.00(0.99-1.01)	0.829	1.00(0.99-1.02)	0.593
Male	5-year	1.00(0.98-1.03)	0.700	1.00(0.98-1.03)	0.800
	8-year	1.00(0.99-1.01)	0.561	1.00(0.99-1.01)	0.572
	9-year	1.00(0.98-1.03)	0.934	1.00(0.97-1.03)	0.997
	10-year	1.01(0.99-1.04)	0.201	1.01(0.98-1.03)	0.512
Female	5-year	1.01(1.00-1.02)	0.146	1.00 (0.99-1.02)	0.423
	8-year	1.00(0.99-1.02)	0.669	1.00(0.99-1.01)	0.935
	9-year	1.01(0.99-1.02)	0.292	1.00(0.99-1.02)	0.615
	10-year	1.00(0.99-1.02)	0.882	1.00(0.98-1.02)	0.914

OR: Odds Ratio, represented every 1-degree increase in the alpha angle and adjusted for age, sex (only in the sex-combined group), body mass index, and follow-up Kellgren & Lawrence grade.

DISCUSSION

In this study, cam morphology was not associated with the presence of self-reported hip pain throughout 10 years of follow-up in females and inconclusive results were found in males. The magnitude of the alpha angle showed no association with hip pain severity in either males or females.

Our results mostly align with studies that did not find an association between the presence of cam morphology and hip pain. However, other studies have shown a significant association between cam morphology and hip pain in populations comprising both sexes¹⁰⁻¹³. These studies have several similarities. Firstly, the definitions of cam morphology used differed from the current recommendations to use an alpha angle threshold of 60°. The threshold value for the alpha angle used in those studies ranged from 50.5°¹¹ to 55.5°¹⁰, potentially leading to an overestimation of the prevalence of cam morphology. Secondly, the populations in these studies had higher average alpha angles exceeding 60° which points toward populations with a high prevalence of cam morphology (ranging from 65.0% to 88.9%)^{10, 12}. This contrasts with the findings of the present study, where the average alpha angle value was 47°. None of the previous studies focused on sex differences except for one cross-sectional study by Faber et al²⁰, which also found an association between cam morphology and hip pain in males but not in females. Our results at 5-year follow-up are in line with this finding, although we did not find significant associations at the other time points, which may be attributable to the fluctuating nature of pain.

In our results, we found that the prevalence of hip pain fluctuated over 10 years, which is supported by the previous findings in the CHECK study that only 32% of participants showed stable pain over 10 years²². The course of hip pain could be easily influenced by external factors, such as topical temperature, exercise and stretching, or using medication for pain relief^{33, 34}. Internal factors, such as cartilage loss, labral tears, synovitis, bone marrow lesions in hip, and subchondral cyst, also play a role in the fluctuation of hip pain. MRI measurements have shown that the progression of these structural diseases is associated with worsening hip symptoms, complicating the course of hip pain³⁵⁻³⁷. Variation existed in the course of hip pain in previous studies^{38, 39}, which showed that hip pain can be stable or progressive during the follow-up, but also fluctuating²². Therefore, the strength of association between any predictor and outcome of hip pain would also change depending on the time frame of follow-up. Studies focusing on this association should take into account the different selected follow-up time points, rather than solely concentrating on pain outcome at a single point in time. However, none of the aforementioned studies exploring the

relationship between cam morphology and hip pain incorporated multiple follow-up assessments.

Biological sex might play a role in the etiology of hip pain regarding cam morphology. Our findings suggest that there is no association between the presence of cam morphology and hip pain in the female or female-dominated combined groups. However, we observed that cam morphology may nearly double the odds of experiencing hip pain in males at 5 years follow-up, independent of the development of hip OA. Although no significant associations were found at other time points, the ORs were consistently higher than 1, potentially indicating a trend towards pain in hips with cam morphology. Such a trend was not observed in females. The difference might be explained by different manifestations of cam morphology and pain between sexes. Firstly, numerous studies have demonstrated that males have greater magnitudes of cam morphology than females^{23, 24}. In our results, the average alpha angle at baseline differed significantly between sexes, with 54.6° in males and 45.4° in females. Secondly, men and women experience pain differently, with women generally having a lower pain threshold and tolerance^{40, 41}. Experimental pain studies have shown that women exhibit heightened pain sensitivity, increased pain facilitation, and reduced pain inhibition compared to men⁴². In our results, the prevalence of hip pain is consistently higher in the female group, at baseline and at nearly all follow-up time points (except at the 9-year follow-up), with the most significant difference observed at the 2-year follow-up (37.2% in females vs. 28.0% in males). Less cases with cam morphology and more painful hips without cam morphology may indicate that there are other causes for experiencing hip pain than cam morphology in females, for which we could not adjust, given the self-reported nature of the pain variable used.

We found no association between the alpha angle and severity of hip pain at four follow-ups within 10 years in all three groups. Those results align with prior findings by Scholes et al¹⁴ that the alpha angle (quantified on an AP view) was not significantly associated with pain intensity, as measured by scores from the International Hip Outcome Tool-33 (iHOT-33) and Copenhagen Hip and Groin Outcome Score (HAGOS). In addition, the alpha angle measured on a Dunn view previously demonstrated a modest correlation with worse iHOT-33 scores, suggesting that the location of cam morphology may be related to pain intensity¹⁴. Future research might further elucidate what the influence of cam morphology location on pain is.

Our study has several notable strengths. First, we conducted ten consecutive annual follow-up assessments to provide a more precise understanding of the association between cam morphology and hip pain. Most importantly, we conducted separate risk

analyses for males and females due to the observed differences in both cam morphology characteristics and hip pain between the sexes. The main limitation of this study is that we capture the outline of the cam morphology solely in the coronal plane by using AP radiographs. Given that cam morphology is inherently a three-dimensional construct, our study may have underestimated its prevalence. Nevertheless, it's important to note that cam morphology is predominantly located at the anterolateral part of the femoral head-neck junction⁷, making the AP view a good choice for capturing most morphological information. Another limitation is that our study participants, drawn from the CHECK study, exhibited initial symptoms in the hip, knee, or both, and were aged between 45 and 65 years at baseline. Therefore, the generalizability of our findings to asymptomatic or younger populations may be limited. The data on hip pain in this study only reflects the past week from the time of collection. As a result, the duration and the course of pain cannot be measured. Future studies with available data should consider these aspects when investigating cam morphology.

In conclusion, no consistent associations were found between cam morphology quantified on an AP radiograph and self-reported hip pain at multiple follow-ups. Only in male participants, baseline cam morphology was associated with hip pain at the 5-year follow-up. This might indicate a weak relationship between cam morphology and hip pain in males, while no such relation was found in females. We did not identify an association between the alpha angle and severity of hip pain.

REFERENCES

1. Griffin DR, Dickenson EJ, O'Donnell J, Agricola R, Awan T, Beck M, et al. The Warwick Agreement on femoroacetabular impingement syndrome (FAI syndrome): an international consensus statement. *Br J Sports Med* 2016; 50: 1169-1176.
2. Clohisy JC, Dobson MA, Robison JF, Warth LC, Zheng J, Liu SS, et al. Radiographic structural abnormalities associated with premature, natural hip-joint failure. *J Bone Joint Surg Am* 2011; 93 Suppl 2: 3-9.
3. Rogers MJ, Sato EH, LaBelle MW, Ou Z, Presson AP, Maak TG. Association of Cam Deformity on Anteroposterior Pelvic Radiographs and More Severe Chondral Damage in Femoroacetabular Impingement Syndrome. *Am J Sports Med* 2022; 50: 2980-2988.
4. Heerey J, Kemp J, Agricola R, Srinivasan R, Smith A, Pizzari T, et al. Cam morphology is associated with MRI-defined cartilage defects and labral tears: a case-control study of 237 young adult football players with and without hip and groin pain. *BMJ Open Sport Exerc Med* 2021; 7: e001199.
5. Khan M, Bedi A, Fu F, Karlsson J, Ayeni OR, Bhandari M. New perspectives on femoroacetabular impingement syndrome. *Nat Rev Rheumatol* 2016; 12: 303-310.
6. Zadpoor AA. Etiology of Femoroacetabular Impingement in Athletes: A Review of Recent Findings. *Sports Med* 2015; 45: 1097-1106.
7. Dijkstra HP, Mc Auliffe S, Arden CL, Kemp JL, Mosler AB, Price A, et al. Oxford consensus on primary cam morphology and femoroacetabular impingement syndrome: part 1-definitions, terminology, taxonomy and imaging outcomes. *Br J Sports Med* 2022; 57: 325-341.
8. Agricola R, Heijboer MP, Bierma-Zeinstra SM, Verhaar JA, Weinans H, Waarsing JH. Cam impingement causes osteoarthritis of the hip: a nationwide prospective cohort study (CHECK). *Ann Rheum Dis* 2013; 72: 918-923.
9. Pun S, Kumar D, Lane NE. Femoroacetabular impingement. *Arthritis Rheumatol* 2015; 67: 17-27.
10. Allen D, Beaulé PE, Ramadan O, Doucette S. Prevalence of associated deformities and hip pain in patients with cam-type femoroacetabular impingement. *J Bone Joint Surg Br* 2009; 91: 589-594.
11. Khanna V, Caragianis A, Diprimio G, Rakhra K, Beaulé PE. Incidence of hip pain in a prospective cohort of asymptomatic volunteers: is the cam deformity a risk factor for hip pain? *Am J Sports Med* 2014; 42: 793-797.
12. Larson CM, Sikka RS, Sardelli MC, Byrd JW, Kelly BT, Jain RK, et al. Increasing alpha angle is predictive of athletic-related "hip" and "groin" pain in collegiate National Football League prospects. *Arthroscopy* 2013; 29: 405-410.
13. Guler O, Isyar M, Karatas D, Ormeci T, Cerci H, Mahirogullari M. A retrospective analysis on the correlation between hip pain, physical examination findings, and alpha angle on MR images. *J Orthop Surg Res* 2016; 11: 140.
14. Scholes MJ, Kemp JL, Mentiplay BF, Heerey JJ, Agricola R, King MG, et al. Are cam morphology size and location associated with self-reported burden in football players with FAI syndrome? *Scand J Med Sci Sports* 2022; 32: 737-753.
15. Heerey J, Agricola R, Smith A, Kemp J, Pizzari T, King M, et al. The Size and Prevalence of Bony Hip Morphology Do Not Differ Between Football Players With and Without Hip and/or Groin Pain: Findings From the FORCe Cohort. *J Orthop Sports Phys Ther* 2021; 51: 115-125.

16. Abrahamson J, Jonasson P, Sansone M, Aminoff AS, Todd C, Karlsson J, et al. Hip pain and its correlation with cam morphology in young skiers-a minimum of 5 years follow-up. *J Orthop Surg Res* 2020; 15: 444.
17. van Klij P, Ginai AZ, Heijboer MP, Verhaar JAN, Waarsing JH, Agricola R. The relationship between cam morphology and hip and groin symptoms and signs in young male football players. *Scand J Med Sci Sports* 2020; 30: 1221-1231.
18. Gosvig KK, Jacobsen S, Sonne-Holm S, Gebuhr P. The prevalence of cam-type deformity of the hip joint: a survey of 4151 subjects of the Copenhagen Osteoarthritis Study. *Acta Radiol* 2008; 49: 436-441.
19. Nardo L, Parimi N, Liu F, Lee S, Jungmann PM, Nevitt MC, et al. Femoroacetabular Impingement: Prevalent and Often Asymptomatic in Older Men: The Osteoporotic Fractures in Men Study. *Clin Orthop Relat Res* 2015; 473: 2578-2586.
20. Faber BG, Ebsim R, Saunders FR, Frysz M, Gregory JS, Aspden RM, et al. Cam morphology but neither acetabular dysplasia nor pincer morphology is associated with osteophytosis throughout the hip: findings from a cross-sectional study in UK Biobank. *Osteoarthritis Cartilage* 2021; 29: 1521-1529.
21. Nepple JJ, Vigdorich JM, Clohisy JC. What Is the Association Between Sports Participation and the Development of Proximal Femoral Cam Deformity? A Systematic Review and Meta-analysis. *Am J Sports Med* 2015; 43: 2833-2840.
22. van Berkel AC, Schiphof D, Waarsing JH, Runhaar J, van Ochten JM, Bindels PJE, et al. Course of pain and fluctuations in pain related to suspected early hip osteoarthritis: the CHECK study. *Fam Pract* 2022; 39: 1041-1048.
23. van Klij P, Heerey J, Waarsing JH, Agricola R. The Prevalence of Cam and Pincer Morphology and Its Association With Development of Hip Osteoarthritis. *J Orthop Sports Phys Ther* 2018; 48: 230-238.
24. Ortiz-Declat V, Maldonado DR, Annin S, Yuen LC, Kyin C, Kopschik MR, et al. Nonarthritic Hip Pathology Patterns According to Sex, Femoroacetabular Impingement Morphology, and Generalized Ligamentous Laxity. *Am J Sports Med* 2022; 50: 40-49.
25. Yanke AB, Khair MM, Stanley R, Walton D, Lee S, Bush-Joseph CA, et al. Sex Differences in Patients With CAM Deformities With Femoroacetabular Impingement: 3-Dimensional Computed Tomographic Quantification. *Arthroscopy* 2015; 31: 2301-2306.
26. Wesseling J, Dekker J, van den Berg WB, Bierma-Zeinstra SM, Boers M, Cats HA, et al. CHECK (Cohort Hip and Cohort Knee): similarities and differences with the Osteoarthritis Initiative. *Ann Rheum Dis* 2009; 68: 1413-1419.
27. Wesseling J, Boers M, Viergever MA, Hilberdink WK, Lafeber FP, Dekker J, et al. Cohort Profile: Cohort Hip and Cohort Knee (CHECK) study. *Int J Epidemiol* 2016; 45: 36-44.
28. Mascarenhas VV, Castro MO, Afonso PD, Rego P, Dienst M, Sutter R, et al. The Lisbon Agreement on femoroacetabular impingement imaging-part 2: general issues, parameters, and reporting. *Eur Radiol* 2021; 31: 4634-4651.
29. Notzli HP, Wyss TF, Stoecklin CH, Schmid MR, Treiber K, Hodler J. The contour of the femoral head-neck junction as a predictor for the risk of anterior impingement. *J Bone Joint Surg Br* 2002; 84: 556-560.
30. Agricola R, Reijman M, Bierma-Zeinstra SM, Verhaar JA, Weinans H, Waarsing JH. Total hip replacement but not clinical osteoarthritis can be predicted by the shape of the hip: a prospective cohort study (CHECK). *Osteoarthritis Cartilage* 2013; 21: 559-564.

31. van Klij P, Reiman MP, Waarsing JH, Reijman M, Bramer WM, Verhaar JAN, et al. Classifying Cam Morphology by the Alpha Angle: A Systematic Review on Threshold Values. *Orthop J Sports Med* 2020; 8: 2325967120938312.
32. Agricola R, Waarsing JH, Thomas GE, Carr AJ, Reijman M, Bierma-Zeinstra SM, et al. Cam impingement: defining the presence of a cam deformity by the alpha angle: data from the CHECK cohort and Chingford cohort. *Osteoarthritis Cartilage* 2014; 22: 218-225.
33. Malenbaum S, Keefe FJ, Williams ACC, Ulrich R, Somers TJ. Pain in its environmental context: implications for designing environments to enhance pain control. *Pain* 2008; 134: 241-244.
34. Fu K, Metcalf B, Bennell KL, Zhang Y, Deveza LA, Robbins SR, et al. Association of weather factors with the risk of pain exacerbations in people with hip osteoarthritis. *Scand J Rheumatol* 2021; 50: 68-73.
35. Schwaiger BJ, Gersing AS, Lee S, Nardo L, Samaan MA, Souza RB, et al. Longitudinal assessment of MRI in hip osteoarthritis using SHOMRI and correlation with clinical progression. *Semin Arthritis Rheum* 2016; 45: 648-655.
36. Heerey JJ, Souza RB, Link TM, Luitjens J, Gassert F, Kemp JL, et al. Defining hip osteoarthritis feature prevalence, severity, and change using the Scoring of Hip Osteoarthritis with MRI (SHOMRI). *Skeletal Radiol* 2024; 53: 1599-1609.
37. Neumann G, Mendicuti AD, Zou KH, Minas T, Coblyn J, Winalski CS, et al. Prevalence of labral tears and cartilage loss in patients with mechanical symptoms of the hip: evaluation using MR arthrography. *Osteoarthritis Cartilage* 2007; 15: 909-917.
38. Verkleij SP, Hoekstra T, Rozendaal RM, Waarsing JH, Koes BW, Luijsterburg PA, et al. Defining discriminative pain trajectories in hip osteoarthritis over a 2-year time period. *Ann Rheum Dis* 2012; 71: 1517-1523.
39. Bastick AN, Verkleij SP, Damen J, Wesseling J, Hilberdink WK, Bindels PJ, et al. Defining hip pain trajectories in early symptomatic hip osteoarthritis--5 year results from a nationwide prospective cohort study (CHECK). *Osteoarthritis Cartilage* 2016; 24: 768-775.
40. Staikou C, Kokotis P, Kyzozis A, Rallis D, Makrydakis G, Manoli D, et al. Differences in Pain Perception Between Men and Women of Reproductive Age: A Laser-Evoked Potentials Study. *Pain Med* 2017; 18: 316-321.
41. Racine M, Tousignant-Laflamme Y, Kloda LA, Dion D, Dupuis G, Choiniere M. A systematic literature review of 10 years of research on sex/gender and experimental pain perception - part 1: are there really differences between women and men? *Pain* 2012; 153: 602-618.
42. Bartley EJ, Fillingim RB. Sex differences in pain: a brief review of clinical and experimental findings. *Br J Anaesth* 2013; 111: 52-58.

6

The Different Subtypes of Cam Morphology as Defined by Statistical Shape Modeling and Their Relationship with the Development of Hip Osteoarthritis: a Nationwide Prospective Cohort Study (CHECK) with 10 Years Follow-up

Jinchi Tang, Fleur Boel, Michiel M A van Buuren, Noortje S Riedstra, Jos Runhaar, Sita Bierma-Zeinstra, Rintje Agricola.

ABSTRACT

Objective: To determine if subtypes of cam morphology on anteroposterior (AP) radiographs exist using statistical shape modelling (SSM), and to assess their association with incident radiographic hip osteoarthritis (RHOA) within 10 years.

Design: The nationwide prospective Cohort Hip and Cohort Knee (CHECK) study included 1,002 participants aged 45-65 years with 10-year follow-up. Subtypes of cam morphology were defined as SSM-based shape variations of femoral head-neck junction that are associated with baseline cam morphology (alpha angle $\geq 60^\circ$). The association between each subtype in hips free of osteoarthritis at baseline (Kellgren & Lawrence (KL) grade < 2) and incident RHOA (KL grade ≥ 2 , or a total hip replacement) was estimated using logistic regression at 10-year follow-up and stratified by sex.

Results: In sex-combined group, but also for males and females separately, cam morphology subtypes were captured in modes 1, 3, 4, and 5 with odds ratios (ORs) ranging from 0.39(0.27-0.58) to 2.25(1.64-3.10). For sex-combined group, only mode 3, a flattened head-neck junction, was associated with incident RHOA (OR:1.14, 1.02-1.27). Males' modes 1 and 3 and females' modes 3 and 4 were associated with RHOA. Notably, the female mode 4, a slightly flattened neck but with subtle curvature, was significantly protective for RHOA (OR:0.88, 0.80-0.98).

Conclusions: We identified four distinct morphological subtypes of cam morphology defined by alpha angle. Only some subtypes were found acting as risk factors for RHOA at 10-year follow-up, which differed between males and females. This highlights the need to study cam morphology beyond the alpha angle alone.

Keywords: cam morphology; subtype; radiographic hip osteoarthritis

INTRODUCTION

Osteoarthritis (OA) is the most common form of musculoskeletal disease^{1,2}. After the knee, the hip is the second most frequently affected joint³. The burden of hip OA has increased in the past three decades^{4,5} and as this increasing trend is expected to continue in the coming years⁶, it is of great importance to better understand the etiology of hip OA.

Several risk factors for hip OA have been identified such as heavy physical joint loading⁷, musculoskeletal injury⁸, heritability⁹, age¹⁰, sex¹¹, and obesity¹². The shape of the hip also plays an important role in the development of radiographic hip OA (RHOA)¹³. One of the strongest shape related risk factors for RHOA is cam morphology^{14,15}. Cam morphology is an osseous prominence at the anterolateral part of the femoral head-neck junction acquired during skeletal growth, which results in a non-spherical femoral head^{16,17}. It can cause abnormal contact between the proximal femur and the acetabular rim during motion, thereby creating repetitive stresses on the cartilage and leading to cartilage defects and labral tears, which might eventually evolve to hip OA¹⁸.

Several measures to quantify cam morphology have been proposed, including the alpha angle¹⁹, femoral head-neck offset ratio²⁰, triangular index²¹, femoroacetabular excursion angle (beta angle)²², all of them aiming to capture the asphericity of the femoral head-neck junction. The alpha angle is the most commonly used measure to quantify cam morphology¹⁹ and can be applied to radiographs at various views and to different planes in CT and MRI images^{23,24}. A recent systematic review and an international consensus statement suggested a threshold of $\geq 60^\circ$ to classify the presence of cam morphology^{16,25}.

However, using this threshold, a broad range of 'aspherical femoral heads' or 'subtypes of cam morphology' are captured, including but not limited to: hook shape, peak, flat shape, and a pistol grip shape²³. Although cam morphology defined by an alpha angle $\geq 60^\circ$ is strongly associated with RHOA, it is unknown whether all these subtypes of cam morphology result in an increased risk for RHOA or whether only some of these subtypes are responsible for this effect. To the best of our knowledge, there is no previous research on whether different subtypes of cam morphology as captured by the alpha angle exist and how these relate to incident RHOA. Also, there is only limited literature on the association between cam morphology and incident RHOA with long-term follow-up.

The aims of this study are i) to examine which different subtypes of cam morphology based on an alpha angle $\geq 60^\circ$ exist on anteroposterior (AP) radiographs using statistical shape modeling (SSM); ii) to investigate the association between those subtypes of cam morphology and incident RHOA within 10 years.

METHODS

Study population

The Cohort Hip and Cohort Knee (CHECK) is a multicenter prospective cohort study in the Netherlands^{26, 27}. From October 2002 until September 2005, 1,002 participants aged between 45 and 65 years were recruited in the Netherlands with a total of 10 years follow-up. Participants were eligible if they had initial symptoms of knee or hip pain and/or stiffness and either not have consulted their general practitioner (GP) for these symptoms previously, or their first consultation occurred within 6 months prior to enrollment. Exclusion criteria encompassed individuals presenting with any other pathological conditions potentially accounting for the symptoms, any comorbidities impeding physical evaluation and/or follow-up period of at least 10 years, malignancy in the past 5 years, or inability to understand the Dutch language. Radiological data were collected from 11 general and academic hospitals in the Netherlands.

Ethical approval for the study was obtained from the medical ethics committees of all participating centers, and written informed consent was secured from all enrolled participants.

Radiography

Standardized weight-bearing AP radiographs of the hips or pelvis were obtained at baseline and 10-year follow-up. During the acquisition of the AP pelvic radiograph, participants were positioned with the lower extremities parallel and with 15° internal rotation, resulting in the touch of the medial sides of the distal part of the big toes. The X-ray beam was centered on the proximal edge of the pubic symphysis. The tube-to-film distance was 100 cm. The first 124 participants who entered the CHECK study had an AP hip radiograph of each hip obtained according to the same protocol, but with the x-ray beam centered on the groin.

Statistical shape modeling (SSM)

To capture the different types of femoral head-neck morphology, SSM was used to quantify the shape variations observed in this population. The shape of the femoral head-neck junction was outlined by a series of landmark point which were automati-

cally annotated using SSM software as described previously (BoneFinder[®], Manchester University, United Kingdom)^{28, 29}. For the current study, a total of 15 landmark points along the contour of the femoral head-neck junction were used to create the SSM of the superior head-neck junction (**Figure 1**). Considering that males generally have cam morphology with greater magnitude than females³⁰, we also study the shape of femoral head-neck junction stratified by biological sex. Therefore, three SSMs were built, based on the radiographs of 1) males only, 2) females only, and 3) two sexes combined.

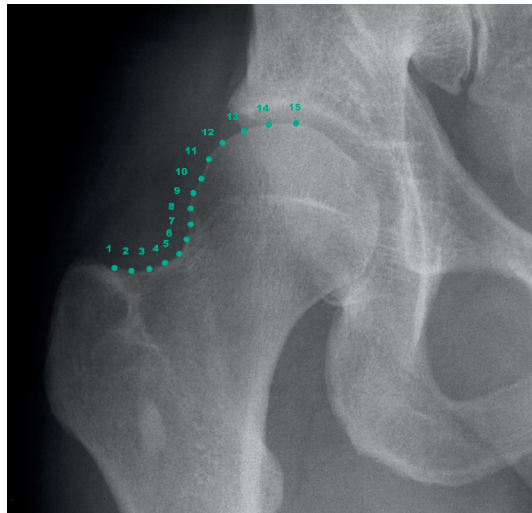


Figure 1. The femoral head and head-neck junction was outlined by 15 landmark points on the AP radiograph. The first point is located where the anterior greater trochanter joins the femoral neck, and the last one is located around the top of the best fitting circle of the femoral head.

Within each SSM, we identified the main variations in shape modes via principal component analysis. The modes of variation were ordered in ascending order based on their contribution to the total shape variance, with the first mode explaining the greatest variation in shape. Given the nature of SSM that all resulting modes of shape variation are statistically independent of each other and not interconnected, each identified shape mode describes a distinct pattern. These modes are described as a set of continuous variables and standardized to have a mean of 0 and a standard deviation of 1. For all three SSMs, we selected the number of modes that together explained at least 99% of the total variation in shape, with each individual mode explaining at least 1% of the total variation. Because all three SSMs were generated based on different inputs (all hips, male hips or female hips) the resulting modes of shape variation cannot be directly compared between these groups.

Alpha angle

The alpha angle is calculated as the angle between the line from the center of the femoral head through the middle of the femoral neck and a second line from the center of the femoral head through the point where the contour of the superior femoral head-neck junction exceeds the radius of the best fitting circle of the femoral head (**Figure 2**). Using in-house developed software (Python Version 3.7.0), the alpha angle was automatically calculated using the landmark points placed by the SSM software. This method previously showed good intraclass correlation coefficients when compared with manual measurement by two orthopedic surgeons: 0.81 (95%CI 0.46 – 0.92) for inter-method reliability, and 0.77(95%CI 0.58 – 0.89) for interobserver reliability³¹. The presence of cam morphology at baseline was defined by the recommended alpha angle threshold of $\geq 60^\circ$, which previously showed a consistent association with development of radiographic hip OA in the CHECK cohort over 10 years follow-up³².

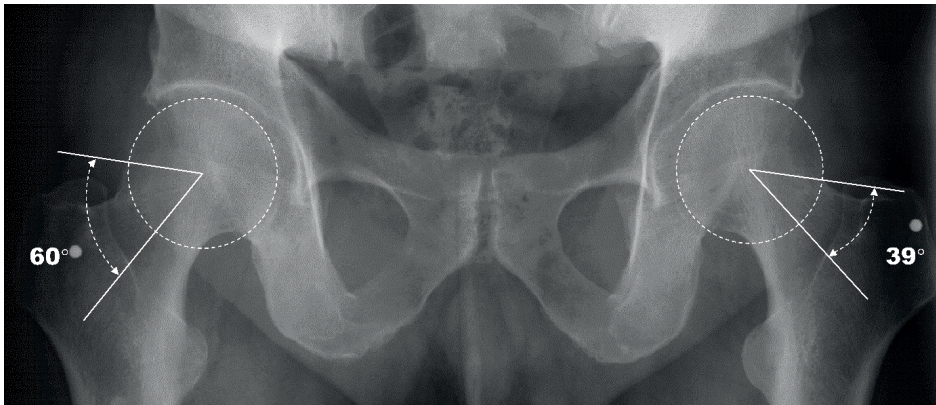


Figure 2. The measurement of alpha angle on AP pelvic radiograph. The left hip (right on the image) has an alpha angle of 39° and the right hip was classified as having cam morphology based on an alpha angle of $\geq 60^\circ$.

Definition of radiographic hip OA

At baseline and 10-year follow-up, the AP pelvic and hip radiographs were scored for RHOA according to the Kellgren and Lawrence (KL) classification. All consecutive radiographs available for each participant were independently scored by five trained medical professionals simultaneously, ensuring that the information from all images was used for KL scoring at each time point. This approach has demonstrated greater reliability when compared to scoring each radiograph independently³³. At baseline, we only included hips without definite RHOA (KL grade < 2) to avoid misclassification of cam morphology based on osteoarthritic changes such as definite osteophyte

formation or femoral head deformation. Incident RHOA was defined by a KL grade ≥ 2 or a total hip replacement (THR) at the 10-year follow-up.

Statistical Analysis

Differences in characteristics between included and excluded hips at baseline were evaluated. We used the independent samples t-test for continuous variables and the chi-square test for categorical variables. A logistic regression model was used to analyze the association between each mode of shape variation and the presence of cam morphology at baseline. Then, a logistic regression model was also used to study the association between each baseline mode of shape variation and incident radiographic hip OA at 10-year follow-up. All regression analyses were performed with generalized estimating equations (GEE), as GEE accounts for statistical dependency between two hips within one individual. All regression analyses were adjusted for age, biological sex, and body mass index (BMI). Finally, we repeated all analyses with exclusion of BMI from the confounders. The strength of association was expressed in odds ratios (OR) per 1 standard deviation (SD) increase in standardized shape mode value with 95% confidence intervals. The effect was considered significant at $P < 0.05$. All statistical analyses were performed in SPSS Statistics, version 26.0 (IBM Corp., Armonk, New York, USA).

RESULTS

Population

Of the 2,004 hips from 1,002 individuals in the CHECK cohort, 588 hips were excluded: 218 hips had definite RHOA at baseline; 2 hips and 294 hips lacked KL grade data at baseline and the 10-year follow-up, respectively; in 72 hips, the alpha angle could not be measured reliably due to insufficient radiographic quality; and 2 hips had missing baseline BMI data. The result of the exploration of all 588 excluded hips were shown in **Table 1**. In total, 1,416 hips from 755 participants were included at baseline (259 male hips [18.3%] and 1,157 female hips [81.7%]) (**Table 2**). The complete flow of participants (hips) is provided in the flowchart (**Figure 3**).

Table 1. The difference in baseline characteristics among included and excluded hips.

Baseline characteristics	2,004 hips from the CHECK cohort			
	Included (n=1,416)	Excluded (n=588)	95% Confidence Interval	
			Lower	Upper
Age in years: mean (SD)	55.6(5.2)	56.6(5.2)	-1.51	-0.49
Women: No (%)	1,157(81.7)	423(71.9)	-0.14	-0.06
BMI, kg/m ² : mean (SD)	26.2(4.0)	26.0(4.0)	-0.20	0.60
Alpha angle, °: mean (SD)	46.4(9.9)	50.9(13.7)	-5.73	-3.27
Cam morphology: No (%)	122(8.6)	89(20.1)	0.03	0.10
KL grade 0: No (%)	1,045(73.8)	170(65.6)	-0.49	-0.41
KL grade 1: No (%)	371(26.2)	89(34.4)	-0.15	-0.07
KL grade 2 or missing: No (%)	0(0.0)	240(40.8)	0.37	0.45

SD: standard deviation; BMI: body mass index; KL: Kellgren and Lawrence. The difference is considered significant if the 95% confidence interval does not include 0.

Table 2. Baseline characteristics among sex-combined, male and female groups.

Baseline characteristics	Three groups from included 1,416 hips of the CHECK cohort				
	Sex-combined group (n=1,416)	Male group (n=259)	Female group (n=1,157)	95% Confidence Interval	
				Lower	Upper
Age in years: mean (SD)	55.6(5.2)	55.8(5.4)	55.6(5.1)	-0.54	0.94
Women: No (%)	1,157(81.7)	0(0.0)	1,157(100.0)	1.00	1.00
BMI, kg/m ² : mean (SD)	26.2(4.0)	26.3(3.5)	26.2(4.1)	-0.42	0.62
Alpha angle, °: mean (SD)	46.4(9.9)	53.0(12.0)	44.9(8.7)	6.54	9.66
Cam morphology: No (%)	122(8.6)	63(24.3)	59(5.1)	-0.25	-0.14
KL grade 0: No (%)	1,045(73.8)	170(65.6)	875(75.6)	0.04	0.16
KL grade 1: No (%)	371(26.2)	89(34.4)	282(24.4)	-0.16	-0.04

SD: standard deviation; BMI: body mass index; KL: Kellgren and Lawrence. 95% confidence interval is for the difference between male and female groups. The difference is considered significant if the 95% confidence interval does not include 0.

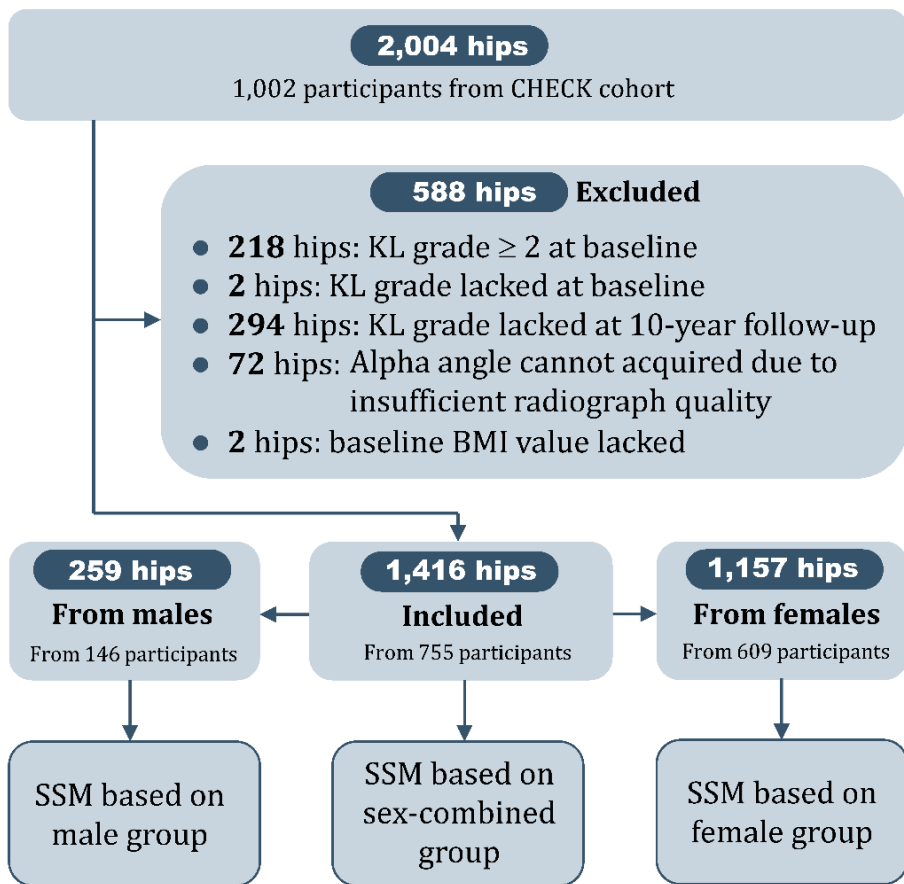


Figure 3. The complete flow of hips

At baseline, the prevalence of cam morphology was 8.6% (24.3% in males; 5.1% in females). These 122 hips with cam morphology came from 95 participants, of which 27 participants had bilateral cam morphology and 68 had unilateral one. Of all hips with cam morphology, 62.3% developed RHOA at 10-year follow-up (69.8% in males; 54.2% in females).

Statistical shape model

For SSMs of the male and sex-combined group, the first 6 modes were extracted from 28 available modes. For the female SSM, the first 6 modes were extracted from 29 available modes. Detailed information was provided in **Supplementary Figure S1**.

Shape modes with the same order (1 to 6) in all three groups are slightly different from each other but share common features (**Figures 4** and **Supplementary Figure S2**). For the combined groups, shape mode 1 shows variation in the head-neck junction with a pistol grip deformity extending towards the major trochanter represented by the lower mode values and an evident spherical femoral head with distinct head-neck junction in the higher mode values. Shape mode 2 represents a slight lateral 'hook shaped' extension of the femoral head with still a distinct concave head-neck junction in the lower values and a flattened head-neck junction in higher values. For shape mode 3, lower values represent a spherical femoral head with a clear concave curvature of the neck while higher values represent a flattened head-neck junction. Shape mode 4 also represents a spherical femoral head in lower values and a flattened head-neck junction in higher values, though with still a subtle concave curvature in the neck, in contrast to mode 3. Shape mode 5 represents a smaller and spherical femoral head with a long femoral neck in lower values and in higher values a prominence in the head-neck junction, though not extending as far to the major trochanter as mode 1. Finally, shape mode 6 shows more subtle variations with a spherical femoral head and long neck in lower values and a very subtle lateral prominence at lateral aspect of the head-neck junction, though with a seemingly spherical femoral head and clear concave head-neck junction. Please note that although the descriptions of modes 1 to 6 are similar between males and females, the shape variations depicted by the extremes of mode 1 and mode 3 might explain the opposite shape variations. For example, the pistol grip deformity in mode 1 was represented by higher values in males, but by lower values in females.

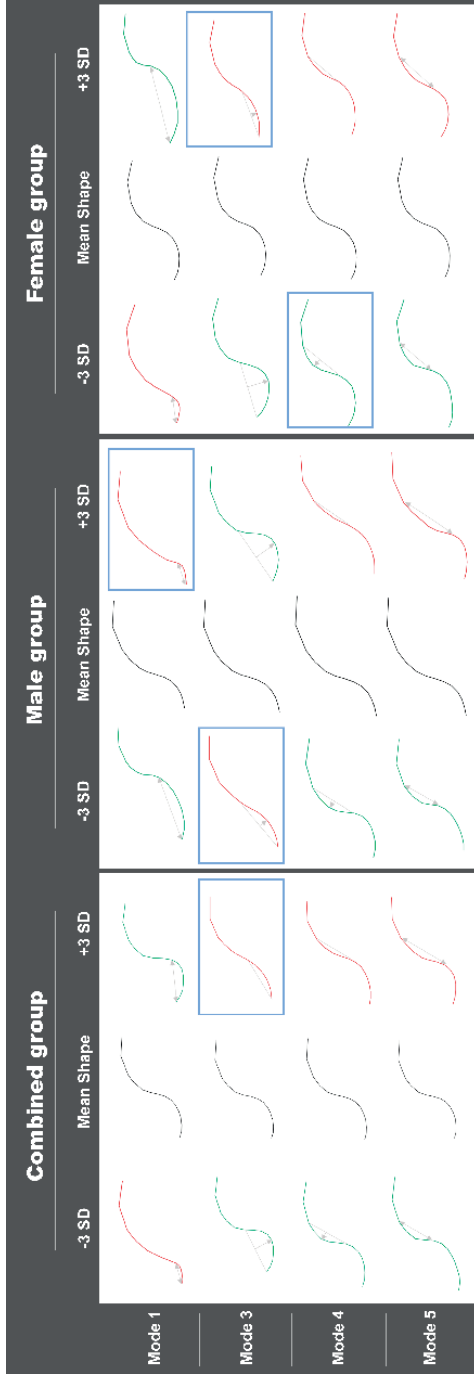


Figure 4. Subtypes of cam morphology defined by SSM based on hips from sexes-combined, male, and female group, respectively. The shapes corresponding to -3 and $+3$ SDs from the mean shape (depicted by the black line) are displayed on the left and right sides, respectively. The extremes that associated with the presence of cam morphology are shown in red line and extremes that are associated with the development of RHOA at 10-year follow-up are indicated in the blue boxes.

Associations between femoral head-neck junction shape variations and cam morphology and incident RHOA

Estimates of associations between femoral head-neck junction shape modes and cam morphology and between subtypes of cam morphology and incident RHOA in all three SSMs are presented in **Table 3** and **Table 4**.

Table 3. Associations between femoral head-neck junction shape modes and the presence of cam morphology in three groups.

Group	Shape mode	Outcome: cam morphology (alpha angle $\geq 60^\circ$)			
		OR (95% CI)	P value	aOR (95% CI)	P value
Combined	mode1	0.584(0.505-0.676)	<0.001	0.591(0.503-0.694)	<0.001
	mode2	1.073(0.868-1.326)	0.515	1.147(0.906-1.452)	0.255
	mode3	1.767(1.441-2.166)	<0.001	1.568(1.303-1.888)	<0.001
	mode4	1.727(1.433-2.080)	<0.001	1.749(1.399-2.186)	<0.001
	mode5	1.814(1.495-2.202)	<0.001	1.819(1.469-2.252)	<0.001
	mode6	1.211(1.011-1.451)	0.038	1.208(0.983-1.484)	0.072
Male	mode1	1.724(1.309-2.270)	<0.001	1.722(1.309-2.266)	<0.001
	mode2	1.143(0.866-1.509)	0.344	1.153(0.873-1.523)	0.316
	mode3	0.396(0.268-0.585)	<0.001	0.394(0.267-0.582)	<0.001
	mode4	2.253(1.638-3.098)	<0.001	2.252(1.637-3.098)	<0.001
	mode5	1.899(1.386-2.601)	<0.001	1.916(1.406-2.612)	<0.001
	mode6	1.207(0.949-1.535)	0.125	1.211(0.951-1.541)	0.12
Female	mode1	0.429(0.336-0.548)	<0.001	0.428(0.331-0.554)	<0.001
	mode2	0.927(0.727-1.183)	0.542	0.949(0.731-1.231)	0.692
	mode3	1.827(1.495-2.233)	<0.001	1.786(1.461-2.183)	<0.001
	mode4	1.435(1.098-1.875)	0.008	1.441(1.102-1.886)	0.008
	mode5	1.687(1.435-1.983)	<0.001	1.808(1.510-2.165)	<0.001
	mode6	1.152(0.949-1.400)	0.153	1.172(0.950-1.447)	0.138

All odds ratios (OR) represent every 1 SD increase in shape mode value; adjusted ORs (aOR) were adjusted for age, sex (only in combined group) and body mass index at baseline.

Table 4. Associations between subtypes of cam morphology and incident radiographic hip osteoarthritis in three groups.

Group	Shape mode	Morphological characteristics	Outcome: the development of RHOA at 10-year follow-up			
			OR (95% CI)	P value	aOR (95% CI)	P value
Combined	mode1	Pistol grip-shaped prominence	0.955(0.860-1.061)	0.389	0.981(0.880-1.093)	0.73
	mode3	Flattened head-neck junction	1.186(1.066-1.319)	0.002	1.140(1.019-1.274)	0.022
	mode4	Flattened neck with curvature	0.921(0.836-1.014)	0.094	0.909(0.823-1.004)	0.059
	mode5	Prominence extending to neck	1.101(0.990-1.224)	0.077	1.100(0.986-1.228)	0.088
	mode1	Pistol grip-shaped prominence	1.413(1.070-1.867)	0.015	1.406(1.063-1.858)	0.017
Male	mode3	Flattened head-neck junction	0.759(0.581-0.993)	0.044	0.758(0.578-0.993)	0.045
	mode4	Flattened neck with curvature	1.135(0.876-1.471)	0.337	1.117(0.860-1.452)	0.407
	mode5	Prominence extending to neck	1.065(0.834-1.361)	0.613	1.081(0.844-1.383)	0.538
	mode1	Pistol grip-shaped prominence	1.073(0.945-1.219)	0.278	1.089(0.957-1.239)	0.197
Female	mode3	Flattened head-neck junction	1.161(1.032-1.305)	0.013	1.134(1.006-1.278)	0.039
	mode4	Flattened neck with curvature	0.884(0.798-0.980)	0.019	0.881(0.795-0.976)	0.015
	mode5	Prominence extending to neck	0.970(0.867-1.084)	0.587	0.983(0.879-1.100)	0.769

All odds ratios (OR) represent every 1 SD increase in shape mode value; adjusted odds ratios (aOR) were adjusted for age, sex (only in combined group) and body mass index at baseline. RHOA: radiographic hip osteoarthritis.

For the SSM modes based on the sex-combined group, shape mode 1(OR: 0.59 95%CI 0.50-0.69), mode 3 (OR:1.57 95%CI 1.30-1.89), mode 4 (OR: 1.75 95%CI 1.40-2.19), and mode 5 (OR: 1.82 95%CI 1.47-2.25) showed significant associations with the presence of cam morphology. Higher value in mode 3-5 and lower value in mode 1 will lead to a higher risk of having cam morphology. Only shape mode 3 also had a significant association with incident RHOA with an adjusted OR of 1.14 (95% CI: 1.02-1.27) per SD increase.

For the SSM based on male group, four out of six analyzed shape modes showed significant association with the presence of cam morphology, which are mode 1 (OR: 1.72 95%CI 1.31-2.27), mode 3(OR: 0.39 95%CI 0.27-0.58), mode 4(OR: 2.25 95%CI 1.64-3.10), and mode 5 (OR: 1.92 95%CI 1.41-2.61). Mode 1 and 3 were also signifi-

cantly associated with incident RHOA with an adjusted OR of 1.41 (95%CI 1.06-1.86) per SD increase for shape mode 1 and an adjusted OR of 0.758 (95%CI 0.58-0.99) per SD increase for shape mode 3.

For the SSM based on female group, similarly, four out of six shape modes showed significant association with the presence of cam morphology. These modes included mode 1 (OR: 0.43 95%CI 0.33-0.55), mode 3 (OR: 1.79 95%CI 1.46-2.18), mode 4 (OR: 1.44 95%CI 1.10-1.89), and mode 5 (OR: 1.81 95%CI 1.51-2.17). Mode 3 and 4 were also significantly associated with incident RHOA, with an adjusted OR of 1.134 (95%CI 1.01-1.28) per SD increase for shape mode 3 and an adjusted OR of 0.88 (95%CI: 0.80-0.99) per SD increase for shape mode 4. Notably, mode 4 was negatively associated with developing RHOA meaning the extreme of this shape mode representing cam morphology was protective for incident RHOA.

The results of the analyses, after excluding BMI from the confounders, are presented in **Table S1**. There were only slight changes in the values of the odds ratios and their corresponding 95% confidence intervals compared to the main analyses conducted above, but with same subtypes of cam morphology and their same effect to RHOA.

DISCUSSION

In this prospective cohort study, we found several morphological subtypes of cam morphology that are distinct from each other. Interestingly, only part of these subtypes of cam morphology were also associated with incident RHOA within 10-year follow-up, suggesting that not all morphological aspects captured by an alpha angle $\geq 60^\circ$ are relevant for the development of RHOA.

To the best of our knowledge, no previous studies have investigated whether different subtypes of cam morphology as defined by the alpha angle exist. However, a number of studies that investigated the entire hip or pelvic shape with SSM have already shed light on the subtypes of cam morphology. Van Buuren et al³⁴ found that certain hip shape variants that might represent cam morphology were associated with cartilage defects while others with cam morphology were not, possibly indicating the existence of different subtypes of cam morphology. Bugeja et al³⁵ used SSM to explore cam morphology through parameters such as cam volume, surface area, and height, however the differences of those radiographic parameters were not used to further classify cam morphology into subtypes.

Among those cam morphology subtypes, only two male (mode 1 and 3), one female subtype (mode 3) and one subtype in combined group (mode 3) acted as a risk factor for incident RHOA, while female shape mode 4 seems to have a protective effect against RHOA. Each SD increase in the combined mode 3, male mode 3/4, and female mode 3 at baseline can lead to 13% to 40% higher risk of developing RHOA 10 years after. Conversely, each SD increase in female mode 4 is associated with approximately a 12% lower risk of developing RHOA. These findings might partly provide an explanation for the substantial difference in the incidence of RHOA in hips with cam morphology between the two sexes. Furthermore, it is essential to recognize that the strength of the association between cam morphology and RHOA has shown significant variation in previous studies. This variation was previously attributed to differences in study populations and definitions³², but it might also be attributable to the distinct distribution of cam morphology subtypes.

Our findings suggest that the impact of cam morphology on incident RHOA may be influenced by biological sex. We found that pistol grip-type cam morphology (mode 1) can be considered a risk factor for RHOA only in males, whereas cam morphology characterized by a flattened head-neck junction (mode 3) was a risk factor in both sexes. In contrast, a slight flattened head-neck junction with still a concave femoral neck curvature appears to act as a protective factor only in females. From the anatomical perspective, females typically have a shallower acetabulum and a smaller femoral head compared to males^{36,37}. This anatomical difference might result in males having greater femoral head coverage compared to females. Consequently, there is a higher probability of abnormal contact between the cam morphology and the acetabulum during hip motion in males, while females have a larger tolerance space for cam morphology. In addition, our study only focuses on the cam morphology while other morphological and orientational factors such as acetabular dysplasia, pincer morphology and femoral version might also be the explanation for the different findings between sexes.

While the alpha angle is a commonly used method to quantify cam morphology, our study reveals that various shape aspects are captured by the alpha angle which are all defined as cam morphology, but they might not all be relevant. The subtypes of cam morphology found in our study exhibit unique characteristics that cannot be distinguished by the alpha angle alone. But they might be differentiated by combined methods with other measurements, such as triangular index or head-neck offset ratio. Future studies should reveal whether our finding also holds in other populations and with three-dimensional imaging and evaluate the potential for classifying cam morphology by integrating the alpha angle with other measurements.

Three confounders were identified in our analyses, which are age, biological sex, and BMI. Both age and sex of participants have already proven to be clear confounders to hip OA, while the association between BMI and hip OA remains somewhat unclear⁵. Recent studies provide evidence suggesting a potential causal role of obesity to the hip OA^{38, 39} and severe cam morphology (higher alpha angle)⁴⁰. Nevertheless, it's plausible that the presence of either cam morphology or hip OA might contribute to changes in weight by affecting individuals' daily activities. However, it's important to note that there is currently insufficient evidence to firmly support this viewpoint. Despite ongoing uncertainty regarding the precise effect of BMI, we opted to include it as a confounder rather than a collider in our analysis.

Our findings may not have direct clinical implication but can provide an insight on a classification of cam morphology. Cam morphology defined by alpha angle greater than 60 degrees should not be treated equally, on the contrary, only some subtypes with typical characteristics need to have priority for intervention.

Our study has several limitations. First, we quantified cam morphology only on AP radiographs. Those two-dimensional shape modes result in a simplified projection of the three-dimensional aspect of cam morphology. However, the alpha angle on an AP view previously showed a strong association with incident hip OA⁴¹. Then, our study solely concentrated on cam morphology, not taking into account other types of hip morphology such as pincer morphology and hip dysplasia which might potentially influence the relationship between cam morphology and RHOA. These types of hip morphology, particularly hip dysplasia, have demonstrated associations with the development of hip OA⁴². Therefore, to better understand the role of cam morphology in RHOA, further validation of our findings stratified by hip morphologies is needed. Furthermore, it is crucial to consider the specific characteristics of our study population. Participants in the CHECK cohort study exhibited first-onset symptoms in either their hip or knee, or both, and were aged between 45 and 65 years at the baseline. Therefore, our findings may not be directly generalizable to individuals without symptoms or to younger populations.

In conclusion, we identified four distinct morphological subtypes of cam morphology on the AP radiographs as defined by SSM. Only some subtypes of cam morphology were found acting as a risk factor for incident RHOA at 10-year follow-up with also differences between males and females. This shows that not all cam-related shape variations as captured by the alpha angle may be relevant in incident RHOA. With regard to RHOA development, it might be necessary to look beyond the alpha angle as a sole measurement for cam morphology.

REFERENCES

1. Martel-Pelletier J, Barr AJ, Cicuttini FM, Conaghan PG, Cooper C, Goldring MB, et al. Osteoarthritis. *Nat Rev Dis Primers* 2016; 2: 16072.
2. Glyn-Jones S, Palmer AJ, Agricola R, Price AJ, Vincent TL, Weinans H, et al. Osteoarthritis. *Lancet* 2015; 386: 376-387.
3. Aresti N, Kassam J, Nicholas N, Achan P. Hip osteoarthritis. *BMJ* 2016; 354: i3405.
4. Diseases GBD, Injuries C. Global burden of 369 diseases and injuries in 204 countries and territories, 1990-2019: a systematic analysis for the Global Burden of Disease Study 2019. *Lancet* 2020; 396: 1204-1222.
5. Fu M, Zhou H, Li Y, Jin H, Liu X. Global, regional, and national burdens of hip osteoarthritis from 1990 to 2019: estimates from the 2019 Global Burden of Disease Study. *Arthritis Res Ther* 2022; 24: 8.
6. Turkiewicz A, Petersson IF, Bjork J, Hawker G, Dahlberg LE, Lohmander LS, et al. Current and future impact of osteoarthritis on health care: a population-based study with projections to year 2032. *Osteoarthritis Cartilage* 2014; 22: 1826-1832.
7. Bierma-Zeinstra SM, Koes BW. Risk factors and prognostic factors of hip and knee osteoarthritis. *Nat Clin Pract Rheumatol* 2007; 3: 78-85.
8. Juhakoski R, Heliövaara M, Impivaara O, Kroger H, Knekt P, Lauren H, et al. Risk factors for the development of hip osteoarthritis: a population-based prospective study. *Rheumatology (Oxford)* 2009; 48: 83-87.
9. Faber BG, Frysz M, Boer CG, Evans DS, Ebsim R, Flynn KA, et al. The identification of distinct protective and susceptibility mechanisms for hip osteoarthritis: findings from a genome-wide association study meta-analysis of minimum joint space width and Mendelian randomisation cluster analyses. *EBioMedicine* 2023; 95: 104759.
10. Prieto-Alhambra D, Judge A, Javaid MK, Cooper C, Diez-Perez A, Arden NK. Incidence and risk factors for clinically diagnosed knee, hip and hand osteoarthritis: influences of age, gender and osteoarthritis affecting other joints. *Ann Rheum Dis* 2014; 73: 1659-1664.
11. Tschon M, Contartese D, Pagani S, Borsari V, Fini M. Gender and Sex Are Key Determinants in Osteoarthritis Not Only Confounding Variables. A Systematic Review of Clinical Data. *J Clin Med* 2021; 10.
12. Yuan J, Wang D, Zhang Y, Dou Q. Genetically predicted obesity and risk of hip osteoarthritis. *Eat Weight Disord* 2023; 28: 11.
13. van Buuren MMA, Arden NK, Bierma-Zeinstra SMA, Bramer WM, Casartelli NC, Felson DT, et al. Statistical shape modeling of the hip and the association with hip osteoarthritis: a systematic review. *Osteoarthritis Cartilage* 2021; 29: 607-618.
14. Saberi Hosnijeh F, Zuiderwijk ME, Versteeg M, Smeele HT, Hofman A, Uitterlinden AG, et al. Cam Deformity and Acetabular Dysplasia as Risk Factors for Hip Osteoarthritis. *Arthritis Rheumatol* 2017; 69: 86-93.
15. Agricola R, Waarsing JH, Arden NK, Carr AJ, Bierma-Zeinstra SM, Thomas GE, et al. Cam impingement of the hip: a risk factor for hip osteoarthritis. *Nat Rev Rheumatol* 2013; 9: 630-634.
16. Dijkstra HP, Mc Auliffe S, Arden CL, Kemp JL, Mosler AB, Price A, et al. Oxford consensus on primary cam morphology and femoroacetabular impingement syndrome: part 1-definitions, terminology, taxonomy and imaging outcomes. *Br J Sports Med* 2022; 57: 325-341.

17. Agricola R, Heijboer MP, Ginai AZ, Roels P, Zadpoor AA, Verhaar JA, et al. A cam deformity is gradually acquired during skeletal maturation in adolescent and young male soccer players: a prospective study with minimum 2-year follow-up. *Am J Sports Med* 2014; 42: 798-806.
18. Heerey J, Kemp J, Agricola R, Srinivasan R, Smith A, Pizzari T, et al. Cam morphology is associated with MRI-defined cartilage defects and labral tears: a case-control study of 237 young adult football players with and without hip and groin pain. *BMJ Open Sport Exerc Med* 2021; 7: e001199.
19. Notzli HP, Wyss TF, Stoecklin CH, Schmid MR, Treiber K, Hodler J. The contour of the femoral head-neck junction as a predictor for the risk of anterior impingement. *J Bone Joint Surg Br* 2002; 84: 556-560.
20. Nemtala F, Mardones RM, Tomic A. Anterior and Posterior Femoral Head-Neck Offset Ratio in the Cam Impingement. *Cartilage* 2010; 1: 238-241.
21. Gosvig KK, Jacobsen S, Palm H, Sonne-Holm S, Magnusson E. A new radiological index for assessing asphericity of the femoral head in cam impingement. *J Bone Joint Surg Br* 2007; 89: 1309-1316.
22. Kim HS, Park JW, Park JW, Ha YJ, Lee YK, Lee YJ, et al. Anterior and Lateral Femoroacetabular Excursion Angles Are Helpful for Assessing Femoroacetabular Impingement Syndrome: A Cross-Sectional Cohort Study. *Arthroscopy* 2023; 39: 2012-2022 e2011.
23. Dijkstra HP, Ardern CL, Serner A, Mosler AB, Weir A, Roberts NW, et al. Primary cam morphology; bump, burden or bog-standard? A concept analysis. *Br J Sports Med* 2021; 55: 1212-1221.
24. Mascarenhas VV, Castro MO, Rego PA, Sutter R, Sconfienza LM, Kassarian A, et al. The Lisbon Agreement on Femoroacetabular Impingement Imaging-part 1: overview. *Eur Radiol* 2020; 30: 5281-5297.
25. van Klij P, Reiman MP, Waarsing JH, Reijman M, Bramer WM, Verhaar JAN, et al. Classifying Cam Morphology by the Alpha Angle: A Systematic Review on Threshold Values. *Orthop J Sports Med* 2020; 8: 2325967120938312.
26. Wesseling J, Boers M, Viergever MA, Hilberdink WK, Lafeber FP, Dekker J, et al. Cohort Profile: Cohort Hip and Cohort Knee (CHECK) study. *Int J Epidemiol* 2016; 45: 36-44.
27. Wesseling J, Dekker J, van den Berg WB, Bierma-Zeinstra SM, Boers M, Cats HA, et al. CHECK (Cohort Hip and Cohort Knee): similarities and differences with the Osteoarthritis Initiative. *Ann Rheum Dis* 2009; 68: 1413-1419.
28. Agricola R, Leyland KM, Bierma-Zeinstra SM, Thomas GE, Emans PJ, Spector TD, et al. Validation of statistical shape modelling to predict hip osteoarthritis in females: data from two prospective cohort studies (Cohort Hip and Cohort Knee and Chingford). *Rheumatology (Oxford)* 2015; 54: 2033-2041.
29. Agricola R, Reijman M, Bierma-Zeinstra SM, Verhaar JA, Weinans H, Waarsing JH. Total hip replacement but not clinical osteoarthritis can be predicted by the shape of the hip: a prospective cohort study (CHECK). *Osteoarthritis Cartilage* 2013; 21: 559-564.
30. Ortiz-Declet V, Maldonado DR, Annin S, Yuen LC, Kyin C, Kopschik MR, et al. Nonarthritic Hip Pathology Patterns According to Sex, Femoroacetabular Impingement Morphology, and Generalized Ligamentous Laxity. *Am J Sports Med* 2022; 50: 40-49.
31. Boel F, de Vos-Jakobs S, Riedstra N, Lindner C, Runhaar J, Bierma-Zeinstra S, et al. Automated radiographic hip morphology measurements: An open-access method. *Osteoarthritis Imaging* 2024; 4: 100181.

32. Tang J, van Buuren MMA, Riedstra NS, Boel F, Runhaar J, Bierma-Zeinstra S, et al. Cam morphology is strongly and consistently associated with development of radiographic hip osteoarthritis throughout 4 follow-up visits within 10 years. *Osteoarthritis Cartilage* 2023.
33. Macri EM, Runhaar J, Damen J, Oei EHG, Bierma-Zeinstra SMA. Kellgren/Lawrence Grading in Cohort Studies: Methodological Update and Implications Illustrated Using Data From a Dutch Hip and Knee Cohort. *Arthritis Care Res (Hoboken)* 2022; 74: 1179-1187.
34. van Buuren MMA, Heerey JJ, Smith A, Crossley KM, Kemp JL, Scholes MJ, et al. The association between statistical shape modeling-defined hip morphology and features of early hip osteoarthritis in young adult football players: Data from the femoroacetabular impingement and hip osteoarthritis cohort (FORCE) study. *Osteoarthr Cartil Open* 2022; 4: 100275.
35. Bugeja JM, Xia Y, Chandra SS, Murphy NJ, Eyles J, Spiers L, et al. Automated volumetric and statistical shape assessment of cam-type morphology of the femoral head-neck region from clinical 3D magnetic resonance images. *Quant Imaging Med Surg* 2022; 12: 4924-4941.
36. Wang SC, Brede C, Lange D, Poster CS, Lange AW, Kohoyda-Inglis C, et al. Gender differences in hip anatomy: possible implications for injury tolerance in frontal collisions. *Annu Proc Assoc Adv Automot Med* 2004; 48: 287-301.
37. Halagatti M, Chelli SB, Rakaraddi S. A Study of Depth of Acetabulum from Adult Human Hip Bones-A Cross Sectional Study. *Medica Innovatica* 2022; 11.
38. Badley EM, Zahid S, Wilfong JM, Perruccio AV. Relationship Between Body Mass Index and Osteoarthritis for Single and Multisite Osteoarthritis of the Hand, Hip, or Knee: Findings From a Canadian Longitudinal Study on Aging. *Arthritis Care Res (Hoboken)* 2022; 74: 1879-1887.
39. Zengini E, Hatzikotoulas K, Tachmazidou I, Steinberg J, Hartwig FP, Southam L, et al. Genome-wide analyses using UK Biobank data provide insights into the genetic architecture of osteoarthritis. *Nat Genet* 2018; 50: 549-558.
40. Ahedi H, Winzenberg T, Bierma-Zeinstra S, Blizzard L, van Middelkoop M, Agricola R, et al. A prospective cohort study on cam morphology and its role in progression of osteoarthritis. *Int J Rheum Dis* 2022; 25: 601-612.
41. Agricola R, Waarsing JH, Thomas GE, Carr AJ, Reijman M, Bierma-Zeinstra SM, et al. Cam impingement: defining the presence of a cam deformity by the alpha angle: data from the CHECK cohort and Chingford cohort. *Osteoarthritis Cartilage* 2014; 22: 218-225.
42. Casartelli NC, Maffiuletti NA, Valenzuela PL, Grassi A, Ferrari E, van Buuren MMA, et al. Is hip morphology a risk factor for developing hip osteoarthritis? A systematic review with meta-analysis. *Osteoarthritis Cartilage* 2021; 29: 1252-1264.

Table S1. Associations between femoral head-neck junction shape modes and the presence of cam morphology and between subtypes of cam morphology and incident radiographic hip osteoarthritis in three groups with adjusting solely for sex and age.

Group	Shape mode	Outcome: cam morphology (alpha angle >60°)		Outcome: the development of RHOA at 10-year follow-up	
		aOR (95% CI)	P value	aOR (95% CI)	P value
Combined	mode1	0.59(0.50-0.69)	<0.001	0.98(0.88-1.09)	0.712
	mode2	1.12(0.89-1.42)	0.329		
	mode3*	1.59(1.32-1.91)	<0.001	1.14(1.02-1.28)	0.021
	mode4	1.77(1.41-2.21)	<0.001	0.91(0.85-1.00)	0.060
	mode5	1.74(1.43-2.13)	<0.001	1.10(0.99-1.23)	0.092
	mode6	1.21 (0.99-1.48)	0.061		
Male	mode1*	1.73(1.31-2.27)	<0.001	1.41(1.07-1.86)	0.016
	mode2	1.15(0.87-1.51)	0.339		
	mode3*	0.39(0.27-0.59)	<0.001	0.760(0.58-0.99)	0.044
	mode4	2.25(1.64-3.09)	<0.001	1.14(0.88-1.47)	0.332
	mode5	1.90(1.39-2.61)	<0.001	1.07(0.84-1.36)	0.605
	mode6	1.21(0.95-1.54)	0.124		
Female	mode1	0.43(0.34-0.55)	<0.001	1.09(0.958-1.239)	0.193
	mode2	0.93(0.73-1.19)	0.571		
	mode3*	1.79 (1.47-2.19)	<0.001	1.13(1.006-1.277)	0.040
	mode4*	1.46(1.13-1.89)	0.004	0.88(0.795-0.975)	0.015
	mode5	1.73(1.46-2.05)	<0.001	0.98(0.879-1.101)	0.772
	mode6	1.16(0.96-1.41)	0.135		

RHOA: radiographic hip osteoarthritis; OR: odds ratios; adjusted odds ratios (aOR) were adjusted for age, sex (only in combined group) at baseline. Shape modes marked with an asterisk (*) are significantly associated with both outcomes.

Selected femoral head-neck junction shape modes and percentage of variance explained per mode

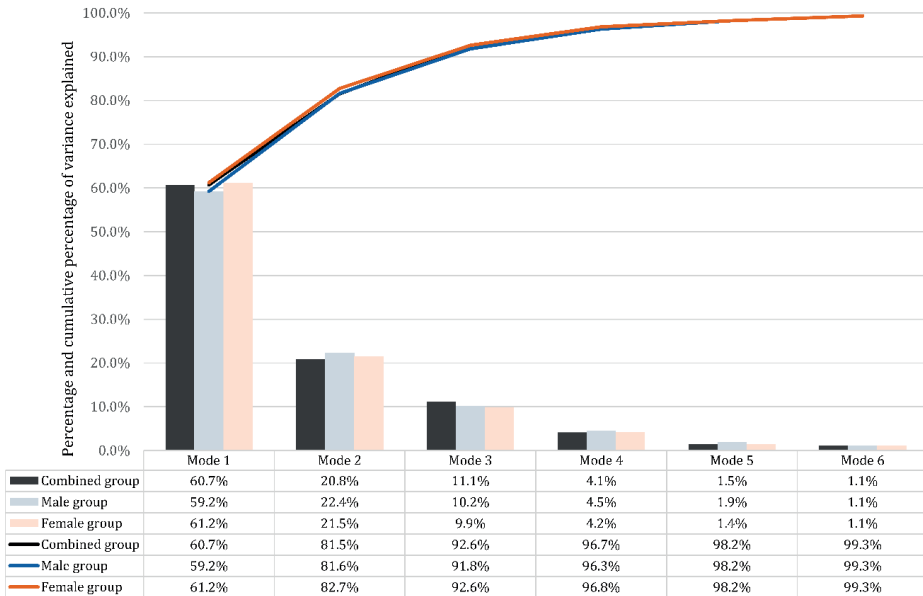


Figure S1. Selected femoral head-neck junction shape modes and percentage of variance explained per mode in three groups. The bar charts represent the percentage of variance explained for each mode and the line charts represent the cumulative percentage of variance in each group.

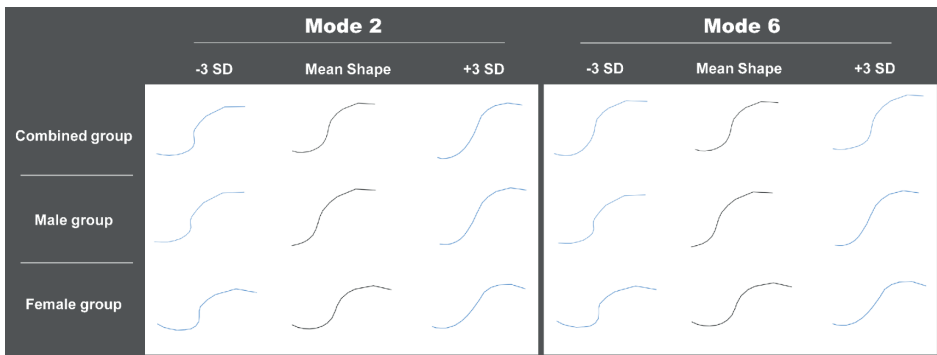


Figure S2. Shape modes defined by statistical shape modeling that are not associated with cam morphology based on hips from combined, male and female group. The shapes corresponding to -3 and +3 standard deviations (SDs) from the mean shape (depicted by the black line) are displayed on the left and right sides (depicted by the blue line), respectively.



Triangular Index Ratio as an Alternative Method to the Alpha Angle for Defining the Presence of Cam Morphology: Data from the CHECK Cohort

Jinchi Tang, Fleur Boel, Michiel M A van Buuren, Noortje S Riedstra, Myrthe A. van den Berg, Jos Runhaar, Sita Bierma-Zeinstra, Rintje Agricola.

Manuscript submitted.

ABSTRACT

Objective: To determine the association between cam morphology defined by triangular index ratio (TIR) and the development of radiographic hip osteoarthritis (RHOA) at 10-year follow-up. Additionally, to compare the predictive performance of cam morphology as defined by the TIR versus the alpha angle (AA) for RHOA development.

Methods: The Cohort Hip and Cohort Knee (CHECK) study included 1,002 participants aged 45-65 years with 10-year follow-up. The associations between cam morphology in hips free of RHOA at baseline (Kellgren & Lawrence (KL) grade <2) and the development of RHOA (KL \geq 2) were estimated using logistic regression adjusted for age, sex, and body mass index. Sensitivity, specificity, positive predictive value (PPV), and negative predictive value (NPV) for the development of RHOA for the two measures of cam morphology (TIR \geq 1.05 and AA \geq 60°) were evaluated.

Results: TIR-defined cam morphology was associated with the development of RHOA at follow-up with an adjusted Odds Ratio of 2.48 (95% CI 1.38-4.46). The PPVs of cam morphology defined by TIR (70.6%, 95% CI 59.0%-80.0%) for RHOA was somewhat higher than that of AA-defined cam morphology (62.3%, 95% CI 53.8%-70.1%), while the sensitivity for AA (12.3%, 95% CI 9.8%-15.2%) was higher than that of TIR (7.8%, 95% CI 5.8%-10.2%).

Conclusions: Cam morphology defined by a TIR \geq 1.05 at baseline is associated with the development of RHOA 10 years later. TIR can offer a more precise definition of the presence of cam morphology while AA can avoid losing too many target cases.

Keywords: radiographic hip osteoarthritis; cam morphology; triangular index ratio; alpha angle

INTRODUCTION

Cam morphology, a hip shape variation characterized by an osseous prominence at the anterolateral femoral head-neck junction, has been recognized as a significant morphological risk factor for hip osteoarthritis¹⁻³. Currently, there is no consensus on the gold standard for detecting or quantifying cam morphology. The alpha angle (AA) has emerged as the most widely used measurement due to its relative simplicity and wide applicability to various radiographic views and planes in both 2D and 3D imaging^{1,4,5}. It serves as a measure of the extent of asphericity of the femoral head, with a higher value indicating a greater deviation towards an aspherical femoral head. Previously, a threshold of AA $\geq 60^\circ$ was recommended to define the presence of cam morphology^{6,7}.

However, the alpha angle also has limitations. First, considerable variability was observed in its reliability previously. Interobserver intraclass correlation coefficient (ICC) ranged from 0.05 (95%CI -0.36-0.44)⁸ to 0.92 (95%CI 0.89-0.95)^{9,10}. Second, the AA only identifies the point where the femoral head-neck junction begins to protrude and is therefore potentially unable to capture the most prominent part of the cam morphology. Consequently, a small sliver of protruding bone may result in a similar AA value as a large bump. Additionally, the AA captures a broad range of 'aspherical femoral heads', some of which may not be consistent with our idea of what a cam morphology is and would not be relevant for the development of hip OA¹¹. These findings suggest that using AA alone to define cam morphology may yield inaccuracies.

The triangular index ratio (TIR) is an alternative method for quantifying cam morphology on an anteroposterior (AP) radiograph. Different than the AA, it quantifies cam morphology by measuring the extent to which a potential cam morphology laterally deviates at a predefined point at the head-neck junction. Given that the AA and TIR measure different aspects, the TIR may serve as an alternative measurement to AA. However, there is a lack of studies using TIR to quantify cam morphology and how this measure relates to the AA.

The aim of this study is to investigate the association between cam morphology defined by TIR and the development of radiographic hip osteoarthritis (RHOA) at follow-up. Additionally, we aim to assess and compare the predictive performance of the AA and TIR for RHOA development.

METHODS

Study population

The study population was drawn from the Cohort Hip and Cohort Knee (CHECK) study, a longitudinal multicenter prospective cohort study in the Netherlands. It included 1,002 individuals aged between 45 and 65 years with 10 years follow-up. These participants were experiencing their first episode of hip and/or knee complaints yet and had not sought medical assistance or initiated consultations with a general practice within six months before entry. The inclusion and exclusion criteria of the CHECK study have been previously outlined¹². In this study, we focused on the development of RHOA and included only individuals who met the following criteria: availability of both baseline and 10-year follow-up radiographs, complete baseline demographic data, and no evidence of RHOA at baseline.

Ethical approval for the study was granted by the medical ethics committees of all participating centers, and written informed consent was obtained from all participants.

Radiographic measurements

Standardized weight-bearing AP radiographs of the pelvis or hip were obtained at both baseline and 10-year follow-up. Both AP pelvis and hip radiographs used the same acquisition protocol; participants were positioned with 15° internal rotation of their hips, leading to contact between the medial side of the distal part of the big toes. For this study, we only used radiographs from the baseline and 10-year follow-up.

The AA is the angle between the femoral neck axis and a line connecting the femoral head center and the alpha point (red point in **Figure 1**), where the contour of the femoral head-neck junction begins to leave the best-fitting circle of the femoral head¹³. A previously validated threshold value of $\geq 60^\circ$ was used to define the presence of cam morphology⁶.

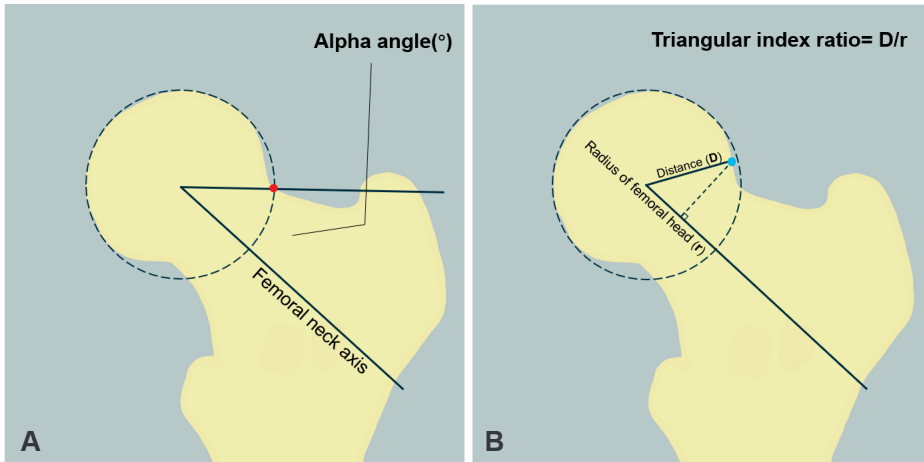


Figure 1. The measurement of alpha angle (figure A) and triangular index ratio (figure B).

By applying the Pythagorean law for triangular figures, triangular index defines cam morphology by comparing a specific distance (D) and the radius of femoral head (r). This distance (D) is measured from the center of the femoral head to the point (blue point in **Figure 1**) on the superior cortex of the head-neck junction. The blue point is located on the perpendicular (dotted) line drawn at half the radius of the femoral head, along the line that passes through the axis of the femoral neck. Initially, the asphericity of femoral head (cam morphology) was defined by Gosvig et al. if $D \geq r + 2$ mm at 1.2 magnification¹⁴. However, this measurement relies on radiographs achieving millimeter-level accuracy, with varying magnifications depending on the radiographic protocol used. To address this issue, we can convert the linear measurement into a ratio. This requires evaluating the relationship between the 2 mm threshold and the radius of the femoral head. First, an average femoral head diameter of 57.16 ± 0.66 mm in the white population (at no magnification) was used as a reference¹⁵. At 1.2 magnification, 2mm approximately corresponds to $0.058 r$. After rounding to two decimals, we selected the maximum value below this value as the threshold. Consequently, defining cam morphology when the ratio $D/r \geq 1.05$.

Both the AA and TIR were automatically and uniformly calculated by open-access, in-house developed and validated Python script (Version 3.7.0) on the baseline radiographs¹⁶. This method previously showed good inter-method reliability when compared with manual measurement by two experienced orthopedic surgeons on dual-energy X-ray absorptiometry (DXA) images: 0.81 (95%CI 0.46-0.92) for AA and 0.96 (95%CI 0.91-0.98) for TIR¹⁶.

Radiographic hip osteoarthritis

The status of RHOA was scored according to Kellgren and Lawrence (KL) classification. For each participant, the radiographs from baseline and all follow-ups were assessed simultaneously. The development of RHOA was defined by a KL grade ≥ 2 or a total hip replacement (THR) at 10-year follow-up from those having KL grade < 2 at baseline¹⁷.

Statistical Analysis

Univariate differences in baseline characteristics between included and excluded hips were investigated by the independent sample's T-test or chi-square test. To study the association between cam morphology defined by TIR or AA at baseline and the development of RHOA at 10-year follow-up, a logistic regression model was used. This regression analysis was performed with generalized estimating equations (GEE) to adjust for the correlation between measurements of the left and the right hip in the same person. The analysis was adjusted for age, biological sex, and body mass index (BMI) and the strength of association was expressed in odds ratios (OR) with 95% confidence intervals (CI). To assess the predictive performance for the development of RHOA at follow-up of cam morphology defined by AA $\geq 60^\circ$ or TIR ≥ 1.05 , we calculated sensitivity, specificity, positive predictive value (PPV) and negative predictive value (NPV) and their 95% CIs. Sensitivity analyses were conducted to assess predictive performance using TIR thresholds of ≥ 1.04 , 1.03, and 1.02.

All statistical analyses were performed in SPSS Statistics, version 26.0 (IBM Corp., Armonk, New York, USA). The effect was considered significant at $P < 0.05$.

RESULTS

Population

Detailed baseline characteristics of the participants and their hips are presented in **Table 1**. Of the 2,004 hips from 1,002 individuals in the Cohort Hip and Cohort Knee (CHECK) cohort, 588 hips were excluded: 240 hips had definite RHOA at baseline; in 111 hips, automated measurement was unavailable to perform due to the insufficient baseline radiographic quality; 2 hips lacked baseline BMI data; 235 hips lacked KL grade data at 10-year follow-up. In total, 1,416 hips were included at baseline (mean age: 55.6 ± 5.2 years; 81.7% females; mean BMI: 26.2 ± 4.0). The complete flow of participants (hips) is provided in the flowchart (**Figure 2**).

Table 1. Baseline characteristics of included and excluded hips from the CHECK cohort.

Baseline characteristics	CHECK cohort		
	Included hips (N=1416)	Excluded hips (N=586)	P value
Age in years: mean (SD)	55.6(5.2)	56.6(5.2)	0.403
Women, No (%)	1,157(81.7)	423(71.9)	<0.001
BMI, kg/m ² : mean (SD)	26.2(4.0)	26.1(4.0)	0.395
Alpha angle, °: mean (SD)	46.4(9.9)	50.9(13.7)	<0.001
Triangular index ratio: mean (SD)	0.96(0.05)	0.74(0.43)	<0.001

SD: standard deviation; BMI: body mass index.

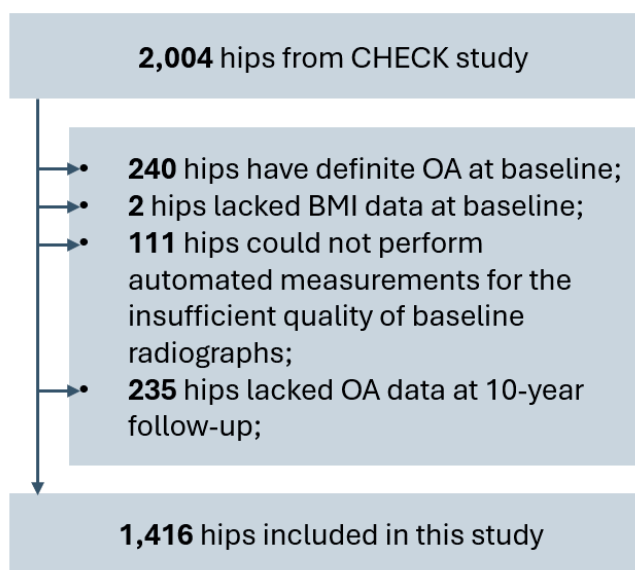


Figure 2. The flow of hips in this study

At baseline, there were 122 hips (8.6%) with cam morphology defined by $AA \geq 60^\circ$ and 69 hips (4.9%) with cam morphology defined by $TIR \geq 1.05$. Among them, 65 hips (4.6%) met both cam morphology definitions. The distribution of values for two measurements is shown in **Figure 3**.

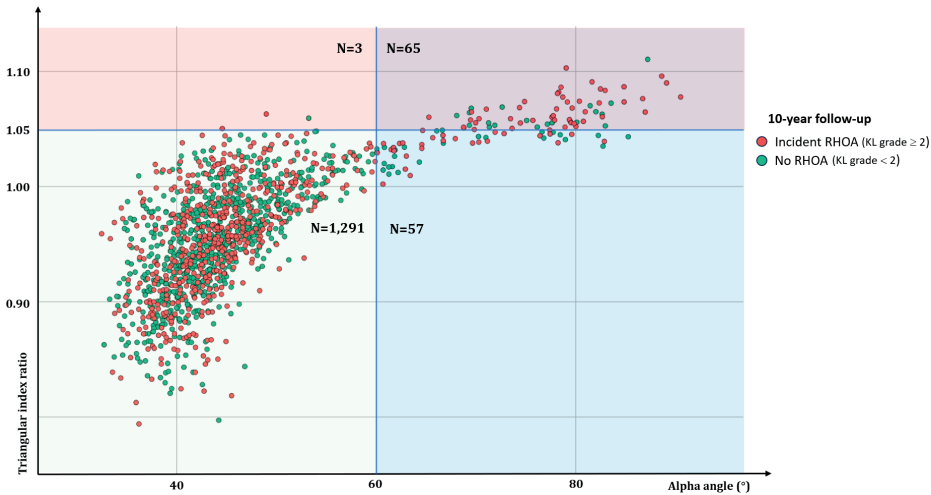


Figure 3. The distribution of included hips according to their value of alpha angle and triangular index ratio with outcome at 10-year follow-up. Two reference lines, indicating the thresholds of two measurements, divided hips into four categories (blue/red area: hips with cam morphology only fulfilling the alpha angle or triangular index ratio threshold; purple area: hips with cam morphology fulfilling both thresholds; green area: hips without cam morphology not fulfilling either threshold).

The incidence of RHOA at 10-year follow-up was 43.6%. Subgroup incidence of RHOA was 70.8% in hips with AA $\geq 60^\circ$ and TIR ≥ 1.05 ; 52.6% in hips with AA $\geq 60^\circ$ and TIR < 1.05 ; 41.8% in hips with AA $< 60^\circ$ and TIR < 1.05 ; 66.6% in hips with AA $< 60^\circ$ and TIR ≥ 1.05 (only 3 cases in this subgroup).

Cam morphology defined by TIR at baseline was significantly associated with the development of RHOA at 10-year follow-up with an unadjusted OR of 2.90 (95%CI 1.69-4.96) and an adjusted OR of 2.48 (95%CI 1.38-4.46). The unadjusted OR for the method of AA is 1.92 (95%CI 1.30-2.83) and the adjusted OR is 1.68 (95%CI 1.10-2.55).

The PPV for developing RHOA was higher in hips with cam morphology defined by TIR ≥ 1.05 (PPV=70.6%, 95%CI 59.0%-80.0%) than in those with cam morphology defined by AA $\geq 60^\circ$ (62.3%, 95%CI 53.8%-70.1%), while the NPV was similar within the two methods (AA: 58.2%; TIR: 57.8%). The sensitivity and specificity of AA were 12.3% and 94.3%, respectively. The corresponding values for TIR were 7.8% (95%CI 5.8%-10.2%) and 97.5% (95%CI 96.2%-98.5%). Results of sensitivity analysis for the predictive performances of TIR ≥ 1.04 , 1.03, or 1.02 were also shown in **Table 2**.

Table 2. Predictive performances of cam morphology defined by alpha angle or triangular index ratio for the development of RHOA at follow-up.

Method for defining cam morphology	The development of RHOA		Sensitivity (95%CI)	Specificity (95%CI)	PPV (95%CI)	NPV (95%CI)	
	Yes	No					
AA	≥ 60°	76	46	12.3% (9.8%-15.2%)	94.2% (92.4%-95.8%)	62.3% (53.8%-70.1%)	58.2% (57.4%-59.2%)
	< 60°	541	753				
	≥1.05	48	20	7.8% (5.8%-10.2%)	97.5% (96.2%-98.5%)	70.6% (59.0%-80.0%)	57.8% (57.3%-58.5%)
	<1.05	569	779				
TIR	≥1.04	64	37	10.4% (8.1%-13.1%)	95.4% (93.7%-96.7%)	63.4% (53.9%-71.9%)	58.0% (57.2%-58.7%)
	<1.04	553	762				
	≥1.03	92	52	14.9% (12.2%-18.0%)	93.5% (91.6%-95.1%)	63.9% (56.2%-71.0%)	58.7% (57.8%-59.6%)
	<1.03	525	747				
	≥1.02	120	82	19.45% (16.4%-22.8%)	89.7% (87.4%-91.7%)	59.1% (58.0%-60.2%)	59.1% (56.5%-61.7%)
<1.02	497	717					

AA: alpha angle; TIR: triangular index ratio; PPV: positive predictive value; NPV: negative predictive value.

DISCUSSION

This prospective cohort study showed a significant association between cam morphology defined by TIR ≥ 1.05 and the development of RHOA within 10 years follow-up. As an alternative method of AA for defining cam morphology, TIR offers both advantages and disadvantages. This makes each method better suited for different research or clinical purposes.

Although the original definition of TIR was initially proposed as a radiological index for evaluating femoral head asphericity in 2005¹⁴, it has seen limited application in prior research. In contrast, the AA, which serves the same purpose, is commonly used. This is likely due to the simplicity of measuring the AA and the ease with which it can be applied to various views of plain radiographs and multiplanar imaging^{18, 19}. Conversely, measuring the TIR involves more complex procedures and there is no evidence that the TIR can be used on radiographic views other than the AP view.

The limitations of the AA are becoming increasingly apparent. With the widespread adoption of automated measurements, the practicality of AA measurement is becoming less of an advantage. In addition, a recent study reported an inter-method ICC of 0.46 (95% CI 0.12-0.70) for AA, compared to 0.78 (95% CI 0.59-0.89) for TIR²⁰.

This variance can be attributed to the different measurement procedures for both measurements. The value of AA is defined by the position of the alpha point, which is related to the position of the best-fitting circle of the femoral head. In contrast, the measurement of TIR is less influenced by this factor²⁰. Moreover, we previously identified several distinct subtypes of cam morphology defined by an alpha angle $\geq 60^\circ$, where only some were relevant to RHOA development. These findings suggest that relying solely on the alpha angle to define cam morphology may be not suitable for researches aiming to efficiently identify high-risk subgroups for RHOA through the presence of cam morphology.

The TIR is a promising method for quantifying cam morphology. Our result of the logistic regression model indicates that hips with cam morphology defined by the TIR with a threshold value of ≥ 1.05 have 2.5 times higher odds (95%CI 1.38-4.46) of developing RHOA at 10-year follow-up compared to those without. As a comparison, the ORs for AA in the same population at the same follow-up is 1.68 (95%CI 1.10-2.55). The TIR therefore can be seen as a valuable tool for quantifying cam morphology and identifying those with high risk of RHOA. Since the TIR focuses on the distance from the most lateral part of the femoral head-neck junction to the femoral head center, slight deviations from a spherical femoral head which result in higher AA values will not be classified as cam morphology with the TIR. In our results, we identified 122 cases with AA-defined cam morphology while only 68 cases were identified by TIR. 46.7% (57 out of 122) of cases with AA-defined cam morphology had TIR values ranging from 1.00-1.05 indicating no to slight prominence at the femoral head-neck junction.

From the distribution of two measurements, both of which aim to serve the same purpose, a positive linear correlation between two values seems to be observed within the included hips. There was some overlap between values of the AA and the TIR, with 65 hips having both an AA $\geq 60^\circ$ and a TIR ≥ 1.05 . These overlapping cases have a high deviation to an aspherical femoral head and also have obvious lateral prominence at the femoral head-neck junction, fitting the description of cam morphology well. Notably, there were 3 cases captured by TIR ≥ 1.05 but with AA $< 60^\circ$, indicating the contour of the femoral head-neck junction exceeded but then re-entered the best-fitting circle of the femoral head. Although such cases are rare and lack an obvious or typical cam morphology, it is not reasonable to classify them as normal based solely on the AA.

The AA and TIR each have their advantages in defining the RHOA-relevant cam morphology. The PPV for RHOA incidence increased from 63.3% to over 70%, when

using the TIR to define cam morphology rather than the AA. However, the sensitivity obtained with the AA (12.3%) is higher than obtained with TIR (7.8%), which also indicates that using TIR alone will lead to a loss of a proportion of interested cases. The difference between the predictive performance of the two measurements primarily stems from a substantial portion of hips having an AA $\geq 60^\circ$ but a TIR < 1.05 . The incidence of RHOA in this subgroup (52.6%) is considerably lower than that in hips with AA $\geq 60^\circ$ and TIR ≥ 1.05 (70.8%), but is higher than in normal hips (AA $< 60^\circ$ and TIR < 1.05) (41.8%). Therefore, TIR ≥ 1.05 provides a more accurate definition for the presence of cam morphology, though it overlooks some RHOA-relevant cases. In contrast, AA $\geq 60^\circ$ can capture more target cases, though this leads to lower accuracy. Depending on the goal of research, the two methods can have different uses. Using the AA could reduce the risk of missing relevant RHOA cases during screening. Conversely, the TIR can more precisely identify individuals at high risk of RHOA, aiding in early intervention decisions.

Our study has several limitations. Firstly, the threshold value of the TIR used lacked extensive support from previous studies, given the limited application of the TIR. The threshold we used, TIR ≥ 1.05 , though showed good predictive performance compared to AA and other TIR thresholds but still needs external validation. Secondly, the generalizability of our findings cannot be generalized to a younger or asymptomatic population. Participants in the CHECK cohort study experienced first-onset symptoms in either their hip or knee, or both, and were aged between 45 and 65 years at baseline. Consequently, future research should focus on externally validating our findings across different demographic groups.

In conclusion, baseline cam morphology defined by a TIR ≥ 1.05 is associated with the development of RHOA 10 years later and showed higher positive predictive values than the alpha angle. The TIR could serve as a promising alternative to the alpha angle for quantifying cam morphology in future research.

REFERENCES

1. Dijkstra HP, Mc Auliffe S, Arden CL, Kemp JL, Mosler AB, Price A, et al. Oxford consensus on primary cam morphology and femoroacetabular impingement syndrome: part 1-definitions, terminology, taxonomy and imaging outcomes. *Br J Sports Med* 2022; 57: 325-341.
2. Agricola R, Waarsing JH, Arden NK, Carr AJ, Bierma-Zeinstra SM, Thomas GE, et al. Cam impingement of the hip: a risk factor for hip osteoarthritis. *Nat Rev Rheumatol* 2013; 9: 630-634.
3. Casartelli NC, Maffiuletti NA, Valenzuela PL, Grassi A, Ferrari E, van Buuren MMA, et al. Is hip morphology a risk factor for developing hip osteoarthritis? A systematic review with meta-analysis. *Osteoarthritis Cartilage* 2021; 29: 1252-1264.
4. Roling MA, Mathijssen NMC, Bloem RM. Diagnostic sensitivity and specificity of dynamic three-dimensional CT analysis in detection of cam and pincer type femoroacetabular impingement. *BMC Musculoskelet Disord* 2020; 21: 37.
5. Sutter R, Dietrich TJ, Zingg PO, Pfirrmann CW. How useful is the alpha angle for discriminating between symptomatic patients with cam-type femoroacetabular impingement and asymptomatic volunteers? *Radiology* 2012; 264: 514-521.
6. van Klij P, Reiman MP, Waarsing JH, Reijman M, Bramer WM, Verhaar JAN, et al. Classifying Cam Morphology by the Alpha Angle: A Systematic Review on Threshold Values. *Orthop J Sports Med* 2020; 8: 2325967120938312.
7. Agricola R, Waarsing JH, Thomas GE, Carr AJ, Reijman M, Bierma-Zeinstra SM, et al. Cam impingement: defining the presence of a cam deformity by the alpha angle: data from the CHECK cohort and Chingford cohort. *Osteoarthritis Cartilage* 2014; 22: 218-225.
8. Dessouky R, Chhabra A, Zhang L, Gleason A, Chopra R, Chatzinoff Y, et al. Cam-type femoroacetabular impingement-correlations between alpha angle versus volumetric measurements and surgical findings. *Eur Radiol* 2019; 29: 3431-3440.
9. Laborie LB, Lehmann TG, Engesaeter IO, Sera F, Engesaeter LB, Rosendahl K. The alpha angle in cam-type femoroacetabular impingement: new reference intervals based on 2038 healthy young adults. *Bone Joint J* 2014; 96-B: 449-454.
10. F. Boel NSR, J. Tang, D.F. Hanff, H. Ahedi, V. Arbabi, N.K. Arden, S.M.A. Bierma-Zeinstra, M.M.A. van Buuren, F.M. Cicuttini, T.F. Cootes, K. Crossley, D. Eygendaal, D.T. Felson, W.P. Gielis, J. Heerey, G. Jones, S. Kluzek, N.E. Lane, C. Lindner, J. Lynch, J. van Meurs, A.E. Nelson, A.B. Mosler, M.C. Nevitt, E.H. Oei, J. Runhaar, H. Weinans, R. Agricola., Reliability and agreement of manual and automated morphological radiographic hip measurements. *Osteoarthritis and Cartilage Open* 2024: 100510.
11. Tang J, Boel F, van Buuren MMA, Riedstra NS, Runhaar J, Bierma-Zeinstra S, et al. The different subtypes of cam morphology as defined by statistical shape modeling and their relationship with the development of hip osteoarthritis: A nationwide prospective cohort study (CHECK) with 10 years follow-up. *Osteoarthritis Cartilage* 2024.
12. Wesseling J, Boers M, Viergever MA, Hilberdink WK, Lafeber FP, Dekker J, et al. Cohort Profile: Cohort Hip and Cohort Knee (CHECK) study. *Int J Epidemiol* 2016; 45: 36-44.
13. Notzli HP, Wyss TF, Stoecklin CH, Schmid MR, Treiber K, Hodler J. The contour of the femoral head-neck junction as a predictor for the risk of anterior impingement. *J Bone Joint Surg Br* 2002; 84: 556-560.

14. Gosvig KK, Jacobsen S, Palm H, Sonne-Holm S, Magnusson E. A new radiological index for assessing asphericity of the femoral head in cam impingement. *J Bone Joint Surg Br* 2007; 89: 1309-1316.
15. Nelson AE, Stiller JL, Shi XA, Leyland KM, Renner JB, Schwartz TA, et al. Measures of hip morphology are related to development of worsening radiographic hip osteoarthritis over 6 to 13 year follow-up: the Johnston County Osteoarthritis Project. *Osteoarthritis Cartilage* 2016; 24: 443-450.
16. Boel F, de Vos-Jakobs S, Riedstra N, Lindner C, Runhaar J, Bierma-Zeinstra S, et al. Automated radiographic hip morphology measurements: An open-access method. *Osteoarthritis Imaging* 2024; 4: 100181.
17. Macri EM, Runhaar J, Damen J, Oei EHG, Bierma-Zeinstra SMA. Kellgren/Lawrence Grading in Cohort Studies: Methodological Update and Implications Illustrated Using Data From a Dutch Hip and Knee Cohort. *Arthritis Care Res (Hoboken)* 2022; 74: 1179-1187.
18. Barton C, Salineros MJ, Rakhra KS, Beaulé PE. Validity of the alpha angle measurement on plain radiographs in the evaluation of cam-type femoroacetabular impingement. *Clin Orthop Relat Res* 2011; 469: 464-469.
19. Cong S, Liu S, Xie Y, Luo Z, Chen J. Evaluation of Cam Deformity on 3-Dimensional Computed Tomography With the Best-Fit Sphere Technique and the Alpha Angle Marking Method. *Am J Sports Med* 2021; 49: 1023-1030.
20. Boel F, Riedstra NS, Tang J, Hanff DF, Ahedi H, Arbabi V, et al. Reliability and agreement of manual and automated morphological radiographic hip measurements. *Osteoarthritis Cartilage* 2024; 6: 100510.

8

General Discussion

In this thesis, cam morphology defined by different methods and its role in the development of RHOA was studied. In the first part, we introduced the automated measurements used to quantify cam morphology. In the second and third parts, we studied the role of cam morphology in the development of RHOA and the presence of hip pain, respectively. In the last part, we explored the cam morphology beyond the alpha angle and defined cam morphology in other ways.

DEFINITION OF CAM MORPHOLOGY

Historically, the terminology of cam morphology has evolved from describing a specific shape (“pistol grip”) to a pathological deformity (“cam deformity”), and now to a more commonly used term reflecting a morphology around the femoral head-neck junction (“cam morphology”)¹. Regardless of its terms, cam morphology essentially is characterized by a cartilage or bony prominence at the femoral head-neck junction, resulting in a deviation from a spherical to an aspherical femoral head.

In **Chapters 3-6**, we quantified cam morphology by the alpha angle on radiographs. This method captures the extent of sphericity of the femoral head and is widely used due to its simplicity and applicability across various radiographic views and 3D imaging scans. Previous studies reported different alpha angle thresholds to dichotomize the presence of cam morphology, ranging from 50.5° up to 83°². Our choice of a 60° threshold is supported not only by a recent international consensus but also by the bimodal distribution of alpha angles observed in the CHECK cohort, which naturally distinguishes hips with and without cam morphology³. Additionally, higher alpha angles have been associated with cartilage defects and labral tears⁴. In **Chapter 3**, we also used a higher threshold value of alpha angle (78°) to define a large cam morphology and found a stronger association with the development of RHOA. There is an argument that dichotomizing the continuous alpha angle can lead to a loss of power and incomplete adjustment for confounding factors^{5,6}. Therefore, we also directly used the continuous alpha angle value in **Chapters 3 and 4**, although this complicates the interpretation of cam morphology.

All alpha angles in this thesis were calculated on anteroposterior (AP) view radiographs. Cam morphology is mostly located at the anterosuperior part of the femoral head-neck junction, therefore the 45° Dunn view could be the optimal view to capture cam morphology^{7,8}. However, radiographic data in such view in large sample is rare and the more superiorly located cam morphologies are captured well in the AP view. Only using radiographs across this thesis might be a limitation, as cam morphology is

a 3D structure at the femoral head-neck junction, the description of its captured contour in a 2D view cannot provide more detailed information. However, the use of CT and MRI for large-scale screening is limited due to being time-consuming, expensive, and higher requirements for facilities and radiologists. Therefore, radiographs may be the best solution as a screening tool for large samples.

Besides the alpha angle, other radiographic measurements have been introduced to assess femoral head sphericity. In **Chapter 7**, we used the triangular index ratio (≥ 1.05) to define cam morphology. This method, derived from the triangular index proposed by Gosvig et al., captures the most lateral part of the femoral head-neck junction, in contrast to the alpha angle, which measures where the femoral head-neck junction begins to deviate from the best-fitting circle of the femoral head. These two methods therefore focus on different aspects of cam morphology, which will be discussed in more detail below.

PREVALENCE OF CAM MORPHOLOGY

The prevalence of cam morphology varies significantly, ranging from 5% to 75%, depending on the study population's characteristics, such as age, sex, ethnicity, athletic activity, and symptomatology⁹. Cam morphology is generally reported to be more prevalent in males than females¹⁰. Our results in **Chapters 3** and **4** support this, with prevalence rates of 23.7% in males versus 5.4% in females in the CHECK cohort and 20.2% in males versus 5.1% in females in the World COACH consortium. This difference may be explained by the fact that females mature earlier than males and likely experience less exposure to repetitive axial loading during their second growth spurt¹⁰. The prevalence of cam morphology tends to increase gradually during skeletal growth¹⁰. Although our data focuses on a middle-aged population, we observed an interesting trend in **Chapter 4**: the prevalence of cam morphology decreases with aging. The 40-50 age group had the highest prevalence at 11.4% compared to other subgroups. Typically, cam morphology stabilizes after skeletal maturation, and thus, its prevalence remains constant over time. However, with increasing age, the dropout rate also increases, particularly in older groups, which may explain our findings. Although this thesis does not aim to provide the prevalence of cam morphology in subgroups categorized by athletic activity, ethnicity, or symptomatology, previous studies have found a higher prevalence in athletic or symptomatic populations^{11,12}, with the lowest prevalence observed in individuals of East Asian ethnicity¹³. These findings suggest that these characteristics could be important factors to consider when studying the prevalence of cam morphology in future research.

DEFINITION OF THE DEVELOPMENT OF RADIOGRAPHIC HIP OSTEOARTHRITIS

In this thesis, the development of RHOA is defined as a transition from being free of OA at baseline to having definite RHOA at follow-up. Hip OA is characterized by the destruction of articular cartilage and reactive bone changes, which are radiographically manifested as joint space narrowing (JSN), the presence of osteophyte formation, the presence of subchondral cysts, or remodeling of the articular surface^{14, 15}. Among these radiographical changes, JSN and osteophyte formation are the most used indicators for assessing the status of hip OA. The JSN refers to the distance between the acetabular roof and the femoral head, reflecting the combined thickness of the acetabular and femoral head cartilages¹⁶. While the osteophytes form as bony lumps compensating for the lost cartilage when the hip bone is damaged by OA or other chronic inflammatory rheumatic disease^{17, 18}.

The definite absence of these two radiographical changes is typically used to define freedom from OA in various classifications, including the Kellgren-Lawrence (KL) classification¹⁹, the Tönnis' classification²⁰, and the Croft classifications²¹. The CHECK cohort used the KL classification to assess the OA status, with grades from 0 (no OA) to 4 (severe OA). Hips were considered free of OA if their baseline KL grade was less than 2, which included hips with doubtful OA (KL grade = 1) in the non-OA group. This dichotomization aimed to simplify OA status classification, as possible JSN or osteophytic lipping alone is insufficient to define definite OA. In **Chapter 4**, the World COACH consortium adopted a harmonized classification system with a trichotomous outcome for radiographic hip osteoarthritis (RHOA), rather than the traditional binary approach. This new classification allowed us to explore whether "doubtful RHOA," often considered a necessary and irreversible stage in the progression from no osteoarthritis to definite OA, plays a role in the development of RHOA. Furthermore, unlike the CHECK cohort, the World COACH consortium's dataset includes over 70,000 hips, providing a large enough sample size to exclude cases of doubtful RHOA at baseline.

Definite RHOA is characterized by the presence of JSN and osteophytes in follow-up radiographs. Additionally, hips that underwent total hip replacement (THR) could be considered as an outcome for both clinical and radiographical end-stage hip OA, therefore these cases were also included in the definition of definite RHOA. Although RHOA status can be classified into early-stage, moderate, and severe (end-stage) based on the extent of JSN, osteophyte size, or other structural changes, we did not delve into these distinctions in most chapters of this thesis. Instead, we grouped them under a single "definite OA" category. The only exception is in **Chapter 3**, where a secondary

outcome—the development of end-stage RHOA—was defined as either a follow-up KL grade of 3 or higher or a THR. This approach allowed us to examine whether cam morphology has varying effects on different stages of osteoarthritis progression. Our findings indicated a stronger association of cam morphology with this outcome compared to incident RHOA (KL grade ≥ 2 or a THR). This suggests that the development of end-stage RHOA may also be a significant and interesting outcome for future studies focusing on cam morphology.

CAM MORPHOLOGY AS A RISK FACTOR FOR RADIOGRAPHIC HIP OSTEOARTHRITIS

The association between cam morphology and the development of RHOA has been well-studied over the past two decades. A recent retrospective study within the Rotterdam study demonstrated a significant risk ratio of 1.80 (1.35–2.38) for cam morphology leading to incident RHOA²². Cross-sectional studies have also reported ORs ranging from 2.12 (1.17–3.83) to 2.91 (1.43–5.93) for the association between cam morphology and joint damage²³, and ORs from 3.20 (2.41–4.25) to 10.38 (5.04–21.44) for the association with hip OA^{24, 25}. In prospective studies^{26–28}, the strength of the association varied greatly with ORs of 1.21 (1.07–1.37) to 4.46 (1.8–11.3) for developing RHOA. All these findings indicate the significant variability for risk of cam morphology to RHOA.

In previous prospective studies, with follow-up periods ranging from 3 to over 20 years, there seemed to be a trend of weaker associations with a longer follow-up²⁹. It has previously been hypothesized that cam morphology can lead to the development of hip OA within a few years of follow-up rather than a gradual development over a decade or more³⁰. Our findings in **Chapter 3** showed a consistent significant association between cam morphology and incident RHOA, with ORs ranging from 2.7 (1.8–4.1) to 2.9 (2.0–4.4). This suggests that for individuals aged 45 to 65 years, the strength of association between cam morphology and RHOA development does not significantly change over time.

The differences in the strength of association between various studies may be attributed to heterogeneity in the populations and definitions of RHOA and cam morphology. The study in **Chapter 4** aimed to address this issue by demonstrating the association between cam morphology and RHOA using harmonized data from nine prospective cohorts. By combining different populations and utilizing a uniform calculation for the alpha angle and a harmonized definition of incident RHOA, the generalizability of

the results is much higher than in individual studies. In this study, cam morphology was associated with the development of RHOA with a lower OR of 1.87 (1.36-2.59), likely due to the exclusion of doubtful RHOA at baseline. In contrast, previous studies typically included hips with doubtful RHOA in the non-RHOA group along with hips free of RHOA. Unlike hips free of RHOA, hips with doubtful RHOA already exhibit some structural changes more likely to progress to definite RHOA. Therefore, including hips with doubtful RHOA at baseline affects the true incidence of RHOA at follow-up.

The size of cam morphology also influences the risk of RHOA. In **Chapter 3**, we found a stronger association with RHOA for large cam morphology (alpha angle $\geq 78^\circ$). In **Chapter 4**, each degree increase in the alpha angle had an OR of 1.02(1.01-1.03) for RHOA. A larger cam morphology may cause earlier and more extensive cartilage damage due to premature contact between the cam and acetabulum during hip motion. Additionally, larger cam morphology can lead to higher peak contact pressures on the acetabular cartilage during extensive hip motion, compared to smaller cam morphology.

Notably, this thesis did not study the role of cam morphology in RHOA at a younger population aged from 20 to 40 years. Cam morphology begins to develop around age 13 and stabilizes after skeletal maturation, whereas hip OA typically appears later, usually in individuals in their late 40s to mid-50s. The role of cam morphology in the period from stabilization to the onset of radiographic OA is rarely studied, therefore it is not fully understood. It is believed that cam morphology may lead to the rapid development of hip OA in young athletes³¹. High alpha angles have been associated with MRI-defined cartilage defects (OR: 1.03, 1.01-1.04) and labral tears (OR: 1.02, 1.01-1.04) in young football players with a mean age of 26 years⁴. Another study in the FORCe cohort found that cam morphology, defined through statistical shape modeling, was associated with cartilage defects (OR: 1.34, 1.05-1.69) and labral tears (OR: 1.30, 1.01-1.69) in high-impact athletes without RHOA³². These findings indicate that individuals with cam morphology may experience OA-related structural changes at a very young age. Notably, these early changes are typically not enough to be classified as definite RHOA and may lead to the development of RHOA only after a prolonged, gradual progression.

CAM MORPHOLOGY AS A KEY TYPE OF FEMOROACETABULAR IMPINGEMENT SYNDROME

Femoroacetabular impingement (FAI) syndrome is a motion-related clinical disorder of the hip, characterized by symptomatic premature contact between the proximal femur and the acetabulum³³. It can be diagnosed by a combination of symptoms, clinical signs, and imaging findings. The primary symptom of FAI syndrome is motion-related or position-related pain in the hip or groin³⁴. By morphological assessment, the FAI syndrome can represent as cam morphology, the focus of this thesis, or/and pincer morphology, which refers to the overcoverage of the femoral head by the acetabulum³⁴. The diagnostic criteria of FAI syndrome indicate that there is a substantial proportion of the population with cam morphology is asymptomatic.

In previous studies, the association between cam morphology and experiencing hip pain showed conflicting results, with some studies finding significant associations³⁵⁻³⁸ and others finding none³⁹⁻⁴³. One potential explanation for these discrepancies might be the fluctuating nature of hip pain over time. The prevalence of hip pain reported in **Chapter 5**, ranges from 27.5% to 40.0% over 10 years, highlighting this character of pain. In all previous, the data of hip are required by participants' self-reporting at one-time point. Past studies have relied on self-reported data at single time points, which introduces subjectivity and affects the observed associations. In **Chapter 5**, baseline cam morphology in males was associated with hip pain at a 5-year follow-up but not at other time points, suggesting that pain fluctuation impacts this association. Therefore, a more objective method for collecting data on pain in future studies is needed. Multiple follow-ups, as conducted in **Chapter 5**, can be a solution. Additionally, using specifically designed tools such as the International Hip Outcome Tool (iHOT), Hip and Groin Outcome Score (HAGOS), and Hip Outcome Score (HOS) can reduce the subjectivity inherent in self-reported outcomes.

Biological sex might play an important role between cam morphology and hip pain. In **Chapter 5**, we observed no significant association between cam morphology and hip pain in females, with odds ratios fluctuating around 1. In contrast, males showed consistent odds ratios exceeding 1. This aligns with findings from a cross-sectional study in UK Biobank, where cam morphology was associated with hip pain only in males (OR: 1.48, 1.05-2.09)⁴³. This difference may be due to variations in cam morphology manifestations and pain sensitivity between sexes. Males typically have higher mean alpha angles, leading to a higher prevalence of cam morphology and a greater risk of cartilage defects and labral tears. In **Chapter 6**, a subtype of cam morphology was found to be protective against RHOA in females, but no such effect was observed in

males, indicating the need for further investigation into the sex-specific effects of cam morphology on hip pain. Experimental pain studies have shown that females exhibit heightened pain sensitivity, increased pain facilitation, and reduced pain inhibition compared to males⁴⁴. In **Chapter 5**, the prevalence of hip pain is consistently higher in the female group, at almost all follow-up time points (10 out of 11), with the most significant difference observed at the 2-year follow-up (37.2% in females vs. 28.0% in males). These findings underscore the importance of considering biological sex in studies on cam morphology and hip pain.

SUBTYPES OF CAM MORPHOLOGY

There were a variety of terms used to describe the shape of cam morphology, including but not limited to “pistol grip deformity”, “tilt deformity”, “hump”, “flattening”, and “oval-shape”⁴⁵. These terms aim to characterize the shape of cam morphology but vary significantly. The alpha angle measures the extent of femoral head asphericity but does not distinguish between different shapes of cam morphology. Statistical shape modeling (SSM), a novel shape analysis technique, can be a useful tool to quantify the shape of cam morphology.

The SSM has gained increasing attention due to the recognized importance of hip morphology. SSM-defined shape variants of the hip had been used to predict an incident or progressive hip OA or future THR previously, demonstrating high effectiveness in quantifying shape variation. However, most of those studies focused on the entire hip or pelvis without further exploring the specific area of the femoral head-neck junction. A study in the FORCe cohort found that certain hip shape variants potentially representing cam morphology were associated with cartilage defects while others with cam morphology were not, possibly indicating the existence of different subtypes of cam morphology³². Another study used SSM to explore cam morphology through parameters such as cam volume, surface area, and height. However, the differences of those radiographic parameters were not used to further classify cam morphology into subtypes⁴⁶.

In **Chapter 6**, we conducted a prospective cohort study using SSM to analyze shape variants in the femoral head-neck junction, which is the first relevant study focused only on cam morphology. Since the shape modes are defined by the population from which they were created, we built three independent SSMs based on hips from only males or females or a combined group. Based on the alpha angle $\geq 60^\circ$, four distinct subtypes of cam morphology were identified, and one subtype representing a “flat-

tened head-neck junction” was the only RHOA-associated subtype in all three groups. Another subtype, described as a “pistol grip-shaped prominence”, was associated with RHOA only in males. Conversely, a flattened femoral neck with clear curvature appeared to be protective against RHOA in females. These findings might help explain the results from **Chapter 4**, where males with cam morphology had a higher relative risk (2.50) of developing RHOA compared to females (1.75).

The clinical implications of those identified subtypes of cam morphology is that by simply identifying the morphological characteristics represented by each independent shape mode, those with RHOA-relevant subtypes can be distinguished. Those with alpha angle $\geq 60^\circ$ but without RHOA-relevant shape variations can therefore be prioritized lower for intervention. Our findings emphasize the need for further validation in diverse populations and with the use of 3D imaging.

THE ALPHA ANGLE AND TRIANGULAR INDEX RATIO

In this thesis, the alpha angle was used to quantify the cam morphology in **Chapters 3-6** with a threshold value of 60° . However, our findings in **Chapter 6** suggest that the alpha angle alone may not accurately define cam morphology, as some subtypes captured were not relevant to RHOA. In **Chapter 2**, we introduced the automated measurement of the alpha angle, which depends on the position of the alpha points. This point refers to where the contour of the femoral head-neck junction begins to leave the best-fitting circle around the femoral head. According to the subtypes of cam morphology we identified, the most prominent part of cam morphology may be located more lateral than this alpha point. Therefore, using alpha angle alone to define cam morphology may yield inaccuracies.

In **Chapter 7**, we investigated the association between cam morphology defined by triangular index ratio and the development of RHOA at 10-year follow-up with a significant OR of 2.48 (1.38-4.46). This value cannot be directly comparable to the ORs for alpha angle-defined cam morphology in **Chapter 3** due to the different included populations of the two studies. However, by comparing the predictive performance for RHOA of the two methods, the triangular index ratio showed a higher positive predictive value (70.6% vs 62.3%) and a lower sensitivity (7.8% vs 12.3%) than the alpha angle for RHOA. These indicate that both of the two methods have their advantages in defining the RHOA-relevant cam morphology. Therefore, triangular index ratio ≥ 1.05 provides a more accurate definition for the presence of cam morphology, though it overlooks some RHOA-relevant cases. In contrast, the alpha angle $\geq 60^\circ$ can capture

more target cases, though this leads to lower accuracy. Depending on the goal of the research, the two methods have different clinical implications. The alpha angle is more suitable as a screening test for large sample sizes, ensuring most suspected cases are identified. Conversely, the triangular index ratio can precisely identify individuals at high risk of RHOA, aiding in early intervention decisions.

THE POPULATION

Data from the CHECK cohort was used across this thesis. The CHECK (Cohort Hip and Cohort Knee study) cohort is a Dutch prospective cohort study aiming to study the course, prognosis, and underlying mechanisms of early symptomatic OA. Therefore, Participants are middle-aged (45-65 years) individuals experiencing their first episode of pain in the hip and/or knee. Those with other pathological conditions explaining the symptoms were excluded, resulting in a baseline cohort of 1,002 participants. These criteria lead to a higher incidence of radiographic hip osteoarthritis (RHOA) in the CHECK cohort compared to other asymptomatic cohorts. Standardized weight-bearing AP hip or pelvic radiographs were obtained at baseline, 2-, 5-, 8-, and 10-year follow-ups. These follow-up data allow for the investigation of the association between cam morphology and RHOA (discussed in **Chapter 3**) and hip pain (discussed in **Chapter 5**) over multiple time points.

The Worldwide Collaboration on Osteoarthritis prediction for the Hip (World COACH) is an international consortium of nine prospective cohort studies worldwide, which are introduced in **Chapter 4**. At baseline, the alpha angle was uniformly calculated using an automated algorithm, enhancing reliability across different cohorts. Follow-up periods varied among these cohorts, ranging from 5 to over 25 years. To ensure consistency, a window period of 4-8 years after baseline was selected for follow-up data. Harmonizing data from multiple cohort studies into an individual participant-level database provides a large sample size and improves the generalizability of the findings. It also allows for subgroup-specific risk estimation for developing RHOA, such as by age, sex, and BMI categories. Utilizing data from the World COACH consortium enhances our understanding of the risk effects of cam morphology on the development of RHOA.

CLINICAL IMPLICATIONS

Cam morphology is a notable risk factor for developing RHOA in individuals without any existing radiographic signs of hip OA. Early identification through simple radiographic measurements can help identify high-risk groups in their early years. This method is also suitable for large-scale population screening. By using the triangular index ratio and identifying morphological characteristics represented by RHOA-relevant subtypes of cam morphology, the detection accuracy can be highly improved. This early detection enables preventive measures through lifestyle and physical activity interventions, potentially mitigating the risk of developing RHOA. Our findings highlight the importance of further investigating the etiology of cam morphology. Although cam morphology remains stable after skeletal maturity, its formation could potentially be influenced during skeletal growth. The prevalence of cam morphology is reported higher in those who long-termly participate high-impact sports than in the nonathletic population, indicating duration of physical activity of high loading can be an interesting target. Notably, there is no strong association between cam morphology and hip pain over a 10-year follow-up. Therefore, the presence of cam morphology on radiographs should not be used to predict future hip pain, especially in females.

FUTURE PERSPECTIVE

In this thesis, most data were derived from the CHECK cohort, which may limit the generalizability of findings to younger or asymptomatic populations. There is a notable gap in research focusing on the association between cam morphology and its development in individuals aged 20 to 40 years. Current studies often target young athletic populations, such as football players, rather than the general population. Therefore, future research should consider including a younger, general population to enhance our understanding of cam morphology.

Using harmonized data from multiple cohorts can improve the generalizability of findings. The World COACH consortium, for instance, provides a valuable resource for such endeavors. However, harmonizing OA scores assessed by different classifications is challenging, emphasizing the need for a uniform definition of RHOA. Excluding hips with doubtful diagnoses from the baseline is crucial, as they can impact the association between cam morphology and definite RHOA.

Sex differences play a significant role in the risk associated with cam morphology. Our findings show different associations between cam morphology and hip pain, as well as

between SSM-defined subtypes of cam morphology and development in males and females. Additionally, we identified a protective subtype of cam morphology in females, but not in males. These results highlight the importance of sex stratification in studies related to cam morphology. The underlying reasons for these sex differences are not fully understood and warrant further investigation through well-designed studies.

This thesis utilized AP radiographs for radiographic measurements. However, cam morphology is a 3D structure at the femoral head-neck junction, and 2D measurements like the alpha angle or triangular index ratio cannot fully capture its morphological information. MRI-based studies have shown that volume, surface area, and height of cam morphology can be assessed through MRI scans, providing more comprehensive data than radiographs. Despite their advantages, 3D imaging scans are less commonly used due to high costs and facility requirements. Future studies on cam morphology should consider incorporating 3D imaging to enhance accuracy.

The triangular index ratio shows potential as a measurement method for quantifying cam morphology with better predictive performance for RHOA. Although this method is seldom used, it has demonstrated high effectiveness in defining RHOA-relevant cam morphology in the CHECK cohort, with a threshold of 1.05. Whether triangular index ratio-defined cam morphology is closer to a real cam morphology than alpha angle-defined cam morphology needs more research explorations.

The identification of cam morphology subtypes is a novel area of research. Our study in **Chapter 6**, though identified four distinct subtypes of cam morphology, serves more as a proof of concept rather than a direct translation of these findings into clinical practice. The morphological characteristics represented by each subtype need validation in SSM studies based on other populations. Future research should also consider using 3D imaging to explore and classify the shapes of cam morphology further.

CONCLUSION

This thesis demonstrated that cam morphology defined by an alpha angle $\geq 60^\circ$ is a significant risk factor for the development of RHOA. This association remained consistently significant over a 10-year follow-up period, although the strength of this association was reduced in a harmonized database excluding hips with doubtful RHOA at baseline. Biological sex appears to play a crucial role in the relationship between cam morphology and hip pain. Specifically, we found a significant association between baseline cam morphology and hip pain at the 5-year follow-up in males, while no

such relationship was observed at other time points or in females. Additionally, sex differences were evident in the subtypes of cam morphology defined by statistical shape modeling. Four distinct subtypes of cam morphology were identified based on an alpha angle $\geq 60^\circ$. Among them, one subtype representing a “flattened head-neck junction” was associated with RHOA development in both males and females; a “pistol grip-shaped prominence” was associated with RHOA only in males; a flattened femoral neck with clear curvature appeared to be protective against RHOA only in females. Given the part of subtypes of cam morphology captured by the alpha angle $\geq 60^\circ$ are non-relevant to RHOA, we therefore tried to use another method to define cam morphology. Cam morphology defined by a triangular index ratio ≥ 1.05 at baseline is associated with the development of RHOA 10 years later. Triangular index ratio can offer a more precise definition of the presence of cam morphology while the alpha angle can ensure the capture of more target cases.

REFERENCES

1. Dijkstra HP, Mc Auliffe S, Ardern CL, Kemp JL, Mosler AB, Price A, et al. Oxford consensus on primary cam morphology and femoroacetabular impingement syndrome: part 1-definitions, terminology, taxonomy and imaging outcomes. *Br J Sports Med* 2022; 57: 325-341.
2. van Klij P, Reiman MP, Waarsing JH, Reijman M, Bramer WM, Verhaar JAN, et al. Classifying Cam Morphology by the Alpha Angle: A Systematic Review on Threshold Values. *Orthop J Sports Med* 2020; 8: 2325967120938312.
3. Agricola R, Waarsing JH, Thomas GE, Carr AJ, Reijman M, Bierma-Zeinstra SM, et al. Cam impingement: defining the presence of a cam deformity by the alpha angle: data from the CHECK cohort and Chingford cohort. *Osteoarthritis Cartilage* 2014; 22: 218-225.
4. Heerey J, Kemp J, Agricola R, Srinivasan R, Smith A, Pizzari T, et al. Cam morphology is associated with MRI-defined cartilage defects and labral tears: a case-control study of 237 young adult football players with and without hip and groin pain. *BMJ Open Sport Exerc Med* 2021; 7: e001199.
5. Altman DG, Royston P. The cost of dichotomising continuous variables. *BMJ* 2006; 332: 1080.
6. Royston P, Altman DG, Sauerbrei W. Dichotomizing continuous predictors in multiple regression: a bad idea. *Stat Med* 2006; 25: 127-141.
7. Saito M, Tsukada S, Yoshida K, Okada Y, Tasaki A. Correlation of alpha angle between various radiographic projections and radial magnetic resonance imaging for cam deformity in femoral head-neck junction. *Knee Surg Sports Traumatol Arthrosc* 2017; 25: 77-83.
8. Barton C, Salineros MJ, Rakhra KS, Beaulé PE. Validity of the alpha angle measurement on plain radiographs in the evaluation of cam-type femoroacetabular impingement. *Clin Orthop Relat Res* 2011; 469: 464-469.
9. Dickenson E, Wall PD, Robinson B, Fernandez M, Parsons H, Buchbinder R, et al. Prevalence of cam hip shape morphology: a systematic review. *Osteoarthritis Cartilage* 2016; 24: 949-961.
10. van Klij P, Heerey J, Waarsing JH, Agricola R. The Prevalence of Cam and Pincer Morphology and Its Association With Development of Hip Osteoarthritis. *J Orthop Sports Phys Ther* 2018; 48: 230-238.
11. Frank JM, Harris JD, Erickson BJ, Slikker W, 3rd, Bush-Joseph CA, Salata MJ, et al. Prevalence of Femoroacetabular Impingement Imaging Findings in Asymptomatic Volunteers: A Systematic Review. *Arthroscopy* 2015; 31: 1199-1204.
12. Mascarenhas VV, Rego P, Dantas P, Morais F, McWilliams J, Collado D, et al. Imaging prevalence of femoroacetabular impingement in symptomatic patients, athletes, and asymptomatic individuals: A systematic review. *Eur J Radiol* 2016; 85: 73-95.
13. Mosler AB, Crossley KM, Waarsing JH, Jomaah N, Weir A, Holmich P, et al. Ethnic Differences in Bony Hip Morphology in a Cohort of 445 Professional Male Soccer Players. *Am J Sports Med* 2016; 44: 2967-2974.
14. Dagenais S, Garbedian S, Wai EK. Systematic review of the prevalence of radiographic primary hip osteoarthritis. *Clin Orthop Relat Res* 2009; 467: 623-637.
15. Gold GE, Cicuttini F, Crema MD, Eckstein F, Guermazi A, Kijowski R, et al. OARSI Clinical Trials Recommendations: Hip imaging in clinical trials in osteoarthritis. *Osteoarthritis Cartilage* 2015; 23: 716-731.

16. Resnick D. Patterns of migration of the femoral head in osteoarthritis of the hip. Roentgenographic-pathologic correlation and comparison with rheumatoid arthritis. *Am J Roentgenol Radium Ther Nucl Med* 1975; 124: 62-74.
17. Roelofs AJ, Kania K, Rafipay AJ, Sambale M, Kuwahara ST, Collins FL, et al. Identification of the skeletal progenitor cells forming osteophytes in osteoarthritis. *Ann Rheum Dis* 2020; 79: 1625-1634.
18. Schett G. Joint remodelling in inflammatory disease. *Ann Rheum Dis* 2007; 66 Suppl 3: iii42-44.
19. Kohn MD, Sassoon AA, Fernando ND. Classifications in Brief: Kellgren-Lawrence Classification of Osteoarthritis. *Clin Orthop Relat Res* 2016; 474: 1886-1893.
20. Kovalenko B, Bremjit P, Fernando N. Classifications in Brief: Tonnis Classification of Hip Osteoarthritis. *Clin Orthop Relat Res* 2018; 476: 1680-1684.
21. Croft P, Cooper C, Wickham C, Coggon D. Defining osteoarthritis of the hip for epidemiologic studies. *Am J Epidemiol* 1990; 132: 514-522.
22. Runhaar J, van Berkel AC, Agricola R, van Meurs J, Bierma-Zeinstra SMA. Risk Factors and Population-Attributable Fractions for Incident Hip Osteoarthritis. *HSS J* 2023; 19: 407-412.
23. Reichenbach S, Leunig M, Werlen S, Nuesch E, Pfirrmann CW, Bonel H, et al. Association between cam-type deformities and magnetic resonance imaging-detected structural hip damage: a cross-sectional study in young men. *Arthritis Rheum* 2011; 63: 4023-4030.
24. Frysz M, Faber BG, Ebsim R, Saunders FR, Lindner C, Gregory JS, et al. Machine Learning-Derived Acetabular Dysplasia and Cam Morphology Are Features of Severe Hip Osteoarthritis: Findings From UK Biobank. *J Bone Miner Res* 2022; 37: 1720-1732.
25. Barros HJ, Camanho GL, Bernabe AC, Rodrigues MB, Leme LE. Femoral head-neck junction deformity is related to osteoarthritis of the hip. *Clin Orthop Relat Res* 2010; 468: 1920-1925.
26. Saberi Hosnijeh F, Zuiderwijk ME, Versteeg M, Smelee HT, Hofman A, Uitterlinden AG, et al. Cam Deformity and Acetabular Dysplasia as Risk Factors for Hip Osteoarthritis. *Arthritis Rheumatol* 2017; 69: 86-93.
27. Faber BG, Baird D, Gregson CL, Gregory JS, Barr RJ, Aspden RM, et al. DXA-derived hip shape is related to osteoarthritis: findings from in the MrOS cohort. *Osteoarthritis Cartilage* 2017; 25: 2031-2038.
28. Pollard TC, Batra RN, Judge A, Watkins B, McNally EG, Gill HS, et al. The hereditary predisposition to hip osteoarthritis and its association with abnormal joint morphology. *Osteoarthritis Cartilage* 2013; 21: 314-321.
29. Tang J, van Buuren MMA, Riedstra NS, Boel F, Runhaar J, Bierma-Zeinstra S, et al. Cam morphology is strongly and consistently associated with development of radiographic hip osteoarthritis throughout 4 follow-up visits within 10 years. *Osteoarthritis Cartilage* 2023.
30. Agricola R, Heijboer MP, Bierma-Zeinstra SM, Verhaar JA, Weinans H, Waarsing JH. Cam impingement causes osteoarthritis of the hip: a nationwide prospective cohort study (CHECK). *Ann Rheum Dis* 2013; 72: 918-923.
31. Wyles CC, Norambuena GA, Howe BM, Larson DR, Levy BA, Yuan BJ, et al. Cam Deformities and Limited Hip Range of Motion Are Associated With Early Osteoarthritic Changes in Adolescent Athletes: A Prospective Matched Cohort Study. *Am J Sports Med* 2017; 45: 3036-3043.

32. van Buuren MMA, Heerey JJ, Smith A, Crossley KM, Kemp JL, Scholes MJ, et al. The association between statistical shape modeling-defined hip morphology and features of early hip osteoarthritis in young adult football players: Data from the femoroacetabular impingement and hip osteoarthritis cohort (FORCE) study. *Osteoarthr Cartil Open* 2022; 4: 100275.
33. Griffin DR, Dickenson EJ, O'Donnell J, Agricola R, Awan T, Beck M, et al. The Warwick Agreement on femoroacetabular impingement syndrome (FAI syndrome): an international consensus statement. *Br J Sports Med* 2016; 50: 1169-1176.
34. Ganz R, Parvizi J, Beck M, Leunig M, Notzli H, Siebenrock KA. Femoroacetabular impingement: a cause for osteoarthritis of the hip. *Clin Orthop Relat Res* 2003: 112-120.
35. Allen D, Beaulé PE, Ramadan O, Doucette S. Prevalence of associated deformities and hip pain in patients with cam-type femoroacetabular impingement. *J Bone Joint Surg Br* 2009; 91: 589-594.
36. Khanna V, Caragianis A, Diprimio G, Rakhra K, Beaulé PE. Incidence of hip pain in a prospective cohort of asymptomatic volunteers: is the cam deformity a risk factor for hip pain? *Am J Sports Med* 2014; 42: 793-797.
37. Larson CM, Sikka RS, Sardelli MC, Byrd JW, Kelly BT, Jain RK, et al. Increasing alpha angle is predictive of athletic-related "hip" and "groin" pain in collegiate National Football League prospects. *Arthroscopy* 2013; 29: 405-410.
38. Guler O, Isyar M, Karatas D, Ormeci T, Cerci H, Mahirogullari M. A retrospective analysis on the correlation between hip pain, physical examination findings, and alpha angle on MR images. *J Orthop Surg Res* 2016; 11: 140.
39. Abrahamson J, Jonasson P, Sansone M, Aminoff AS, Todd C, Karlsson J, et al. Hip pain and its correlation with cam morphology in young skiers—a minimum of 5 years follow-up. *J Orthop Surg Res* 2020; 15: 444.
40. van Klij P, Ginai AZ, Heijboer MP, Verhaar JAN, Waarsing JH, Agricola R. The relationship between cam morphology and hip and groin symptoms and signs in young male football players. *Scand J Med Sci Sports* 2020; 30: 1221-1231.
41. Gosvig KK, Jacobsen S, Sonne-Holm S, Gebuhr P. The prevalence of cam-type deformity of the hip joint: a survey of 4151 subjects of the Copenhagen Osteoarthritis Study. *Acta Radiol* 2008; 49: 436-441.
42. Nardo L, Parimi N, Liu F, Lee S, Jungmann PM, Nevitt MC, et al. Femoroacetabular Impingement: Prevalent and Often Asymptomatic in Older Men: The Osteoporotic Fractures in Men Study. *Clin Orthop Relat Res* 2015; 473: 2578-2586.
43. Faber BG, Ebsim R, Saunders FR, Frysz M, Gregory JS, Aspden RM, et al. Cam morphology but neither acetabular dysplasia nor pincer morphology is associated with osteophytosis throughout the hip: findings from a cross-sectional study in UK Biobank. *Osteoarthritis Cartilage* 2021; 29: 1521-1529.
44. Bartley EJ, Fillingim RB. Sex differences in pain: a brief review of clinical and experimental findings. *Br J Anaesth* 2013; 111: 52-58.
45. Dijkstra HP, Arderin CL, Serner A, Mosler AB, Weir A, Roberts NW, et al. Primary cam morphology; bump, burden or bog-standard? A concept analysis. *Br J Sports Med* 2021; 55: 1212-1221.
46. Bugeja JM, Xia Y, Chandra SS, Murphy NJ, Eyles J, Spiers L, et al. Automated volumetric and statistical shape assessment of cam-type morphology of the femoral head-neck region from clinical 3D magnetic resonance images. *Quant Imaging Med Surg* 2022; 12: 4924-4941.

9

Summary/ Samenvatting

SUMMARY

Cam morphology is a significant risk factor for hip osteoarthritis (OA). Given the current absence of curative treatment for this condition, it is essential to understand the role cam morphology plays in the development of hip OA. This thesis consists of four parts. The first part introduces the radiographic methodology that was used across the whole thesis. In the second part, we aimed to investigate the relationship between baseline cam morphology and the development of radiographic hip osteoarthritis (RHOA) through multiple visits or within a harmonized database. The third part focuses on the relationship between cam morphology and hip pain symptoms. The last part identifies subtypes of cam morphology captured by the alpha angle and examines whether the triangular index ratio is an alternative method to the alpha angle for defining cam morphology.

In **Chapter 2**, we introduced automated measurements for defining cam morphology on pelvic radiographs and assessed the reliability and agreement of both manual and automated measurements. Automated measurements for both the alpha angle and triangular index ratio were found to be valid in a clinical setting. The inter-method intraclass correlation coefficients (ICCs) were 0.46 for the alpha angle and 0.78 for the triangular index ratio, demonstrating comparable performance to manual measurements by trained observers. These automated measurements were used in subsequent chapters.

The association between cam morphology and the development of RHOA has been explored in several prior studies, though with varying strengths of association. In **Chapter 3**, we proposed that time may be a key factor influencing this relationship, therefore we investigated the association between the two across multiple visits over 10 years in the CHECK cohort. Our findings indicate that cam morphology is consistently associated with the development of RHOA at all follow-ups with adjusted odd ratios (aORs) ranging from 2.7 (95%CI 1.8–4.1) to 2.9 (95%CI 2.0–4.4).

The different definitions of both cam morphology and RHOA as well as the diverse demographics of study populations might also be the explanation for the considerable heterogeneity in the results of previous studies. To address this, **Chapter 4** investigated the association of cam morphology with the development of RHOA in the World COACH consortium. In this study, the alpha angle was uniformly calculated, and the definition of cam morphology was standardized. We also harmonized the OA scores across different classification systems, resulting in a three-categories outcome for RHOA (free of RHOA, doubtful RHOA, and definite RHOA) instead of a binary one.

All hips with doubtful RHOA at baseline were excluded from the analysis of this study. In this harmonized dataset, cam morphology was associated with the development of RHOA with aORs of 1.87 (95%CI 1.36-2.59). The strength of this association was weaker but more generalized than previous findings.

Chapter 5 aimed to investigate the association between cam morphology and the presence of hip pain over 10 consecutive annual follow-ups. Hips from the CHECK cohort were divided into three subgroups : male, female and sex-combined group. Significant association was found in the male group at five-year follow-up [aOR: 1.77 (95%CI: 1.01-3.09)], while no such association was observed at other time points or in the other subgroups. Notably, all aORs in the male group were consistently above 1, whereas in the female group, they fluctuated around 1 over the 10-year period. Our findings suggested that biology sex might play a role between cam morphology and RHOA.

In **Chapter 6**, we identified four distinct morphological subtypes of cam morphology on the AP radiographs using statistical shape modeling. Only certain subtypes, such as a flattened head-neck junction or a pistol grip-shaped prominence (only in males), were found acting as risk factors for the development of RHOA at 10-year follow-up. This indicates that not all cam-related shape variations as captured by the alpha angle may be relevant in the development of RHOA, suggesting the need to look beyond the alpha angle as a sole measurement for cam morphology.

Given the inaccuracy of the alpha angle for defining cam morphology, we explored whether the triangular index ratio could serve as an alternative method. In **Chapter 7**, we investigated the association between cam morphology, defined by triangular index ratio ≥ 1.05 , and the development of RHOA at 10-year follow-up in the CHECK cohort. Meanwhile, we compared the predictive performance for RHOA of two methods by calculating sensitivity, specificity, positive predictive value (PPV), and negative predictive value (NPV). With an aOR of 2.48 (95% CI 1.38-4.46), a higher PPV (70.6% vs 62.3%), and a lower sensitivity (7.8% vs 12.3%), we believe the triangular index ratio offers a more precise definition of the presence of cam morphology while the alpha angle can ensure to capture more target cases.

Finally, **Chapter 8** generally discussed the main findings, interpretations, clinical implications, strengths, and limitations of this thesis.

SAMENVATTING

Cam-morfologie is een significante risicofactor voor heupartrose. Aangezien er momenteel geen curatieve behandeling voor artrose beschikbaar is, is het essentieel om de rol van cam-morfologie in de ontwikkeling van heupartrose te begrijpen. Dit proefschrift bestaat uit vier delen. Het eerste deel introduceert de methodologie die door het gehele proefschrift heen wordt gebruikt. In het tweede deel hebben we de relatie tussen cam-morfologie en het ontstaan van radiologische heupartrose onderzocht. Zowel op meerdere tijdstippen binnen het CHECK cohort als binnen het World COACH consortium; een verzameling van alle wereldwijd beschikbare prospectieve cohort studies. Het derde deel richt zich op de relatie tussen cam-morfologie en symptomen. Het laatste deel identificeert subtypes van cam-morfologie, gemeten met de alfahoek, en onderzoekt of de triangular index ratio een alternatief is voor de alfahoek bij het definiëren van cam-morfologie.

In **hoofdstuk 2** introduceerden we geautomatiseerde metingen voor het definiëren van cam-morfologie op röntgenfoto's van het bekken en evalueerden we de betrouwbaarheid en overeenstemming van zowel handmatige als geautomatiseerde metingen. Geautomatiseerde metingen van zowel de alfahoek als de triangular index ratio bleken matig tot goed reproduceerbaar te zijn. De intraclass correlatiecoëfficiënten (ICC's) tussen deze twee methodes waren 0.46 voor de alfahoek en 0.78 voor de triangular index ratio, wat vergelijkbaar is met de reproduceerbaarheid van handmatige metingen door getrainde waarnemers. Deze geautomatiseerde metingen werden gebruikt in de volgende hoofdstukken.

De associatie tussen cam-morfologie en het ontstaan van radiologische heupartrose is al in verschillende studies onderzocht, hoewel met wisselende sterktes van associatie. In **hoofdstuk 3** stellen we dat follow-up tijd een mogelijke factor kan zijn in de sterkte van associatie en daarom onderzochten we de associatie tussen cam-morfologie en radiologische heupartrose gedurende meerdere bezoeken over een periode van 10 jaar in de CHECK-cohort. Onze bevindingen tonen aan dat cam-morfologie consequent geassocieerd is met de ontwikkeling van RHOA bij alle follow-ups, met geadjusteerde odds ratio's (aOR's) variërend van 2.7 (95% CI 1.8–4.1) tot 2.9 (95% CI 2.0–4.4).

De verschillende definities van zowel cam-morfologie als radiologische heupartrose, evenals de diverse demografieën van studiepopsaties, kunnen de aanzienlijke heterogeniteit in de resultaten van eerdere studies mogelijk verklaren. Om dit aan te testen, onderzochten we in **hoofdstuk 4** de associatie tussen cam-morfologie en het ontstaan van radiologische heupartrose in het world COACH-consortium. In deze

studie werd de alfahoek uniform berekend en werd de definitie van cam-morfologie gestandaardiseerd. We harmoniseerden ook de radiologische artrose scores van de verschillende classificatiesystemen, wat resulteerde in een uitkomst met drie categorieën voor radiologische heupartrose (vrij van artrose, twijfelachtige artrose, en evidente artrose) in plaats van een binaire uitkomst. Alleen heupen vrij van radiologische heupartrose bij aanvang werden geïnccludeerd. In deze geharmoniseerde dataset was cam-morfologie geassocieerd met het ontstaan van radiologische heupartrose met een aOR van 1.87 (95% CI 1.36-2.59). De sterkte van deze associatie was zwakker dan eerder gerapporteerd maar beter toepasbaar op de algemene populatie.

Hoofdstuk 5 had tot doel de associatie tussen cam-morfologie en de aanwezigheid van heuppijn gedurende 10 opeenvolgende jaarlijkse follow-ups te onderzoeken. Heupen uit het CHECK-cohort werden verdeeld in drie subgroepen: mannen, vrouwen en een gecombineerde groep. Een significante associatie tussen cam-morfologie bij aanvang en het hebben van heuppijn bij de 5 jaars follow-up werd gevonden in de mannengroep [aOR: 1.77 (CI: 1.01-3.09)], terwijl er geen dergelijke associatie werd waargenomen op andere tijdstippen of in de andere subgroepen. Opmerkelijk was dat alle aOR's in de mannengroep consequent boven de 1 lagen, terwijl deze in de vrouwengroep rond de 1 schommelden gedurende de 10-jarige periode. Onze bevindingen suggereren dat geslacht mogelijk een rol speelt in de relatie tussen cam-morfologie en heuppijn.

In **hoofdstuk 6** identificeerden we vier verschillende morfologische subtypes van cam-morfologie op de AP rontgenfoto's met behulp van statistical shape modeling. Alleen bepaalde subtypes, zoals een afgeplatte kop-hals overgang of een pistool-greepvormige prominentie (alleen bij mannen), bleken risicofactoren te zijn voor de ontwikkeling van radiologische heupartrose bij de 10-jarige follow-up. Dit geeft aan dat niet alle cam-gerelateerde vormvariëaties zoals gedefinieerd door de alfahoek relevant zijn voor de ontwikkeling van artrose, wat suggereert dat verder gekeken moet worden dan de alfahoek als enige maat voor cam-morfologie.

Gezien de onnauwkeurigheid van de alfahoek bij het definiëren van cam-morfologie, onderzochten we of de triangular index ratio als een alternatieve methode zou kunnen dienen. In **hoofdstuk 7** onderzochten we de associatie tussen cam-morfologie, gedefinieerd door een triangular index ratio van ≥ 1.05 , en de ontwikkeling van radiologische heupartrose bij de 10-jarige follow-up in het CHECK-cohort. Tegelijkertijd vergeleken we de voorspellende prestaties voor radiologische heupartrose van beide methoden door het berekenen van de sensitiviteit, specificiteit, positief voorspellende waarde (PPV) en negatief voorspellende waarde (NPV). Met een aOR van 2.48 (95%

CI 1.38-4.46), een hogere PPV (70.6% vs. 62.3%) en een lagere sensitiviteit (7.8% vs. 12.3%), denken we dat de triangular index ratio een nauwkeurigere definitie biedt van de aanwezigheid van cam-morfologie, terwijl de alfahoek ervoor kan zorgen dat meer gevallen worden gedefinieerd.

Tot slot worden in **hoofdstuk 8** de belangrijkste bevindingen, interpretaties, klinische implicaties, sterke punten en beperkingen van dit proefschrift in het algemeen besproken.

总结

髌关节凸轮形态 (cam morphology) 是指股骨头颈连接处因发育或形态异常导致的骨性隆起 (缺乏正常的凹度), 是髌骨关节炎的重要危险因素之一。由于目前缺乏针对骨关节炎的根治性治疗手段, 深入了解凸轮形态在髌骨关节炎发生与发展中的作用显得尤为重要。本论文分为四个部分。第一部分介绍了整篇论文中使用的影像学测量方法; 第二部分研究了基线凸轮形态与放射学髌骨关节炎发展之间的关联; 第三部分探讨了凸轮形态与髌关节疼痛的关系; 第四部分进一步分析了基于alpha角的凸轮形态亚型, 并探索三角指数比 (triangular index ratio) 作为替代定义指标的可能性。

在第二章中, 我们提出了基于骨盆X光片的自动测量方法, 用于定义凸轮形态, 并对其与传统手动测量的可靠性和一致性进行了评估。结果表明, 无论是alpha角还是三角指数比, 自动测量在临床背景下均表现出良好的有效性。自动测量与手动测量的组内相关系数 (ICC) 表明两者一致性较高, 其中alpha角的ICC为 0.46, 三角指数比的ICC为 0.78。

尽管许多研究已经探讨了凸轮形态与髌骨关节炎发展之间的关联, 但既往研究中关联强度的差异较大。在第三章中, 我们认为随访时间可能是导致这种差异的原因之一。因此, 在CHECK队列中, 我们通过10年多次随访探索了两者之间的关联。结果显示, 在所有随访时间点, 凸轮形态始终与放射学髌骨关节炎的发展相关, 矫正后的比值比 (adjusted odds ratio) 介于 2.7 (95%CI 1.8 - 4.1) 至 2.9 (95%CI 2.0 - 4.4)。

凸轮形态和髌骨关节炎定义的不一致以及研究人群人口特征的多样性可能是既往研究结果差异显著的原因之一。为了解决这一问题, 第四章利用World COACH Consortium数据库, 该数据库整合了来自全球九个独立队列的研究数据。在本研究中, alpha角的测量实现了重新定义和标准化, 凸轮形态的定义也达到了统一。为了提高分析精度, 我们整合了多种关节炎评分系统, 将放射学髌骨关节炎的状态分为健康、疑似和明确三类, 而非以往的二元分类 (有或无)。所有基线时疑似病例的髌关节均被排除在分析之外。结果显示, 凸轮形态与放射学髌骨关节炎的发展存在显著关联, 矫正比值比为 1.87 (95%CI 1.36 - 2.59)。尽管这一关联强度弱于既往研究, 但普适性更强。

第五章探讨了凸轮形态与髌关节疼痛之间的关联, 分析CHECK队列中10年随访数据。根据受试者性别, 将髌关节分为男性组、女性组和性别混合组。结果显示, 仅在第五年随访中, 男性组存在显著关联[矫正比值比为 1.77 (95%CI 1.01 - 3.09)], 其他时间点及女性组和混合组中均未观察到类似结果。值得注意的是, 男性组的矫正比值比始终高于1, 而女性组则在10年间波动于1左右。这提示生物学性别可能在凸轮形态引发髌关节疼痛中起一定作用。

在第六章中, 我们利用统计形状建模 (statistical shape modeling) 对凸轮形态进行了更精细的分类, 明确了其四种不同亚型。研究发现, 只有部分亚型 (如扁平的头颈连接处

或“手枪柄状”突起，仅见于男性）与髌骨关节炎的发展显著相关。这表明，并非所有由alpha角定义的凸轮形状都与髌骨关节炎的发展相关。

鉴于alpha角在定义凸轮形态时存在一定局限性，我们在第七章中探索了三角指数比作为替代方法的可行性。通过分析CHECK队列数据，研究三角指数比大于1.05所定义的凸轮形态与10年随访期间放射学髌骨关节炎发展的关联，并比较其alpha角在预测髌骨关节炎时的表现。结果显示，三角指数比定义的凸轮形态在矫正比值比上表现出较高的关联性（2.48，95%CI 1.38-4.46），并在阳性预测值（PPV）上优于alpha角（70.6% vs. 62.3%），但敏感度稍低（7.8% vs. 12.3%）。因此，我们认为三角指数比更适合用于准确定义凸轮形态，而alpha角则更适用于大规模筛查。

最后，第八章对本论文集的主要发现进行了全面总结，并讨论了研究结果的解释、临床意义、优势与局限性。

APPENDICES



PhD portfolio
Acknowledgments
About the author
List of publications

PHD PORTFOLIO

PhD student	Jinchi Tang
Department	Orthopaedics and Sports Medicine
PhD Period	January 2021- February 2025
Promotor	Prof. dr. S.M.A. Bierma - Zeinstra
Co-promotor	Dr. R. Agricola

	Year	Workload (ETCS*)
courses		
Master of Science in Health Sciences	2021-2024	70
Research Integrity	2021	0.3
Diversity & Inclusivity	2023	0.1
Presentations		
Poster Presentation OARSI World Congress on Osteoarthritis 2023	2023	1
Poster Presentation OARSI World Congress on Osteoarthritis 2024	2024	1
Poster Presentation OARSI World Congress on Osteoarthritis 2024	2024	1
Poster Presentation OARSI World Congress on Osteoarthritis 2024	2024	1
Oral Presentation Nederlandse Orthopaedische Vereniging Jaarcongres 2023	2023	1
Oral Presentation Combined 61st NOF Congress and NOV Jaarcongres 2024	2024	1
Oral Presentation Combined 61st NOF Congress and NOV Jaarcongres 2024	2024	1
Oral Presentation Combined 61st NOF Congress and NOV Jaarcongres 2024	2024	1
Conferences		
OARSI World Congress on Osteoarthritis 2022	2022	0.5
2023 European Sports Orthopedic Congress	2023	0.5
Total		79.4

*One ETCS (European Credit Transfer and Accumulation System) credit corresponds to a workload of 28 hours.

A

ACKNOWLEDGMENTS

From January 2021 to today, the four years I've spent living, studying, and researching in the Netherlands have been an unforgettable chapter in my life. I would like to take this opportunity to express my heartfelt gratitude to everyone who has helped and encouraged me throughout this journey.

First and foremost, I owe a great deal to my promotors, **Prof. Dr. Sita Bierma-Zeinstra** and **Dr. Rintje Agricola**, for granting me the opportunity to pursue this PhD and for their support throughout my studies. Your guidance was invaluable during my research and the writing of this thesis.

Dear Sita, thank you for your confidence in my potential and for accepting me into the PhD program, which laid the foundation for all that followed. Your insightful advice has been essential in shaping my research on hip osteoarthritis, and I deeply appreciate our discussions, which often gave me new perspectives and direction.

Dear Rintje, there is so much I want to thank you for. From the moment you picked me up at Schiphol Airport, you made me feel welcome and supported. Despite your demanding schedule, you always made time to offer invaluable advice and help me navigate challenges. Working with you on my first academic publication is a memory I will cherish forever—no matter how many papers I write in the future, that milestone will always stand out. Thank you for your consistent encouragement and mentorship.

No academic achievement is possible without a strong team, and I am incredibly fortunate to have been part of the World COACH team. My heartfelt thanks to **Michiel, Fleur, Noortje, Myrthe, and Ninka** for your invaluable support and collaboration on my research projects. The experiences we shared at the OARSI congresses in Berlin, Denver, and Vienna will stay with me always.

Room NC-424 became my second home at Erasmus MC, and my colleagues there were like family. I would like to extend my gratitude to my dear colleagues **Max, Eline, Irene, Erin, Niels, Mark, Merel, Derek, Brechtje, Joshua, Mariska, Floris, Britt, Lichelle, Tjerk, Annika, Abigael, and Sabine**. Thank you for creating such a warm, friendly, and productive work environment, and for many enjoyable Monday afternoon department meetings.

Initially, I was the only Chinese member of our department, but soon **Delong** joined, and this year, **Zhongcan** became part of us as well. I am truly grateful for their pres-

ence—not only because we can speak our mother tongue, but also because they made me feel at home. I treasure our friendship and look forward to reflecting on our time together in the Netherlands in the future.

Beyond my colleagues, I was fortunate to meet many wonderful friends during my time in the Netherlands. Whether they came from other departments of Erasmus MC, EUR, or beyond, these friends have enriched my life in countless ways. Together, we shared dinners, bike rides, travels, card games, barbecues, and movie nights. I am honored to name them here: **Aunt Aifeng, Dawei, Enping, Fang Zhu, Guangjie, Hongzhen, Heng Liu, Haojie, Hui Lin, Hongchao, Jie Deng, Jiawei, Jeff, Jing Yu, Jie Gao, Lun Li, Liang Wu, Letao, Qiuke, Ruud, Wei Zhang, Wenchao, Wenjing, Wenbo, Xiangjun, Xiaoyu, Yahong, Yuwei, Yu Shuai, Yanyan, Yisha, Yubo, Ying Liu, Zhaochen, Zuoluo.** Thank you all for making these years so memorable.

I would also like to express my sincere gratitude to my Master's supervisor, **Prof. Yuntao Wu**, from China-Japan Union Hospital of Jilin University, for his thoughtful guidance and consistent support in shaping my career path. Your encouragement has been instrumental in inspiring me to pursue a doctorate abroad, and for that, I am deeply thankful.

Last but certainly not least, I want to express my deepest gratitude to my beloved family. To my dear wife, **Yifan**, thank you for your companionship over these four years. You've been my rock, and your love has been my greatest motivation. Your sacrifices, patience, and unwavering care have been a constant source of strength for me, and I am truly grateful for everything you've done. It is through you that I've come to understand that love is not only felt but seen and experienced every day. To my beloved parents, thank you for your endless support and encouragement throughout the years. Your unwavering belief in me has been my driving force, and I am forever grateful for all you've done to help me become the best son I can be. 亲爱的妈妈爸爸们，感谢你们这么多年的培养，你们的支持将一直推动我前进，成为你们眼中最棒的儿子。

Jinchi Tang

November 18, 2024

Capelle aan den IJssel

ABOUT THE AUTHOR

Jinchi Tang was born on August 24, 1994, in Yangling, Shaanxi Province, China. He obtained his Bachelor's degree in Medicine from Nanchang University in 2017, followed by a Master's degree in Surgery from Jilin University in 2020. Concurrent with his Master's studies, Jinchi completed medical training and served as a resident surgeon at the China-Japan Union Hospital of Jilin University from 2017 to 2020.

In 2020, Jinchi was awarded a Doctoral Scholarship by the China Scholarship Council. This opportunity led him to begin his PhD journey in January 2021 at the Department of Orthopedics and Sports Medicine, Erasmus Medical Center, Rotterdam, the Netherlands. Under the supervision of Prof. Dr. S.M.A. Bierma-Zeinstra and Dr. R. Agricola, his research focused on hip osteoarthritis and cam morphology.

Given the statistical and epidemiological demands of his research, Jinchi enrolled in a Master's program in Health Science at the Netherlands Institute for Health Sciences (NIHES). He successfully obtained his second Master's degree in Science in 2024.

Upon completing his PhD, Jinchi plans to return to China, where he will continue his career as an orthopedic surgeon. He is also committed to advancing research in the field of osteoarthritis, aiming to contribute to both clinical practice and scientific understanding in this area.



LIST OF PUBLICATIONS

Jinchi Tang, Michiel M. A. van Buuren, Noortje S Riedstra, Fleur Boel, Jos Runhaar, Sita Bierma-Zeinstra, Rintje Agricola. Cam morphology is strongly and consistently associated with development of radiographic hip osteoarthritis throughout 4 follow-up visits within 10 years. *Osteoarthritis Cartilage*. 2023;31(12):1650-1656. doi:10.1016/j.joca.2023.08.006

Jinchi Tang, Fleur Boel, Michiel M. A. van Buuren, Noortje S Riedstra, Jos Runhaar, Sita Bierma-Zeinstra, Rintje Agricola. The different subtypes of cam morphology as defined by statistical shape modeling and their relationship with the development of hip osteoarthritis: A nationwide prospective cohort study (CHECK) with 10 years follow-up. *Osteoarthritis Cartilage*. 2024;32(12):1647-1654. doi:10.1016/j.joca.2024.08.003

Jinchi Tang, Michiel M. A. van Buuren, Fleur Boel, Noortje S Riedstra, Myrthe A van den Berg, Jos Runhaar, Sita Bierma-Zeinstra, Rintje Agricola. The association between cam morphology and hip pain in males and females within 10 years: A national prospective cohort study (CHECK). *Semin Arthritis Rheum*. Published online August 23, 2024. doi:10.1016/j.semarthrit.2024.152539

Fleur Boel, Noortje S. Riedstra, **Jinchi Tang**, David F. Hanff, Harbeer Ahedi, Vahid Arbabi, Nigel K. Arden, Sita Bierma-Zeinstra, Michiel M. A. van Buuren, Flavia M. Cicuttini, Tim F. Cootes, Kay M. Crossley, Denise Eygendaal, David T. Felson, Willem P. Gielis, Joshua Heerey, Graeme Jones, Stefan Kluzek, Nancy E. Lane, Claudia Lindner, John A. Lynch, Joyce van Meurs, Amanda E. Nelson, Andrea Mosler, Michael C. Nevitt, Edwin H.G. Oei, Jos Runhaar, Harrie Weinans, Rintje Agricola. Reliability and agreement of manual and automated morphological radiographic hip measurements. *Osteoarthr Cartil Open*. 2024;6(3):100510. doi:10.1016/j.ocarto.2024.100510

Michiel M. A. van Buuren, Noortje S. Riedstra, Myrthe A van den Berg, Fleur Boel, Harbeer Ahedi, Vahid Arbabi, Nigel K. Arden, Sita Bierma-Zeinstra, Cindy G. Boer, Flavia M. Cicuttini, Tim F. Cootes, Kay M. Crossley, David T. Felson, Willem P. Gielis, Joshua Heerey, Graeme Jones, Stefan Kluzek, Nancy E. Lane, Claudia Lindner, John A. Lynch, Joyce van Meurs, Amanda E. Nelson, Andrea Mosler, Michael C. Nevitt, Edwin H.G. Oei, Jos Runhaar, **Jinchi Tang**, Harrie Weinans, Rintje Agricola. Cohort profile: Worldwide Collaboration on OsteoArthritis prediCtion for the Hip (World COACH) - an international consortium of prospective cohort studies with individual participant data on hip osteoarthritis. *BMJ Open*. 2024;14(4):e077907. doi:10.1136/bmjopen-2023-077907

Jinchi Tang, Fleur Boel, Michiel M. A. van Buuren, Noortje S. Riedstra, Myrthe A. van den Berg, Harbeer Ahedi, Nigel K. Arden, Sita Bierma-Zeinstra, Cindy G. Boer, Flavia M. Cicuttini, Tim F. Cootes, Kay M. Crossley, David T. Felson, Willem P. Gielis, Graeme Jones, Stefan Kluzek, Nancy E. Lane, Claudia Lindner, John A. Lynch, Joyce van Meurs, Amanda E. Nelson, Michael C. Nevitt, Edwin H.G. Oei, Jos Runhaa, Harrie Weinans, Rintje Agricola. Cam morphology and the risk of developing radiographic hip osteoarthritis within 8 years: an individual participant data meta-analysis from the World COACH consortium. *Manuscript submitted.*

Jinchi Tang, Fleur Boel, Michiel M A van Buuren, Noortje S Riedstra, Myrthe A. van den Berg, Jos Runhaar, Sita Bierma-Zeinstra, Rintje Agricola. Triangular Index Ratio as An Alternative Method to The Alpha Angle for Defining the Presence of Cam Morphology: Data from The CHECK Cohort. *Manuscript submitted.*

Jing Yu*, **Jinchi Tang***, Yahong Wu*, Wenjie Kang, Justin Boer, Trudy Voortman, Rintje Agricola, Edwin H.G. Oei, Sita Bierma- Zeinstra, Gennady Roshchupkin, Jukka Hirvasniemi, Joyce van Meurs, Cindy G. Boer. Automatic grading of knee chondrocalcinosis using convolution neural network. *In preparation.*

*Authors denote equal contribution.

